

Computational Plasticity

Chapter 1 – Recent progress of computational plasticity

Li-Wei Liu, Ph.D.

Department of Civil Engineering

National Taiwan University

Teaching assistants



Zhen-En Jian

r11521240@ntu.edu.tw



Po-Ho Chen

r11521244@ntu.edu.tw



Jin-Yan Wang

r11521248@ntu.edu.tw



Cheng-Yuan Chen

r11521253@ntu.edu.tw

Program of short course

- Chapter 1 – Recent progress of computational plasticity
- Chapter 2 – First step in computational plasticity
- Chapter 3 – Numerical integrations in computational plasticity
- Chapter 4 – High accurate integrations in computational plasticity

Overview

- Evidence of plastic behavior in multi-scale mechanics
- Mathematical frameworks of plastic models
- Plastic integrations

Evidence of plastic behavior in multi-scale mechanics

Warp-up

Elastic behavior of materials

Bar (rod)

P : axial load

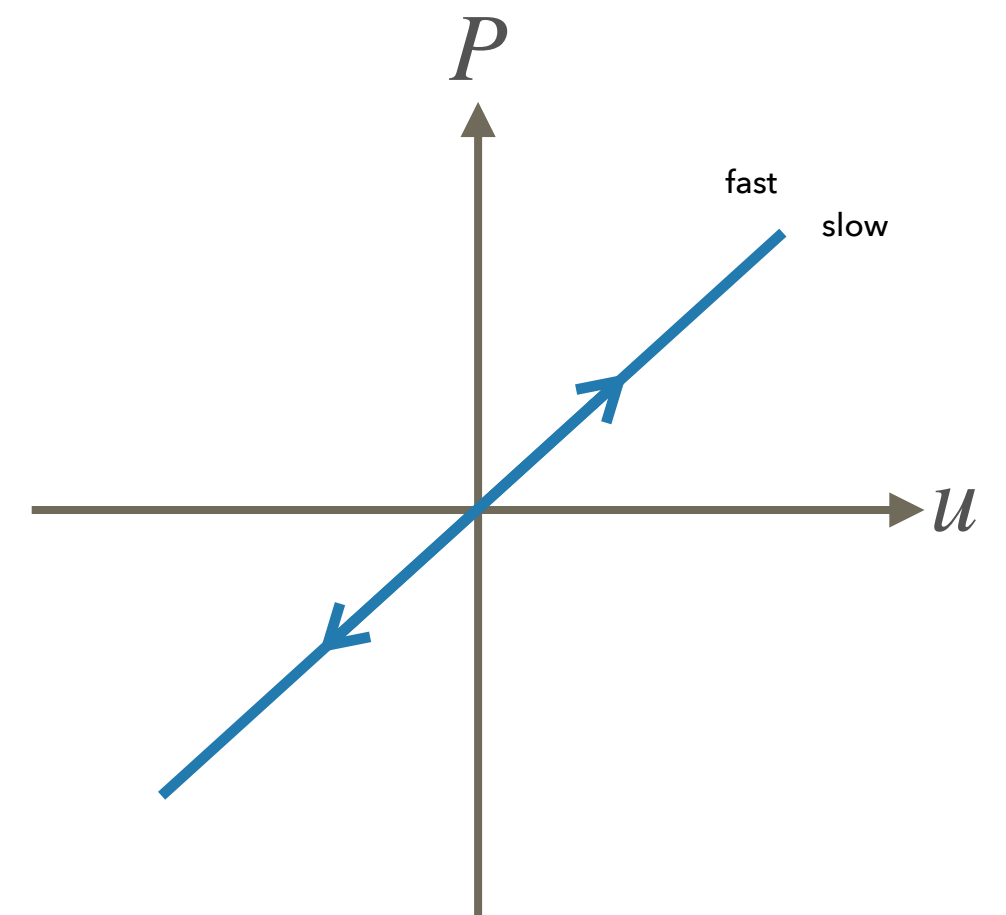
u : axial displacement



E : Young's modulus

A : area of cross section

$$P = \frac{EA}{L}u$$



Elastic behavior of materials

Shaft

T : torque

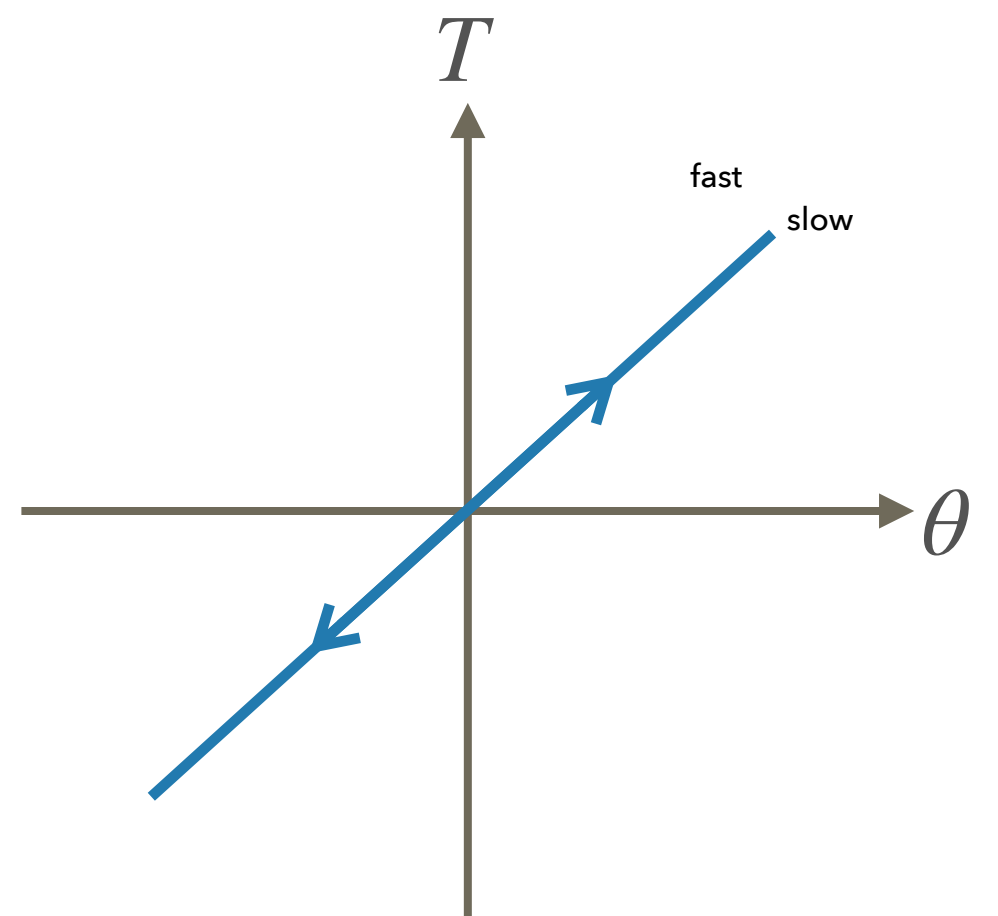
θ : rotation angle



G : shear modulus

J : polar moment of inertia

$$T = \frac{GJ}{L} \theta$$



Elastic behavior of materials

Beam

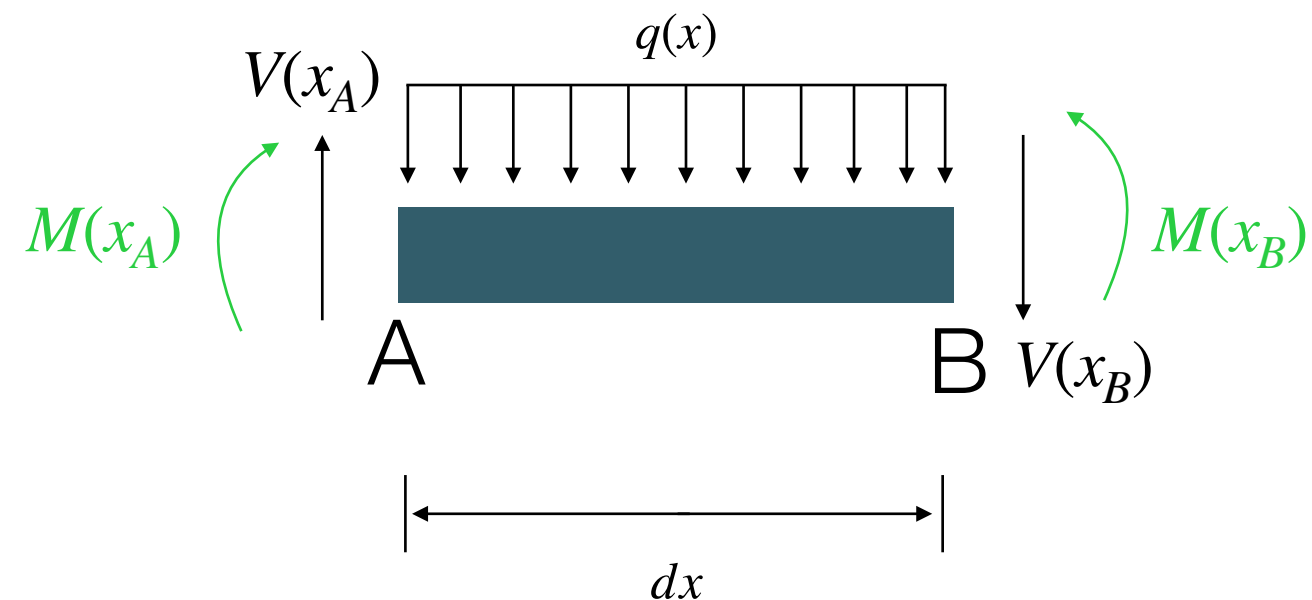
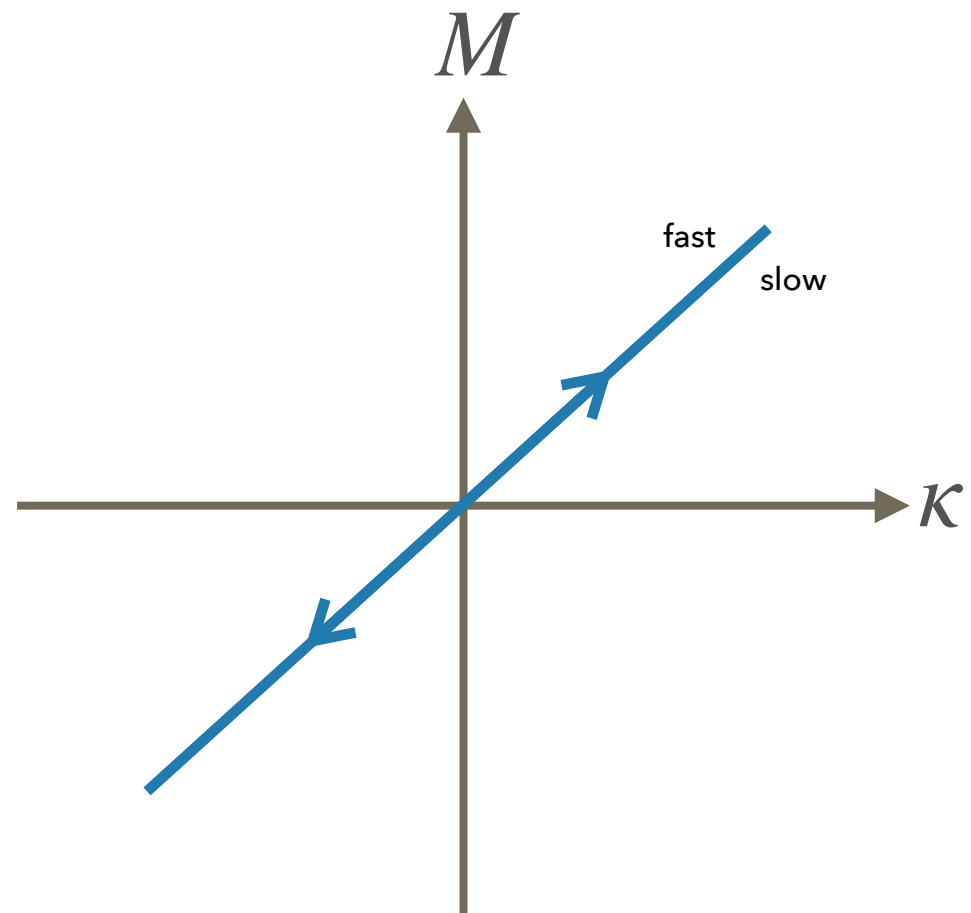
M : bending moment

κ : curvature

E : Young's modulus

I : moment of inertia

$$M = EI\kappa$$



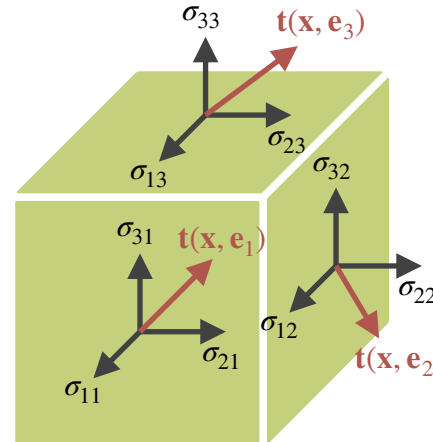
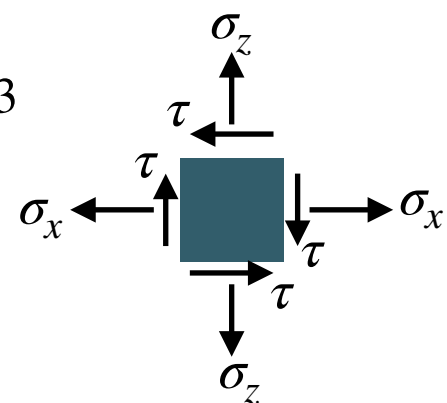
Elastic behavior of materials

Material points

$$\sigma_{ij} = 2G\epsilon_{ij} + \frac{3K - 2G}{3}\delta_{ij}\epsilon_{kk}, \quad i, j = 1, 2, 3$$

$$\sigma_{ij} = 2\mu\epsilon_{ij} + \lambda\delta_{ij}\epsilon_{kk}$$

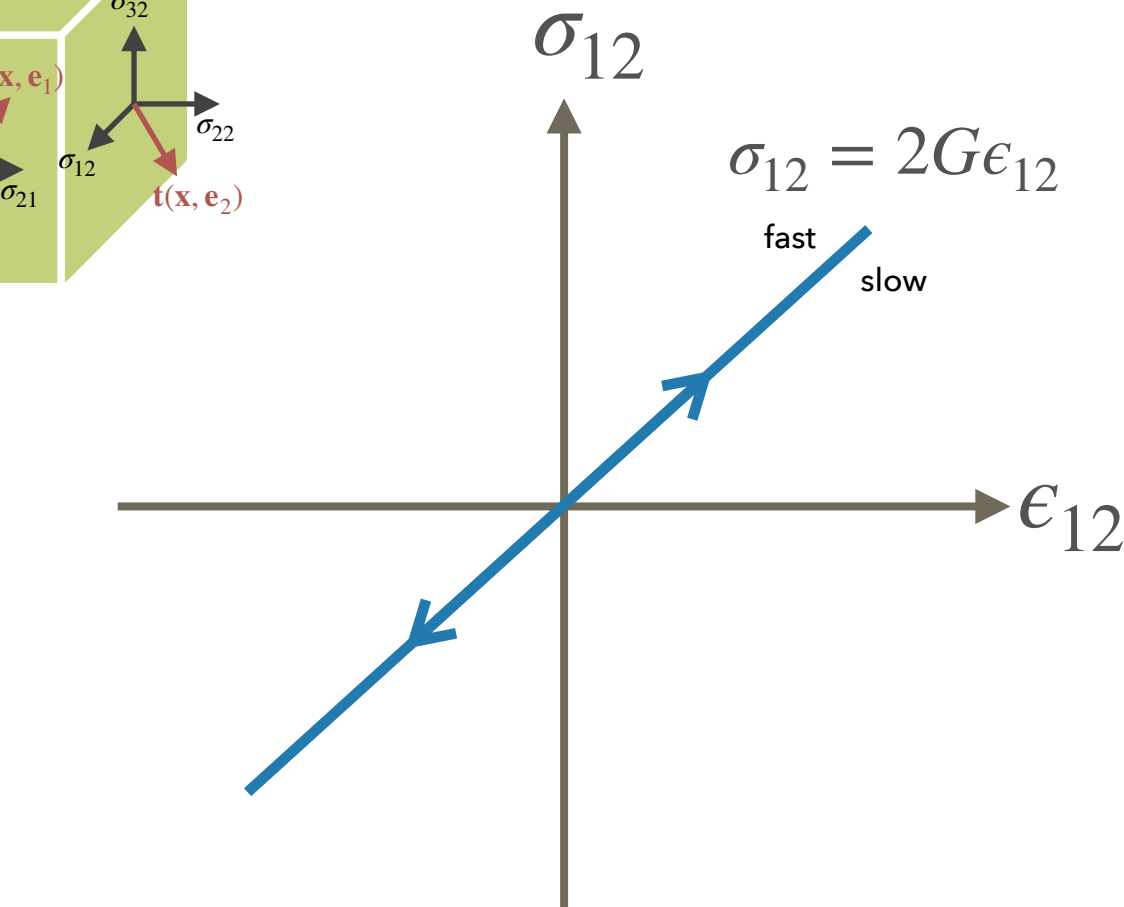
$$\epsilon_{ij} = -\frac{\nu}{E}\sigma_{ij} + \frac{1+\nu}{E}\delta_{ij}\sigma_{kk}$$



$$\begin{bmatrix} \sigma_{11} \\ \sigma_{22} \\ \sigma_{33} \\ \sqrt{2}\sigma_{23} \\ \sqrt{2}\sigma_{13} \\ \sqrt{2}\sigma_{12} \end{bmatrix} = \begin{bmatrix} (3K+4G)/3 & (3K-2G)/3 & (3K-2G) & 0 & 0 & 0 \\ (3K-2G)/3 & (3K+4G)/3 & (3K-2G) & 0 & 0 & 0 \\ (3K-2G)/3 & (3K-2G)/3 & (3K+4G) & 0 & 0 & 0 \\ 0 & 0 & 0 & 2G & 0 & 0 \\ 0 & 0 & 0 & 0 & 2G & 0 \\ 0 & 0 & 0 & 0 & 0 & 2G \end{bmatrix} \begin{bmatrix} \epsilon_{11} \\ \epsilon_{22} \\ \epsilon_{33} \\ \sqrt{2}\epsilon_{23} \\ \sqrt{2}\epsilon_{13} \\ \sqrt{2}\epsilon_{12} \end{bmatrix}$$

$$\begin{bmatrix} \epsilon_{11} \\ \epsilon_{22} \\ \epsilon_{33} \\ \sqrt{2}\epsilon_{23} \\ \sqrt{2}\epsilon_{13} \\ \sqrt{2}\epsilon_{12} \end{bmatrix} = \begin{bmatrix} \frac{1}{E} & -\frac{\nu}{E} & -\frac{\nu}{E} & 0 & 0 & 0 \\ -\frac{\nu}{E} & \frac{1}{E} & -\frac{\nu}{E} & 0 & 0 & 0 \\ -\frac{\nu}{E} & -\frac{\nu}{E} & \frac{1}{E} & 0 & 0 & 0 \\ 0 & 0 & 0 & \frac{1}{2G} & 0 & 0 \\ 0 & 0 & 0 & 0 & \frac{1}{2G} & 0 \\ 0 & 0 & 0 & 0 & 0 & \frac{1}{2G} \end{bmatrix} \begin{bmatrix} \sigma_{11} \\ \sigma_{22} \\ \sigma_{33} \\ \sqrt{2}\sigma_{23} \\ \sqrt{2}\sigma_{13} \\ \sqrt{2}\sigma_{12} \end{bmatrix}$$

Young's modulus E
Shear modulus G
Bulk modulus K



Poisson's ratio ν
Lamé constants λ and μ

σ_{ij} : stress
 ϵ_{ij} : strain

Elastic behavior of materials

Linearly elastic behavior

linear

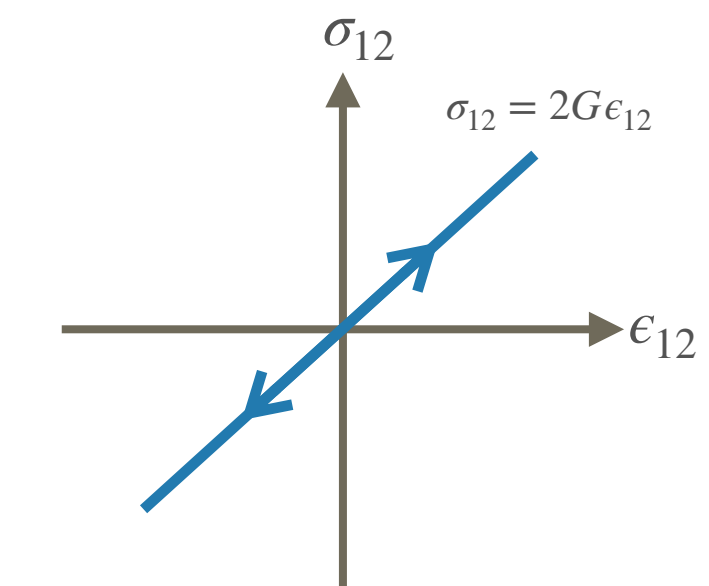
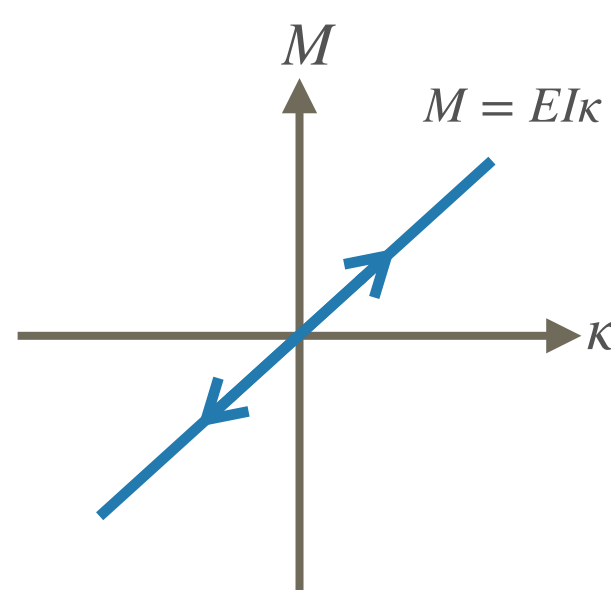
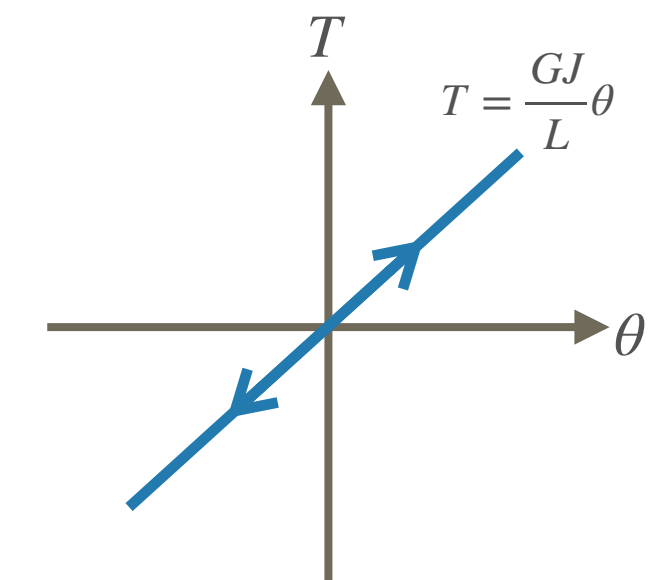
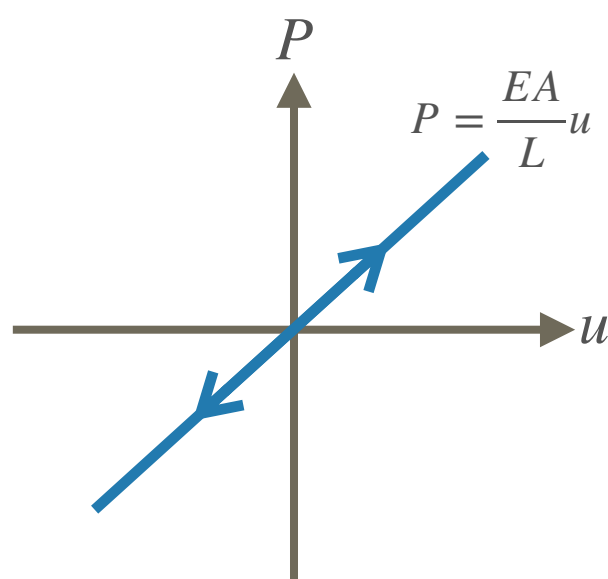
constant moduli

reversible

conservative

single-valued

state vs. state



Generalized stress/strain

Level IV	$\mathbf{Q} = \mathbf{K}\mathbf{q}$		
Level III	$\begin{bmatrix} P_i \\ P_j \end{bmatrix} = \begin{bmatrix} \frac{EA}{L} & -\frac{EA}{L} \\ -\frac{EA}{L} & \frac{EA}{L} \end{bmatrix} \begin{bmatrix} u_i \\ u_j \end{bmatrix} \quad \begin{bmatrix} T_i \\ T_j \end{bmatrix} = \begin{bmatrix} \frac{GJ}{L} & -\frac{GJ}{L} \\ -\frac{GJ}{L} & \frac{GJ}{L} \end{bmatrix} \begin{bmatrix} \theta_i \\ \theta_j \end{bmatrix}$		
Level II	$P = EA\varepsilon \quad T = GJ\phi \quad M = EI\kappa$		
Level I	$\begin{bmatrix} \sigma_{11} \\ \sigma_{22} \\ \sigma_{33} \\ \sqrt{2}\sigma_{23} \\ \sqrt{2}\sigma_{31} \\ \sqrt{2}\sigma_{12} \end{bmatrix} = \begin{bmatrix} E_{1111} & E_{1122} & E_{1133} & 2E_{1123} & 2E_{1131} & 2E_{1112} \\ & E_{2222} & E_{2233} & 2E_{2223} & 2E_{2231} & 2E_{2212} \\ & & E_{3333} & 2E_{3323} & 2E_{3331} & 2E_{3312} \\ & & & 2E_{2323} & 2E_{2331} & 2E_{2312} \\ & & & & 2E_{3131} & 2E_{3112} \\ & & & & & 2E_{1212} \end{bmatrix} \begin{bmatrix} \varepsilon_{11} \\ \varepsilon_{22} \\ \varepsilon_{33} \\ \sqrt{2}\varepsilon_{23} \\ \sqrt{2}\varepsilon_{31} \\ \sqrt{2}\varepsilon_{12} \end{bmatrix}$ <p style="text-align: center;"><i>sym.</i></p>		

$$\mathbf{Q} = \mathbf{K}\mathbf{q}$$

\mathbf{Q} : generalized stress

\mathbf{q} : generalized strain

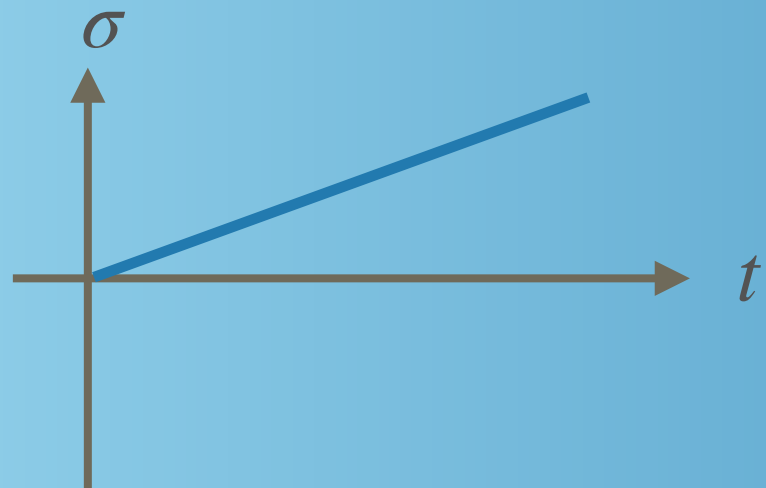
\mathbf{K} : generalized modulus

Framework of solid mechanics

	Name	Subjects	Related theory
Level IV	structure	discrete structure	Theory of structural analysis Structural dynamics
Level III	structural member solid finite element	discrete element	Theory of structural analysis Structural dynamics
Level II	mechanical member	1D or 2D continuum (beam, plate, shell etc)	Mechanics of material The theory of plate & shell
Level I	material	3D continuum	Theory of elasticity
Level -I	microstructure	unit cell representative element	Micromechanics

Evidence of plastic behavior in multi-scale mechanics

Monotonic loading tests



Monotonic loading test

Metal–nickel and copper

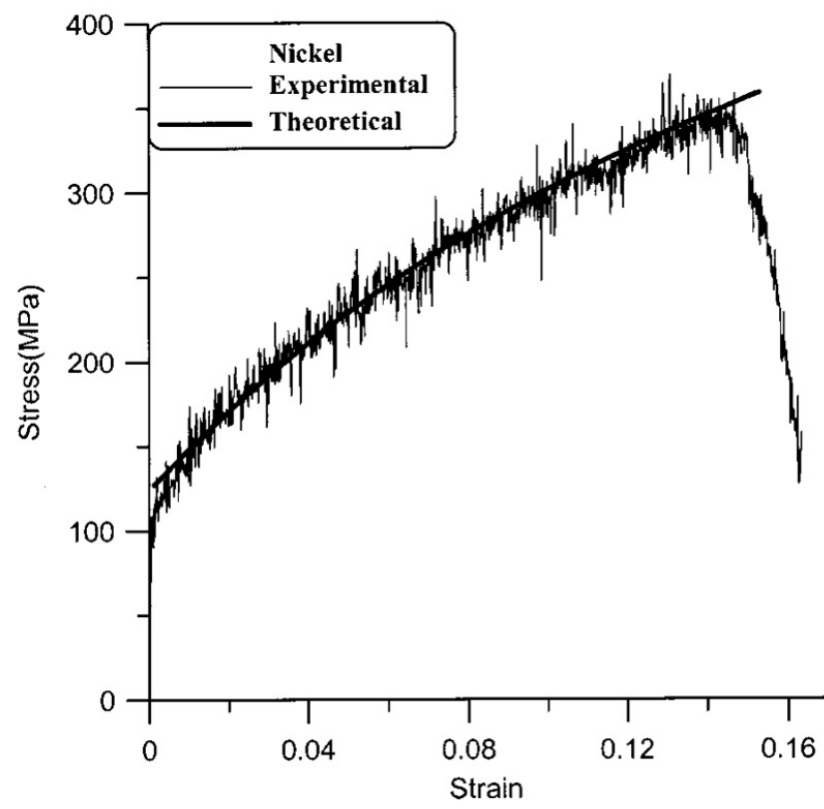


Fig. 6 Comparison of experimental macro data with theoretical simulation for the tensile stress-strain curve of nickel

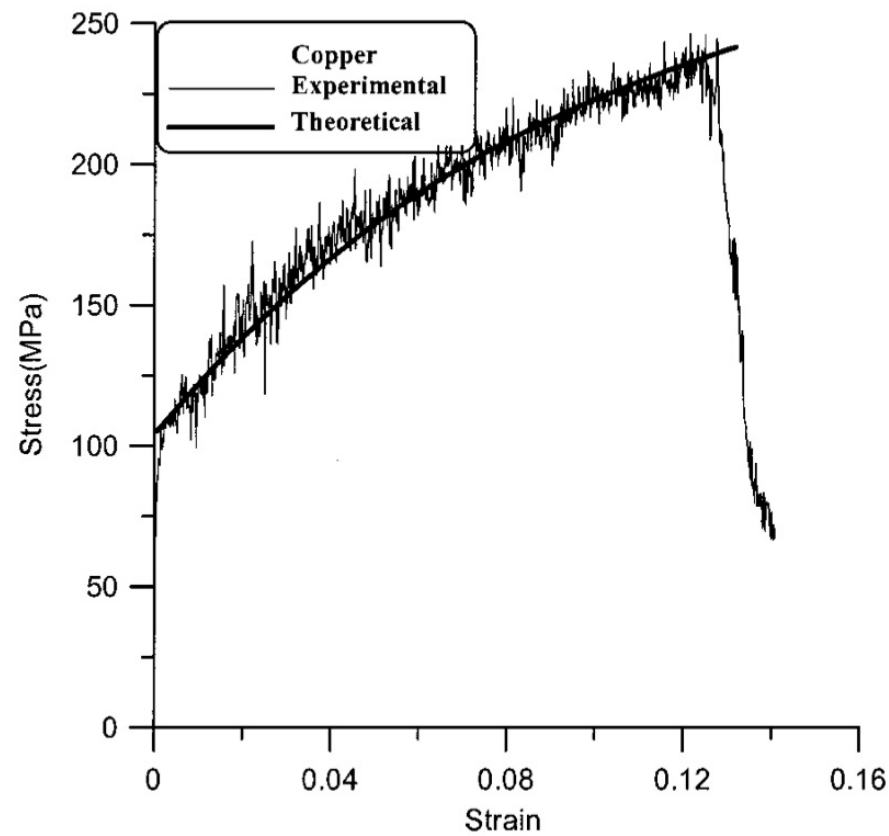
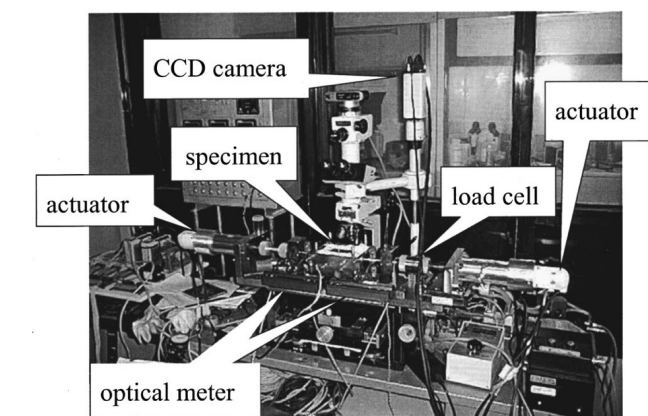
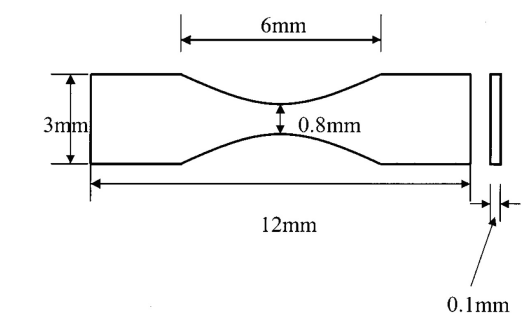
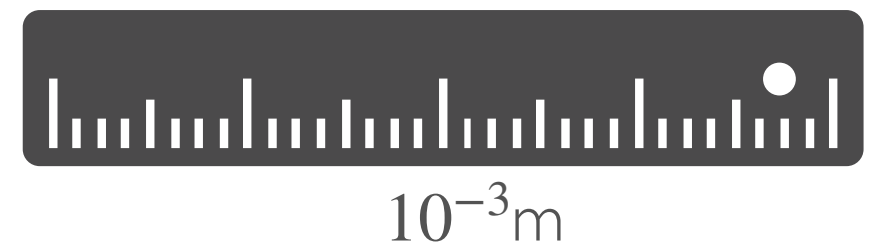


Fig. 8 Comparison of experimental macro data with theoretical simulation for the tensile stress-strain curve of copper

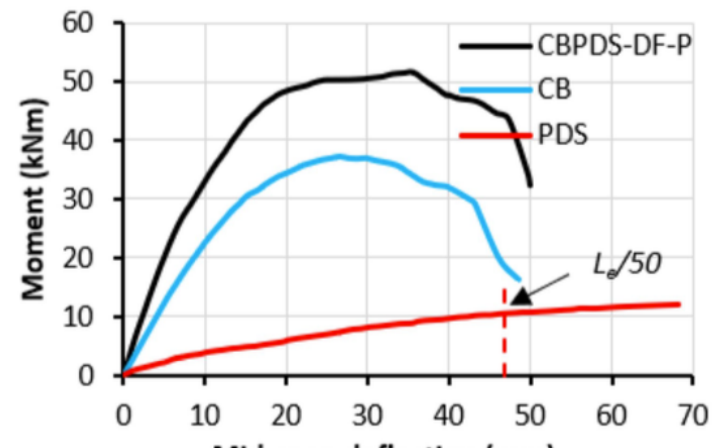


B20 @ College of Engineering building

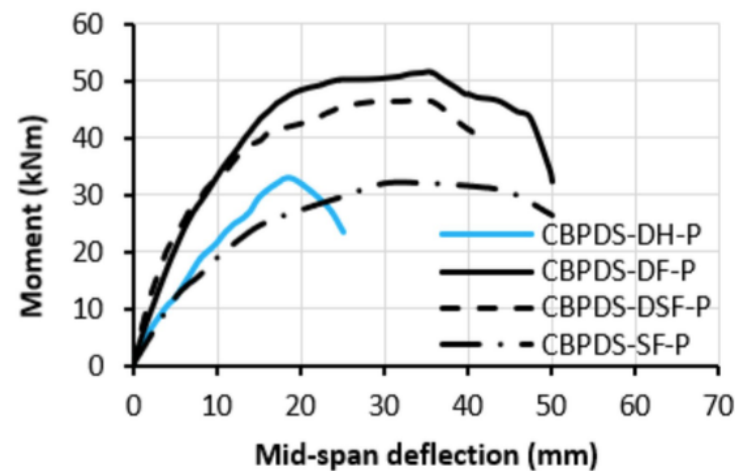
H.-K. Hong, C.-S. Liu, Y.-P. Chiao, B.-C. Shih, Planar double-slip model for polycrystal plasticity and micro tension tests of pure nickel and copper, ASME Journal of Engineering Materials and Technology, Vol. 124, pp. 314-321, 2002.

Monotonic loading test

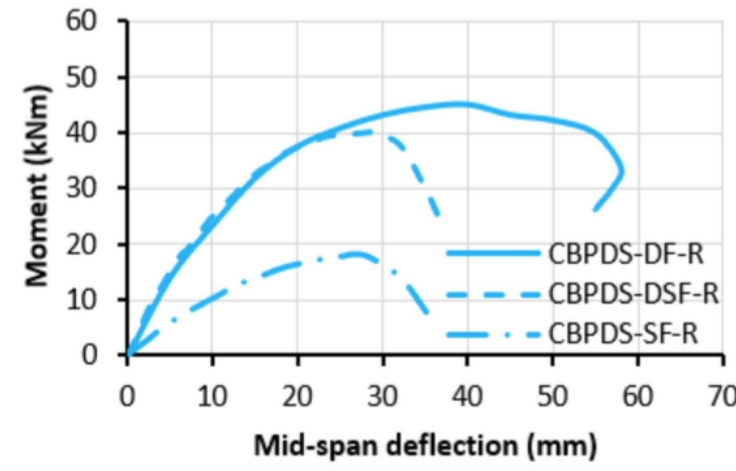
Slab composite



(a) Control specimens



(b) Specimens with parallel PSS

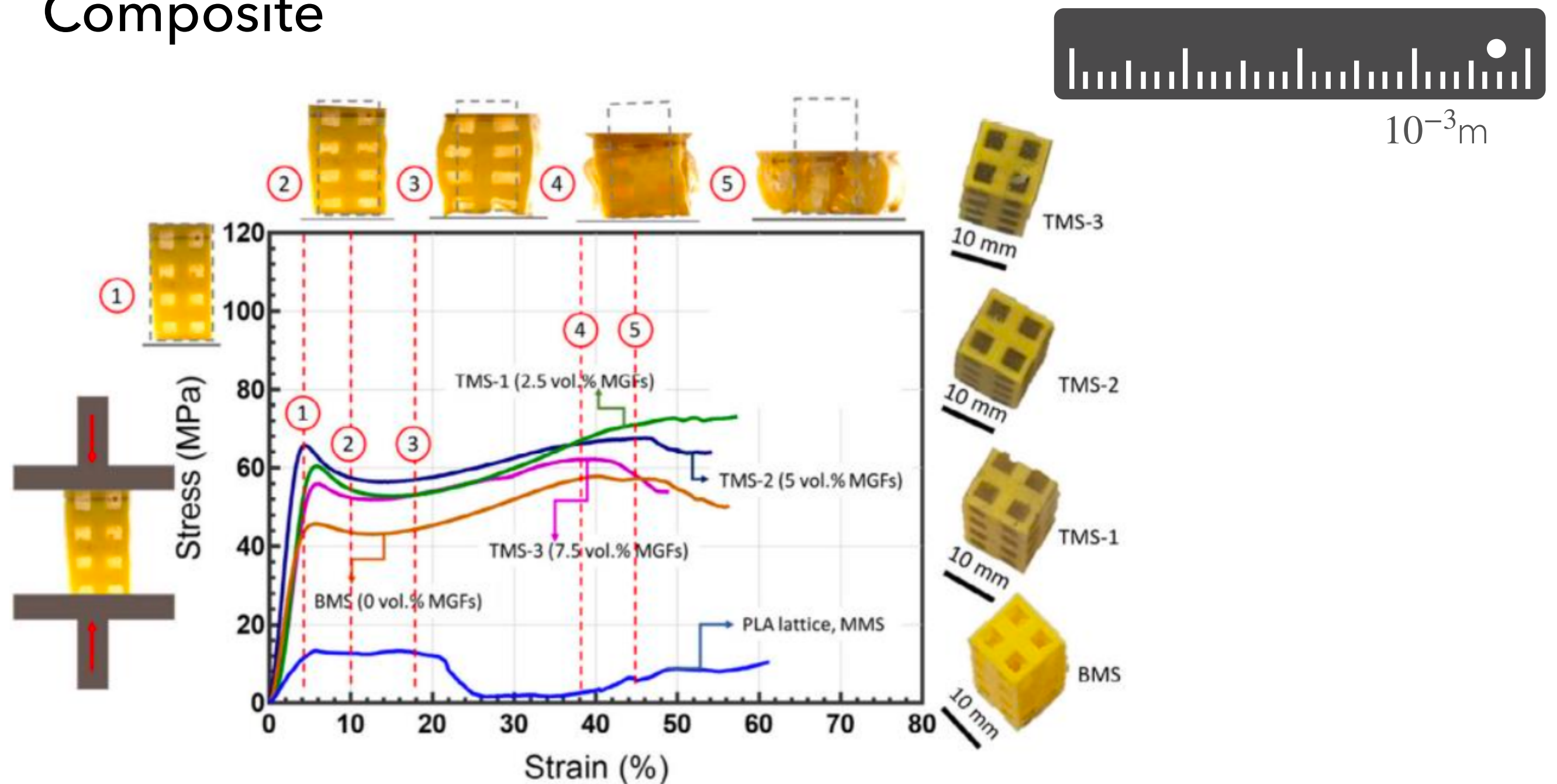


(c) Specimens with perpendicular PSS



Monotonic loading test

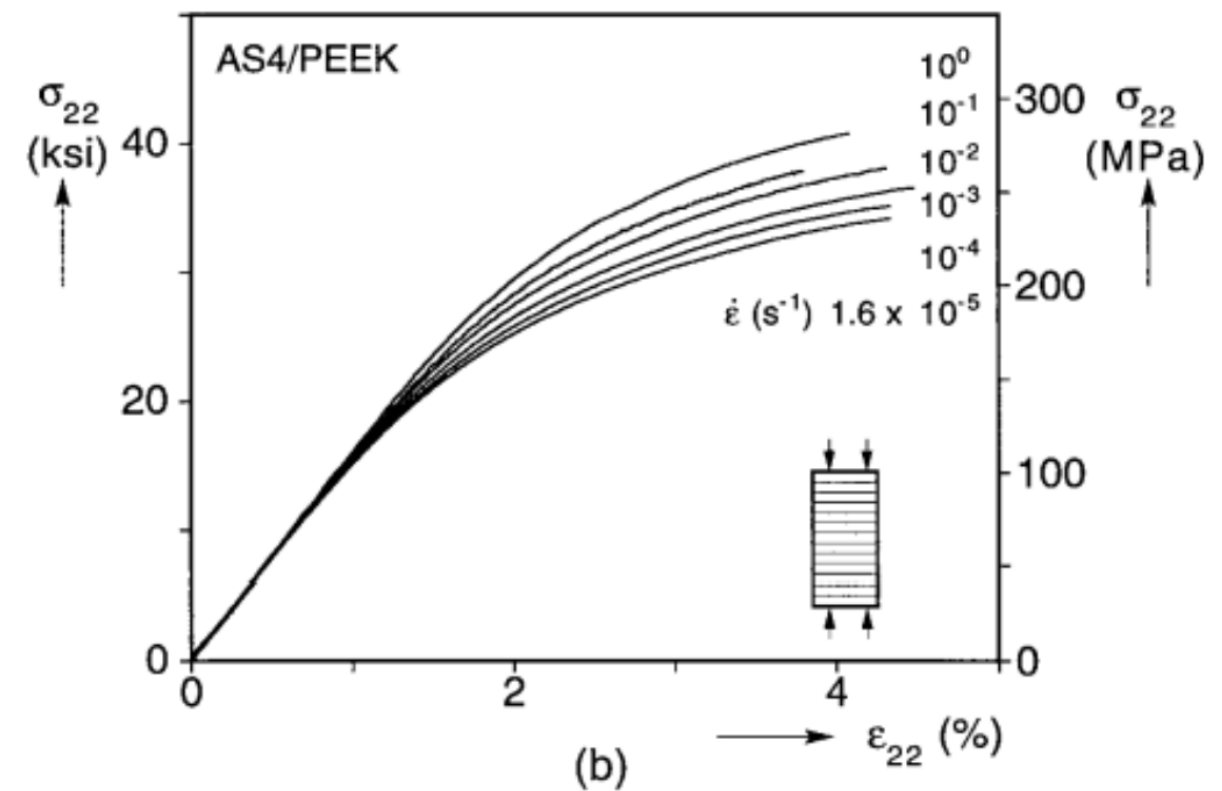
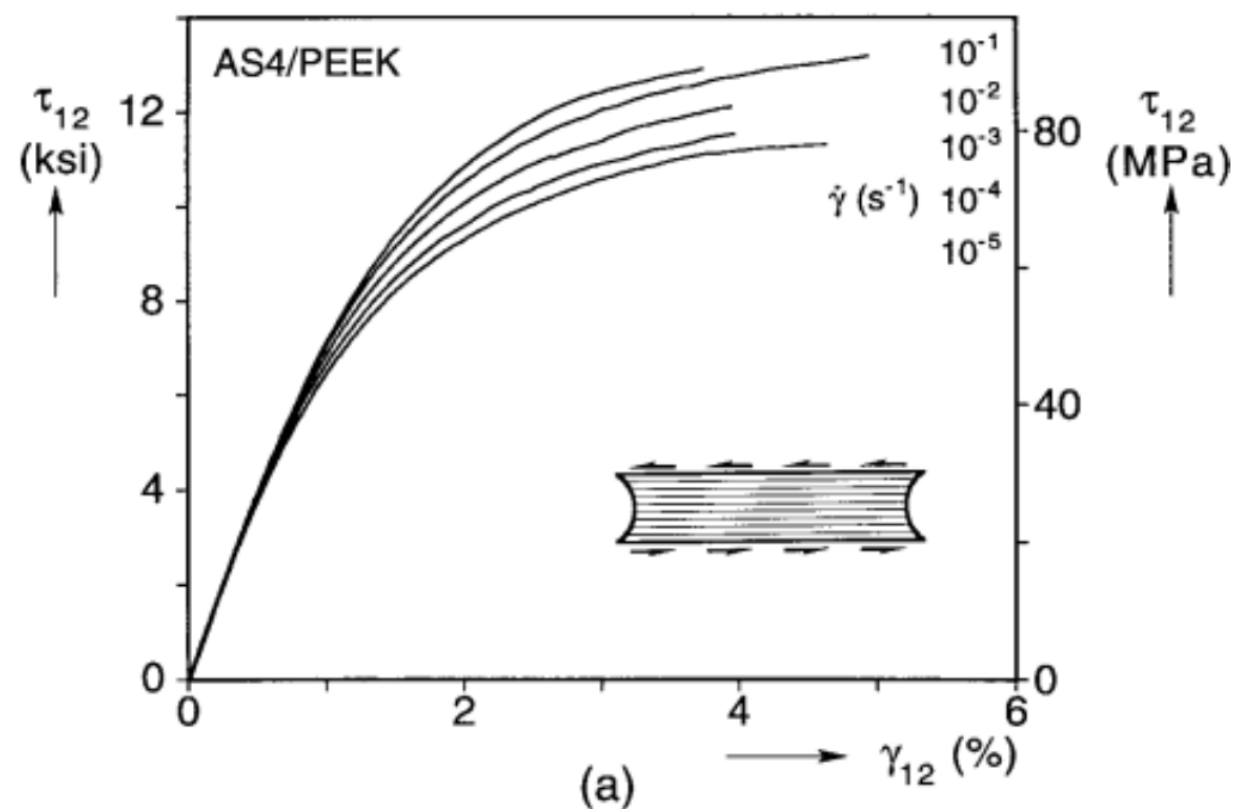
Composite



X. H. Vu, Y. Malécot, L. Daudeville, E. Buzaud, Experimental analysis of concrete behavior under high confinement: effect of the saturation ratio, International Journal of Solids and Structures, Vol. 46, pp. 1105-1120, 2009.

Monotonic loading test

PEEK polymer (polyetheretherketone)



T. J. Vogler & S. Kyriakides, Inelastic behavior of an AS4/PEEK composite under combined transverse compression and shear. Part I: experiments, Vol. 5, pp. 783-806, 1999.

Monotonic loading test

Polymer

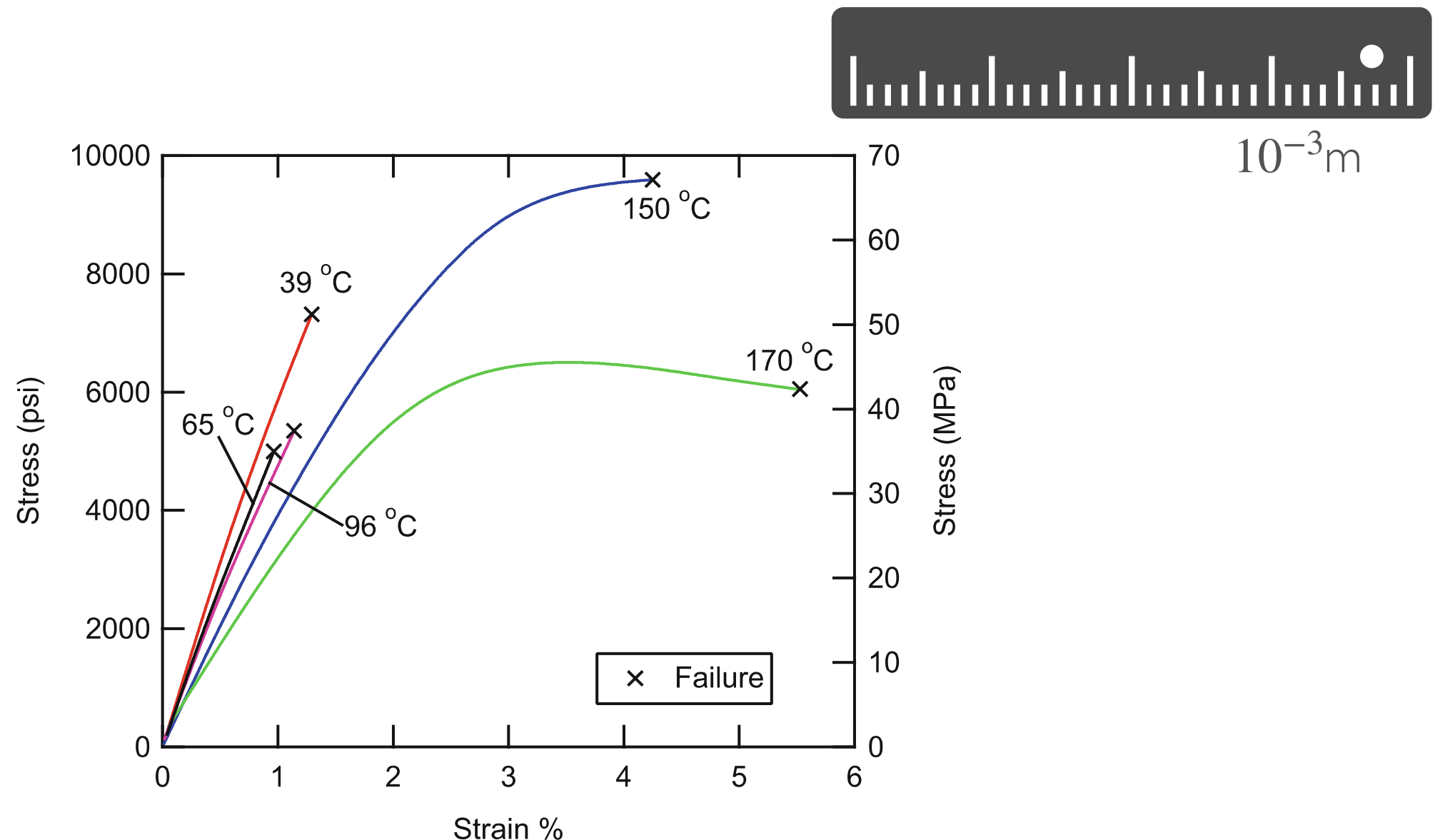
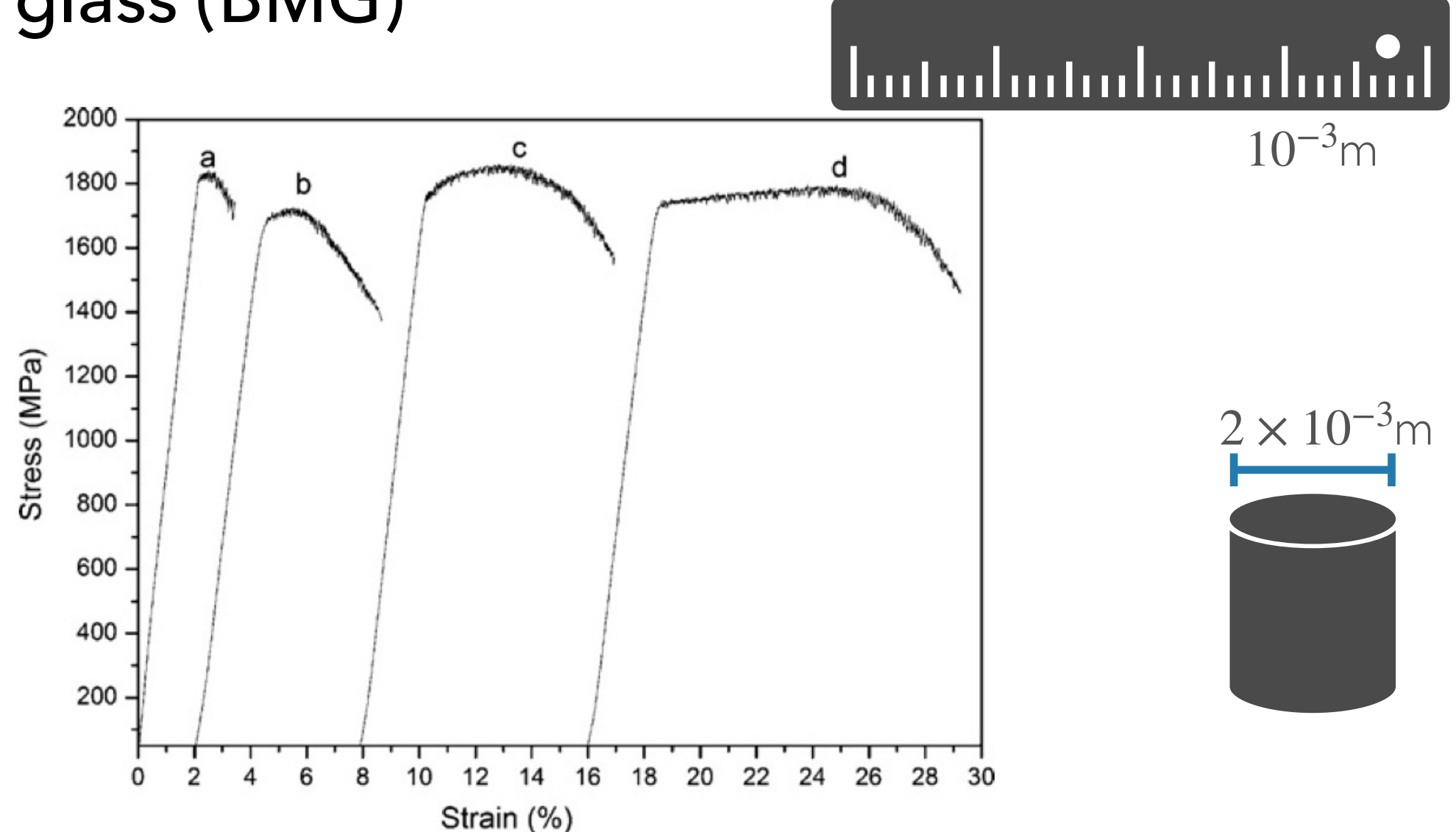


Fig. 3.10 Temperature dependent stress-strain response of a typical brittle epoxy (Data from Hiel et al. 1983)

H. F. Brinson & L. C. Brinson, Polymer Engineering Science and Viscoelasticity, Springer, New York, 2015.

Monotonic loading test

Bulk metallic glass (BMG)



The uniaxial compressive stress-strain curves of different samples: (a) As-cast; (b) Cu coated; (c) Ni coated; and (d) Cu/Ni coated.

W. Chen, K. C. Chan, S. H. Chen, S. F. Guo, W. H. Li, G. Wang, Plasticity enhancement of a Zr-based bulk metallic glass by an electroplated Cu/Ni bilayered coating, Material Science and Engineering A, Vol. 552, pp. 199-203, 2012.

Monotonic loading test

Concrete

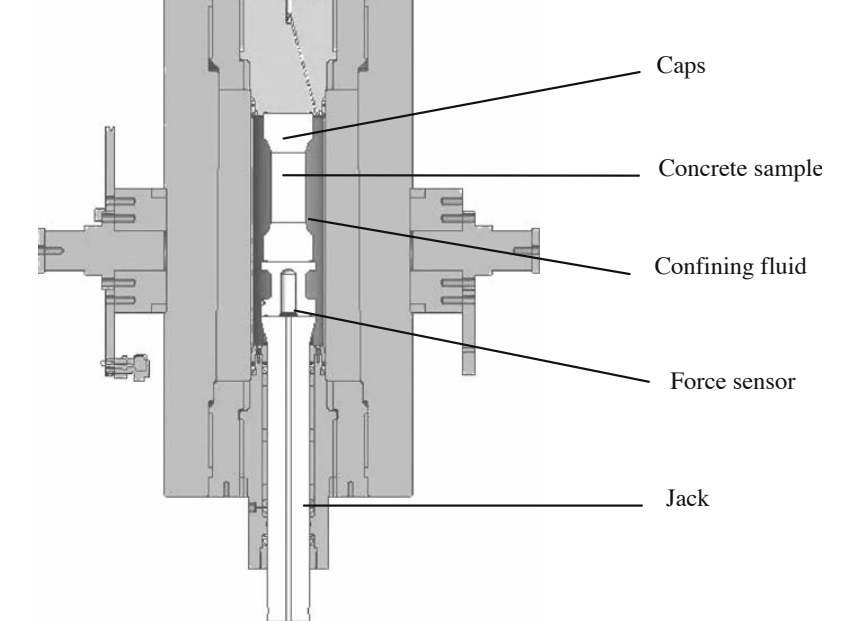
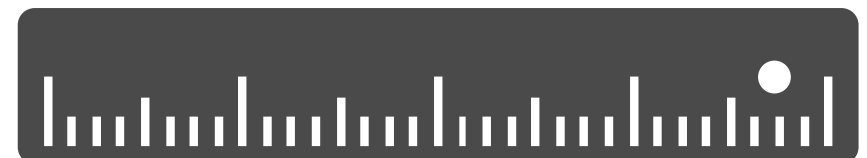
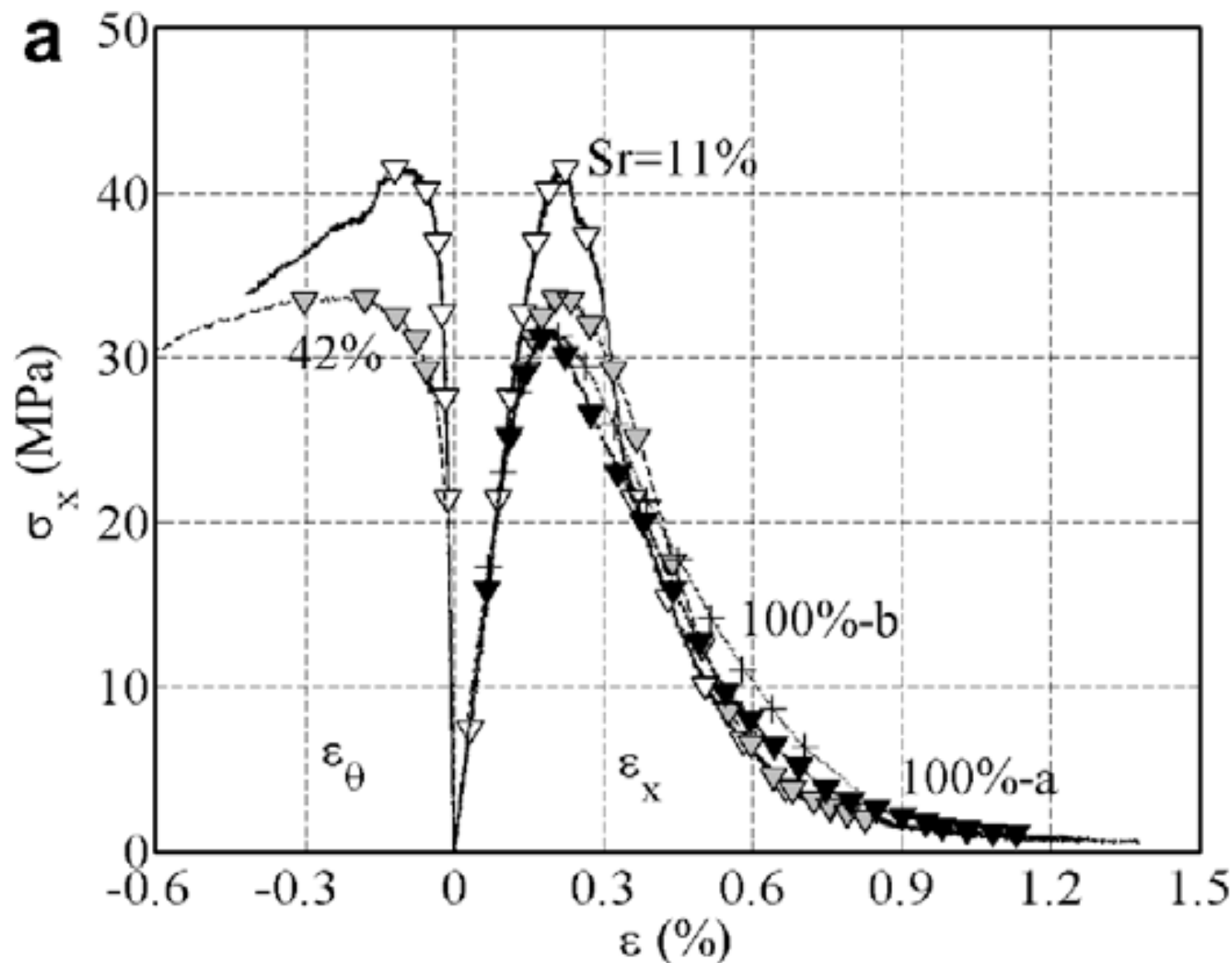


Fig. 2. Cross-section view of the confinement cell.

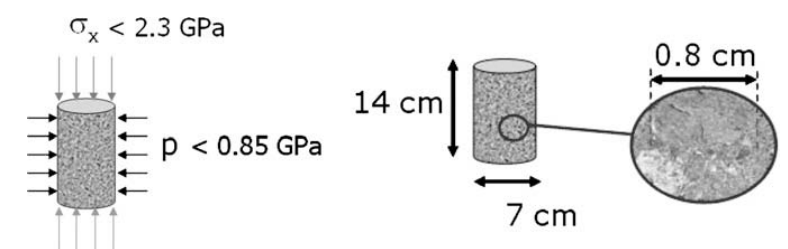
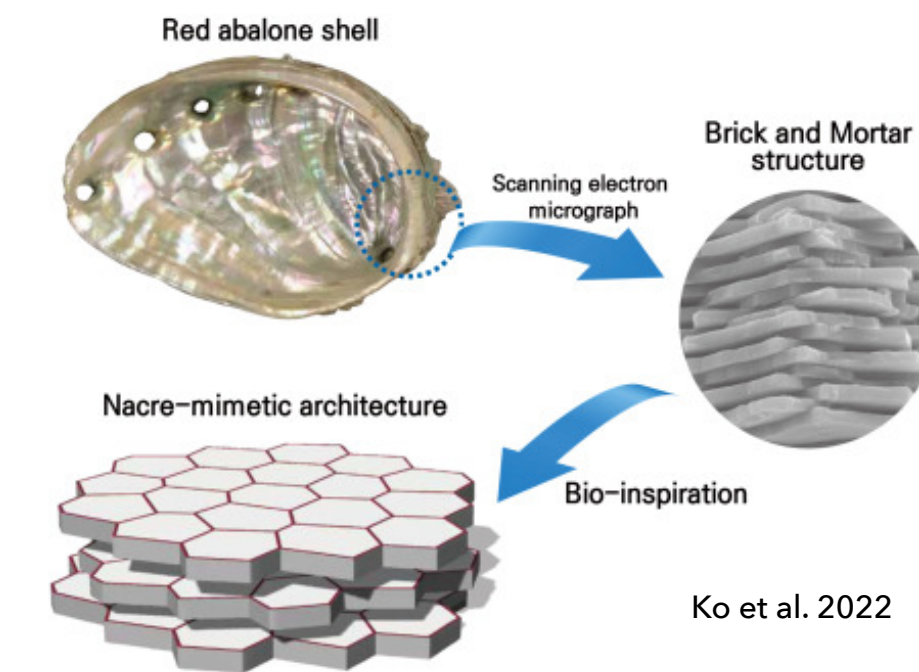


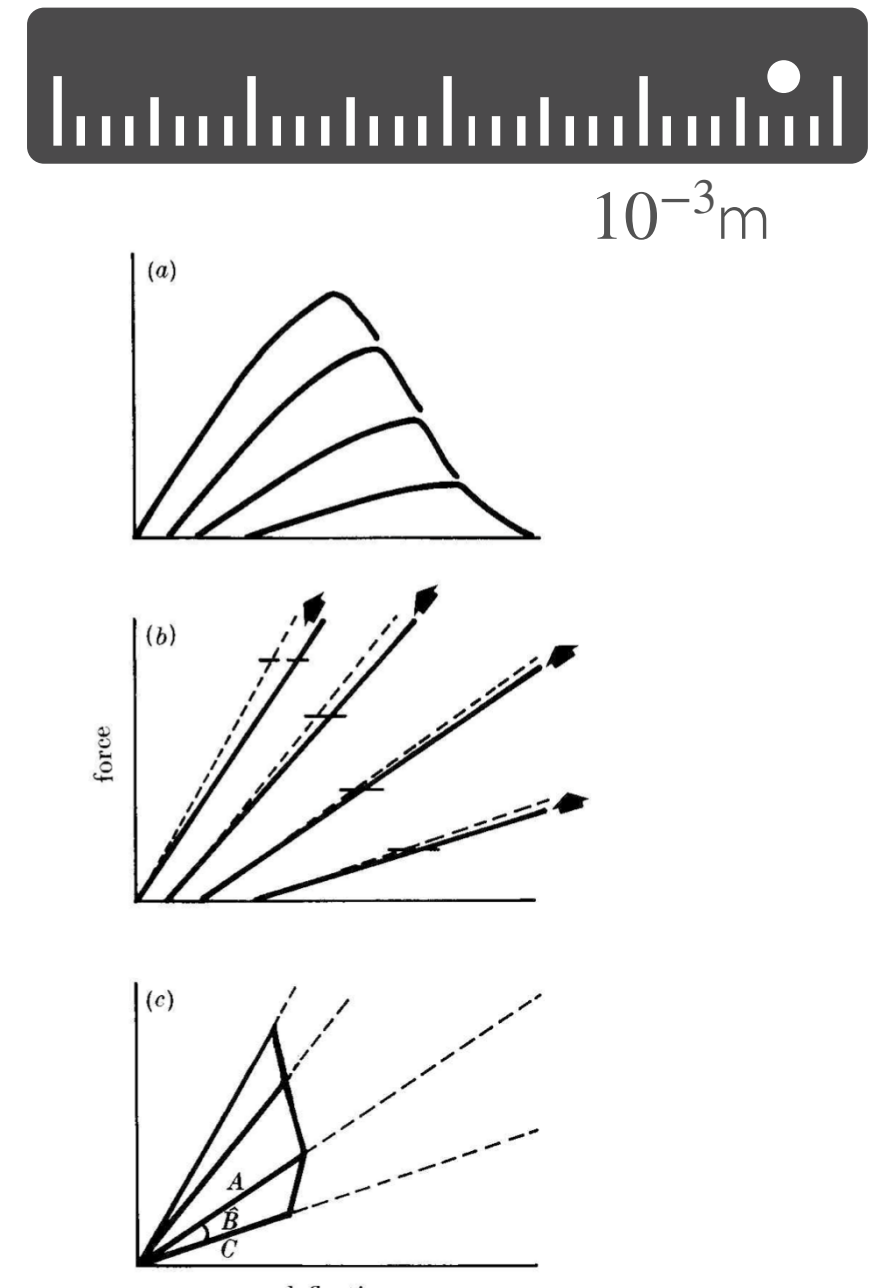
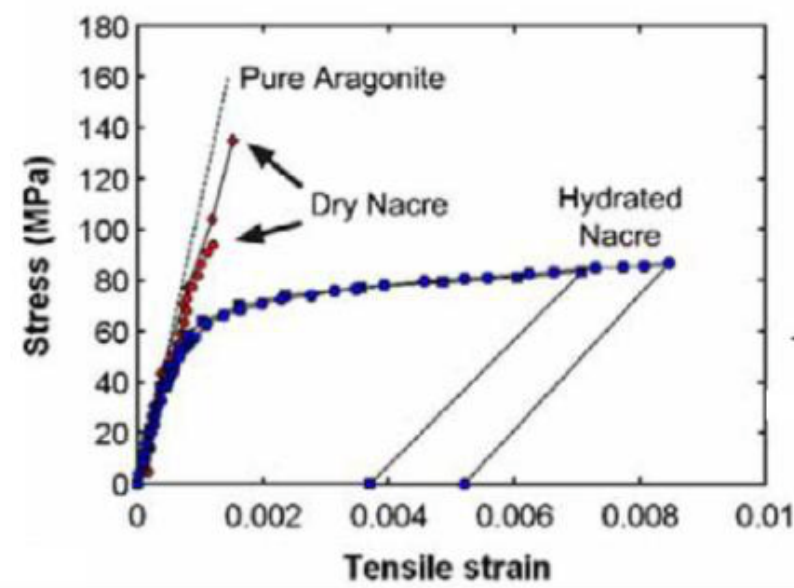
Fig. 3. Maximum press capacity and associated sample sizes of the triaxial cell.

X. H. Vu, Y. Malécot, L. Daudeville, E. Buzaud, Experimental analysis of concrete behavior under high confinement: effect of the saturation ratio, International Journal of Solids and Structures, Vol. 46, pp. 1105-1120, 2009.

Post-yield behavior of nacre



Ko et al. 2022



Jackson et al. 1988

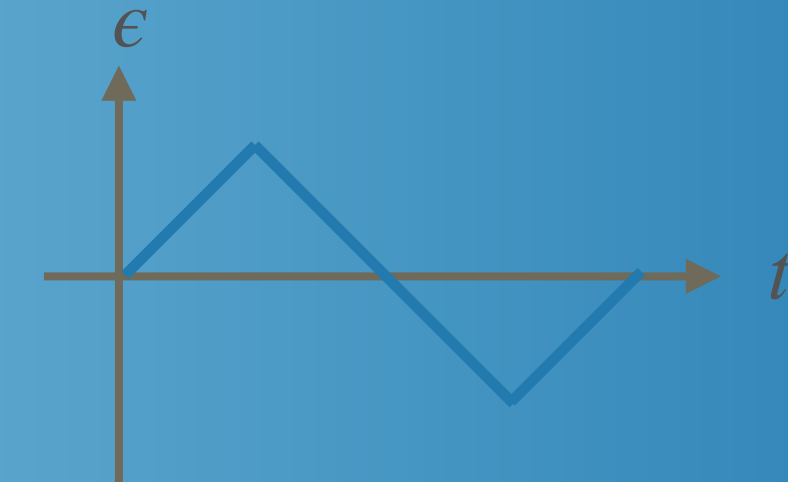
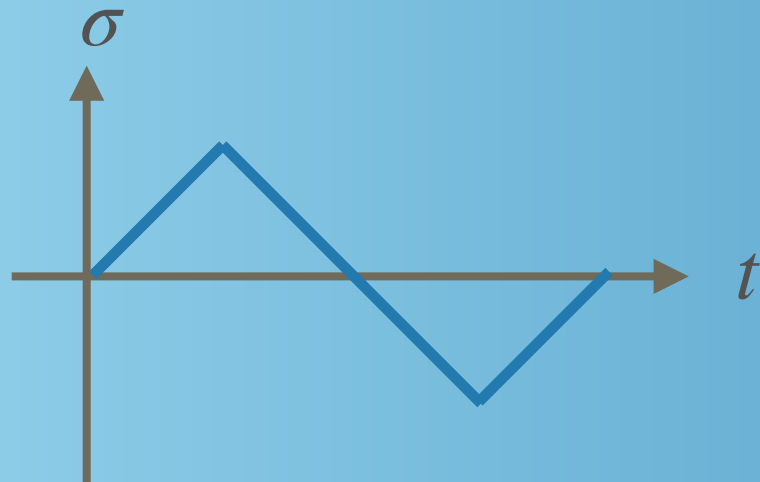
KO, Kwonhwan, et al. Investigation on the impact resistance of 3D printed nacre-like composites. *Thin-Walled Structures*, 2022, 177: 109392.

JACKSON, A. P.; VINCENT, Julian FV; TURNER, R. M. The mechanical design of nacre. *Proceedings of the Royal society of London. Series B. Biological sciences*, 1988, 234.1277: 415-440.

Evidence of plastic behavior in multi-scale mechanics

Uniaxial tests

(loading-unloading & cyclic loading tests)



Loading-unloading loading test

Laminated elastomeric bearing

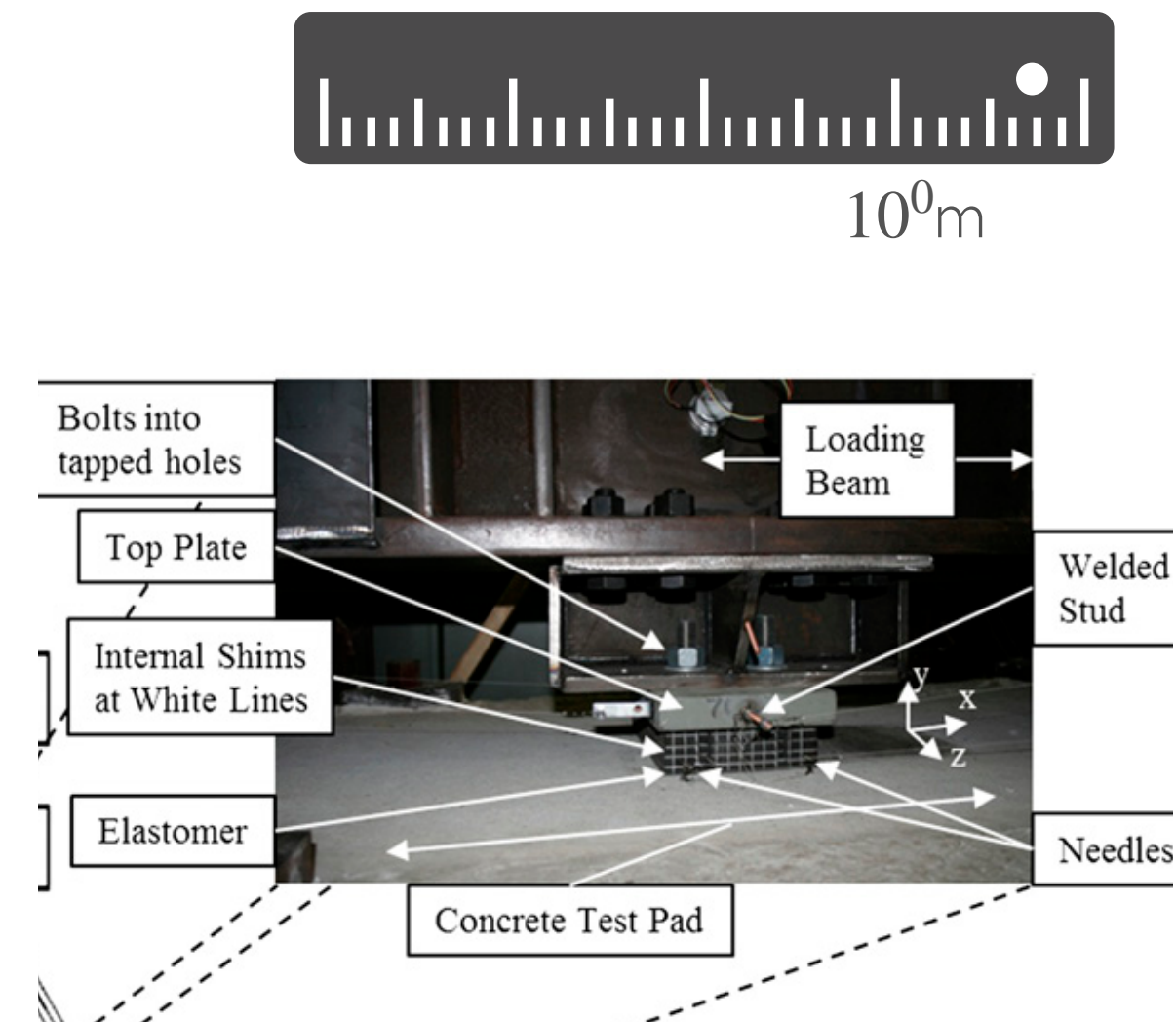
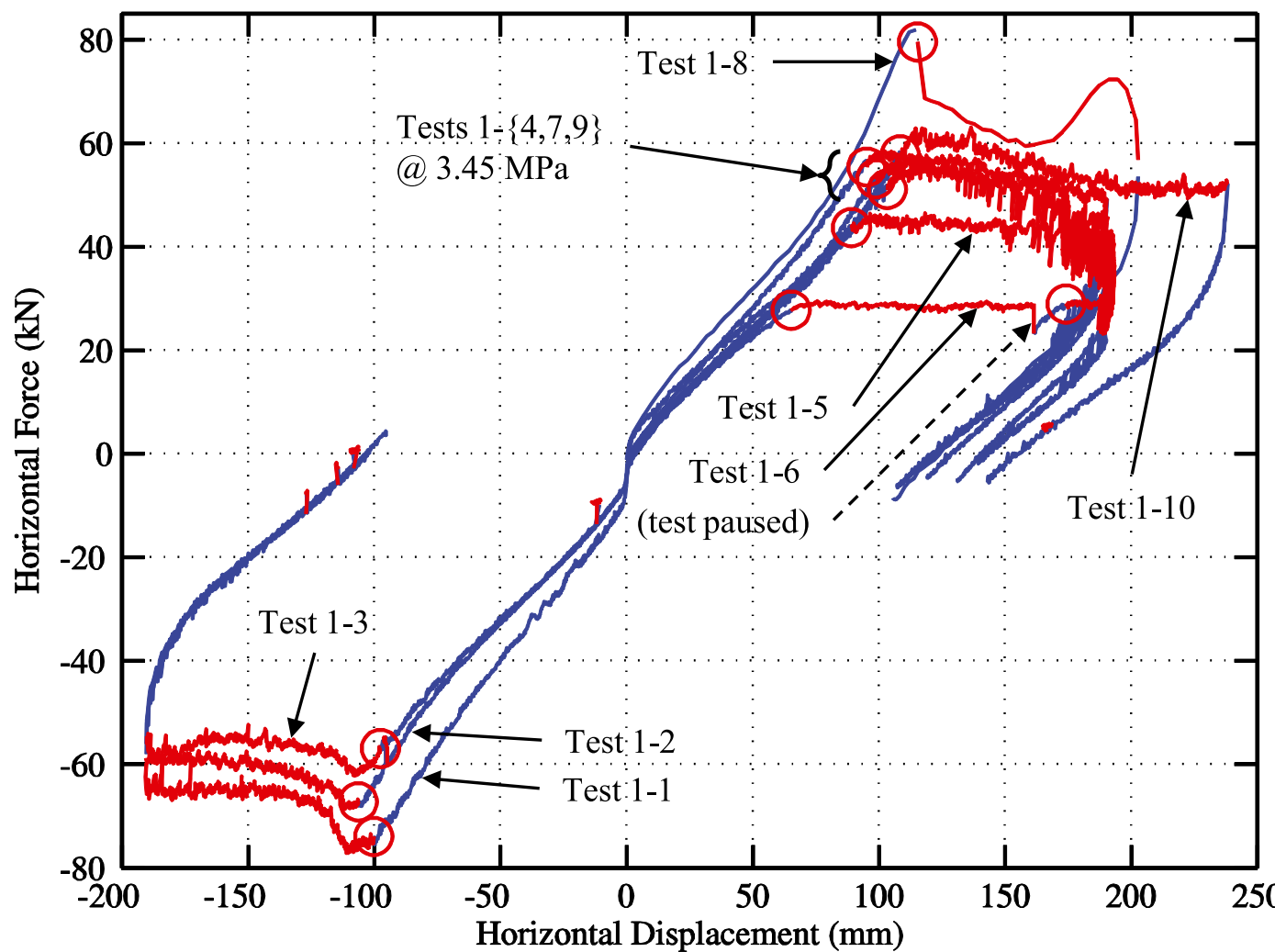
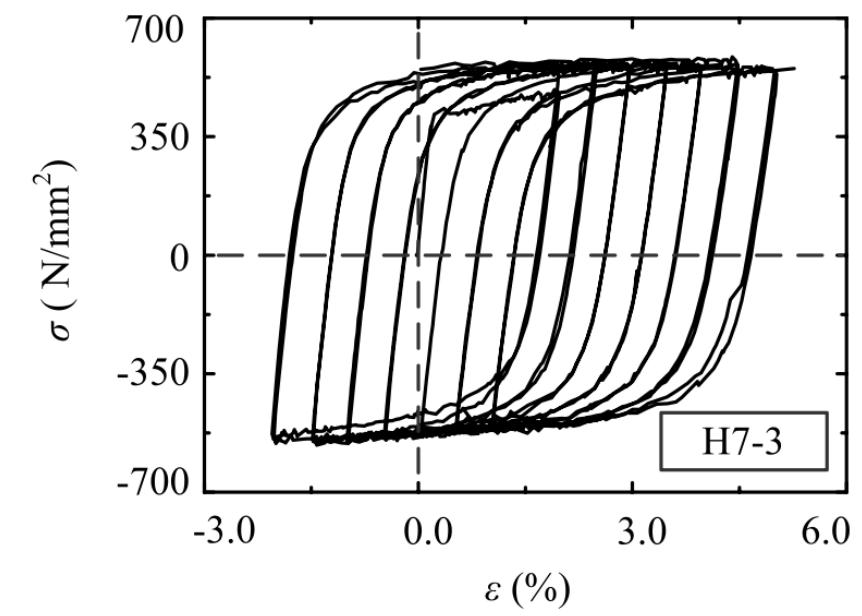
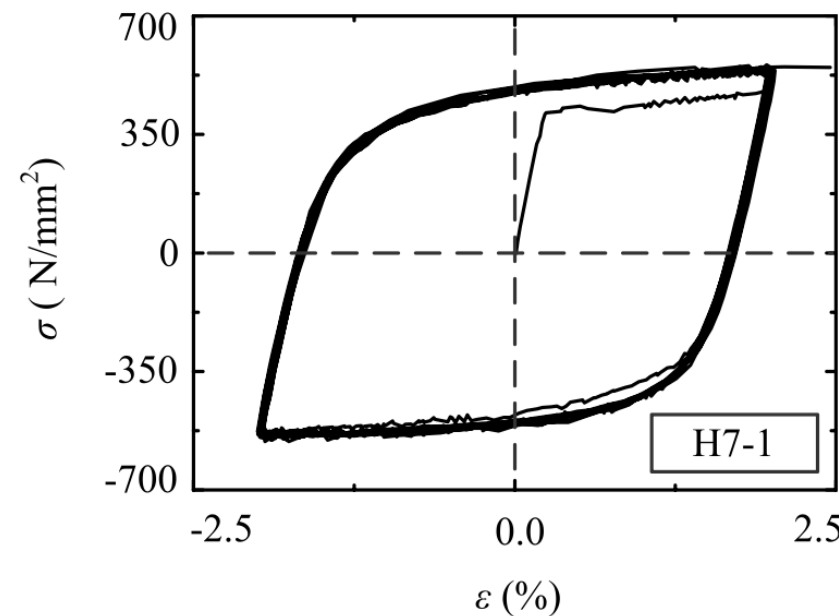
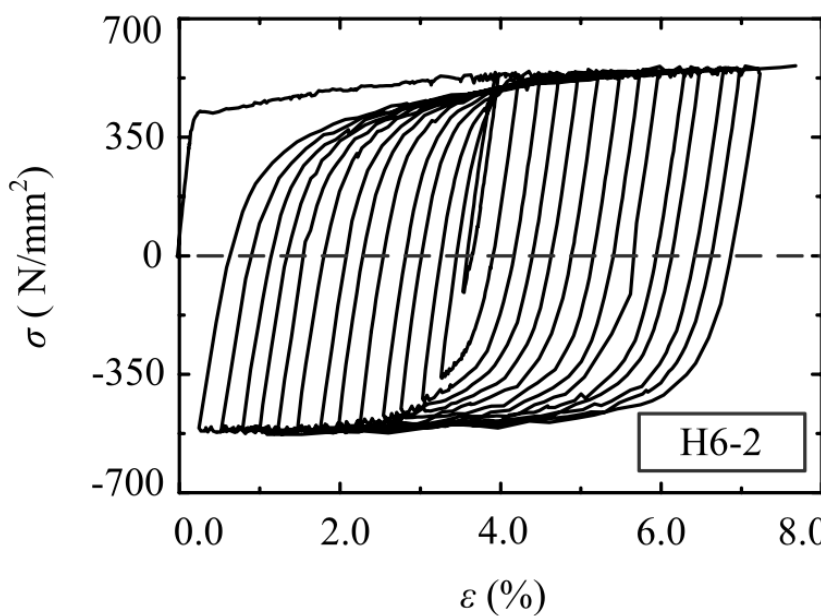


Fig. 4. Specimen 1 force versus displacement

X. H. Vu, Y. Malecot, L. Daudeville, E. Buzaud, Experimental analysis of concrete behavior under high confinement: effect of the saturation ratio, International Journal of Solids and Structures, Vol. 46, pp. 1105-1120, 2009.

Loading-unloading loading test

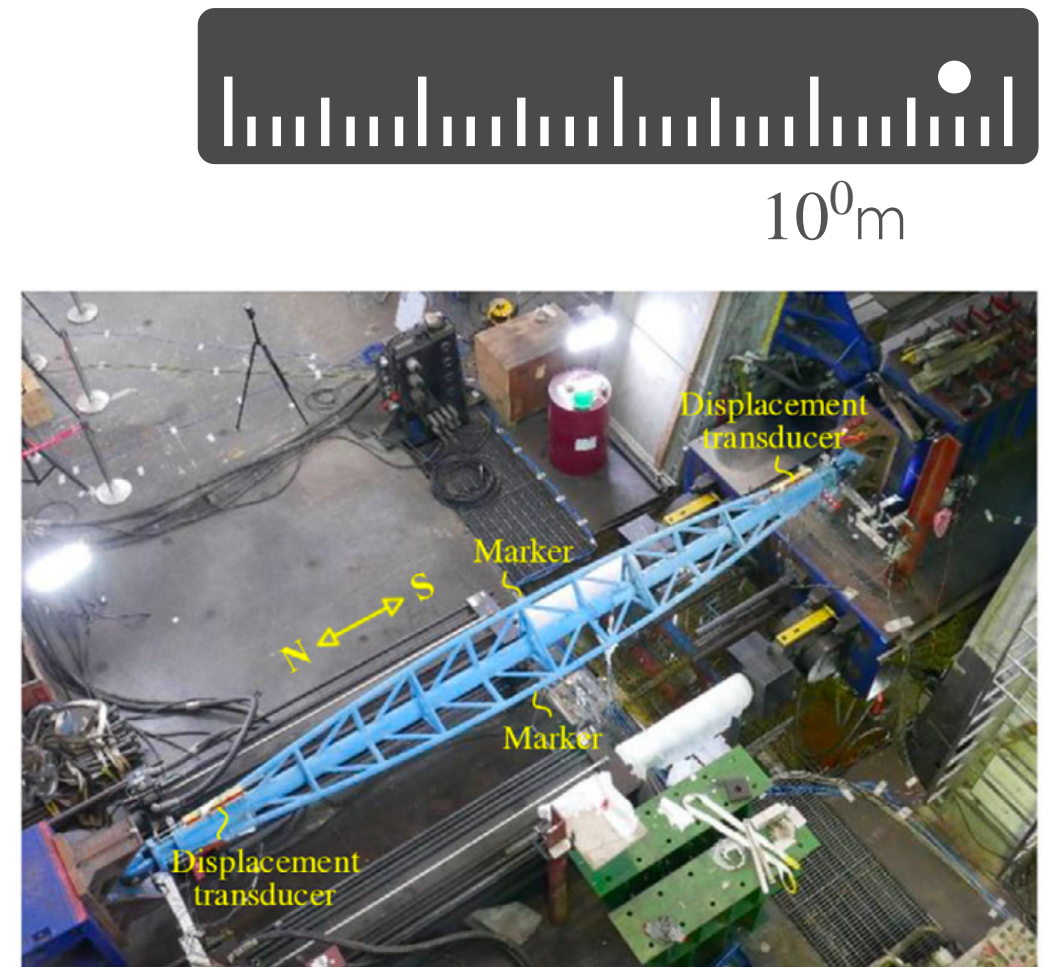
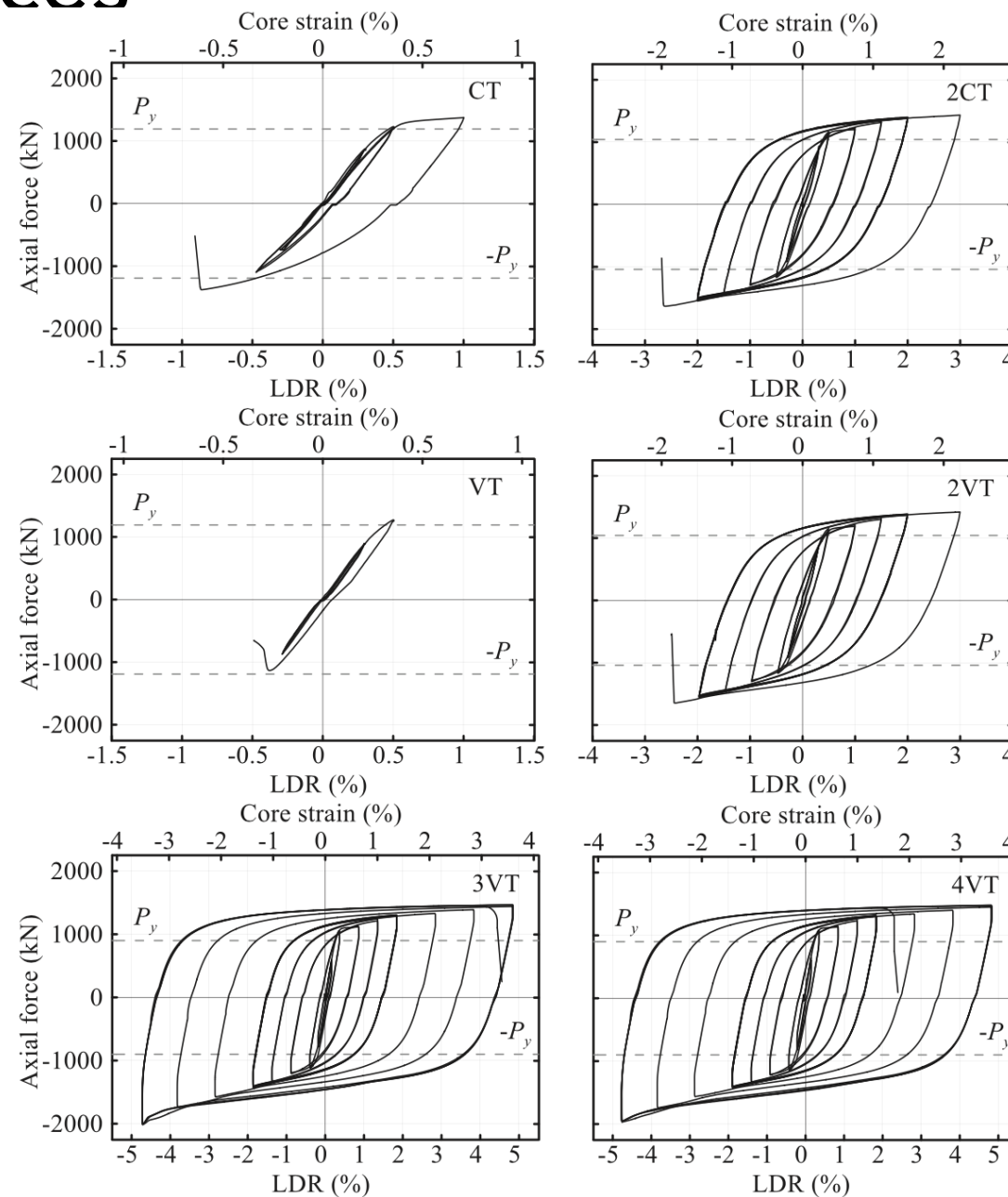
Structural steel



Shi Yongjiu, Wang Meng, & Wang Yuanqing, Experimental and constitutive model study of structural steel under cyclic loading, Journal of Constructional Steel Research, Vol. 67, pp. 1185-1197, 2011.

Loading-unloading loading test

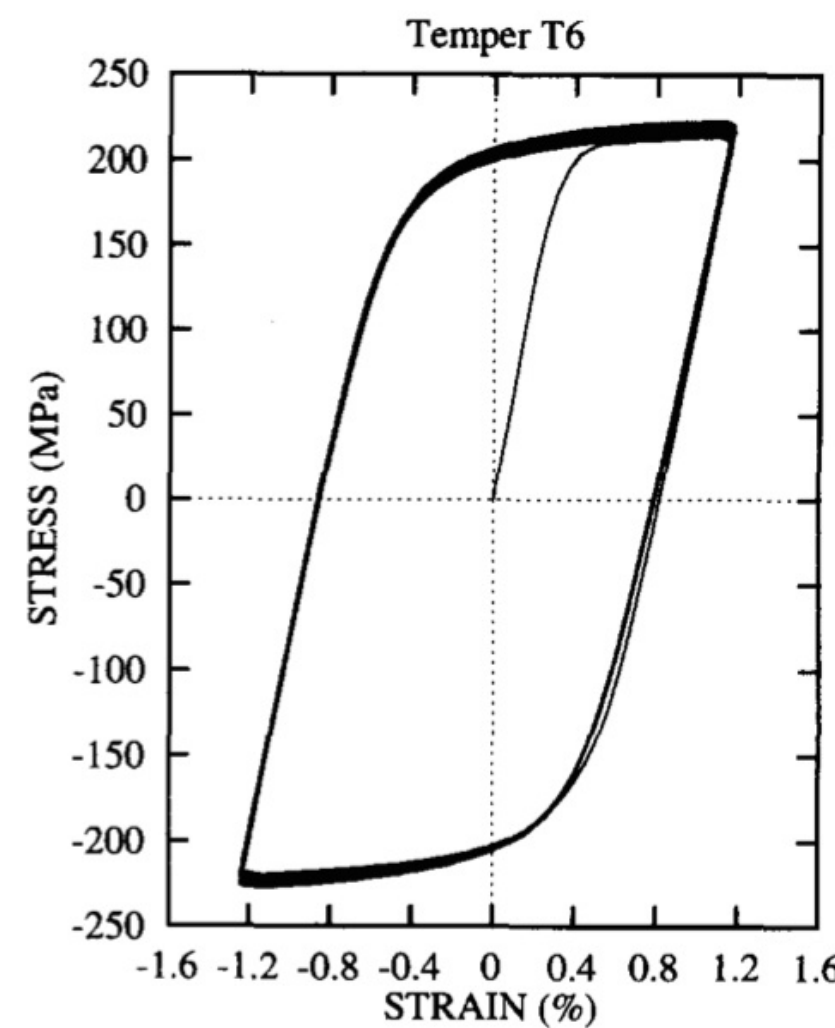
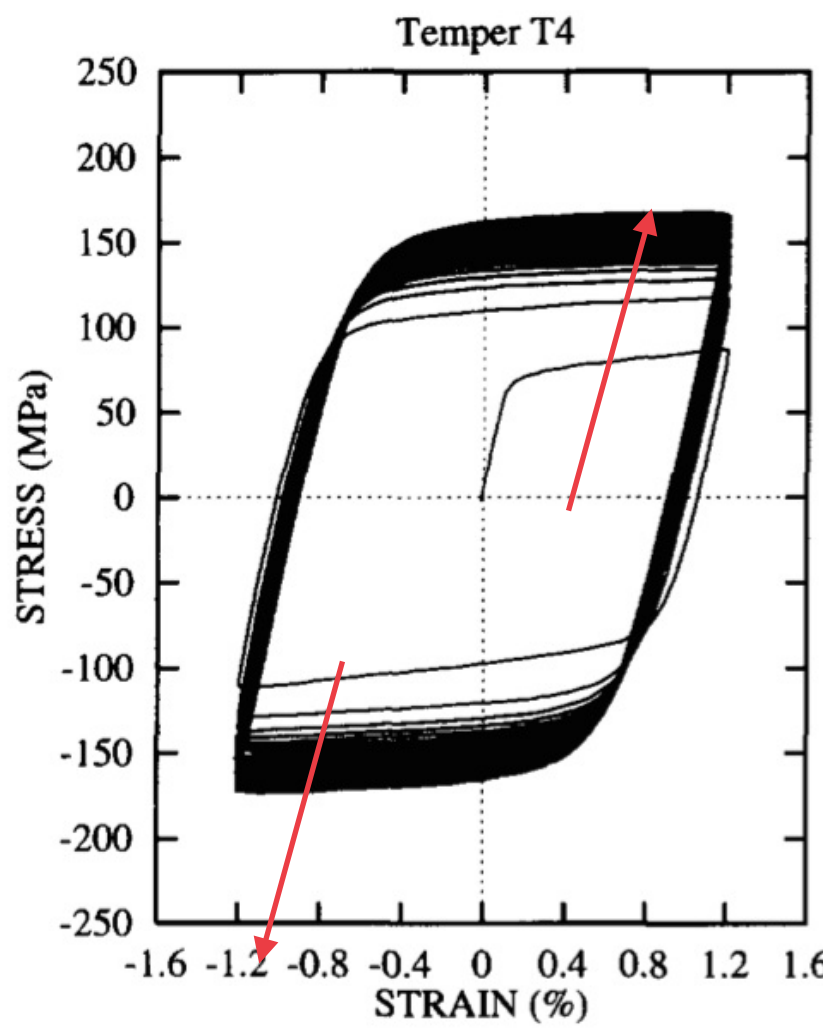
Braces



An-Chien Wu, Keh-Chyuan Tsai, Chun Chen, Lu-An Chen, & Yu-Cheng Lin, Experimental behavior of truss-confined buckling-restrained braces, Earthquake Engineering & Structural Dynamics, Vol. 52, pp. 624– 640, 2023.

Cyclic loading test

Aluminium alloy (Al6060)

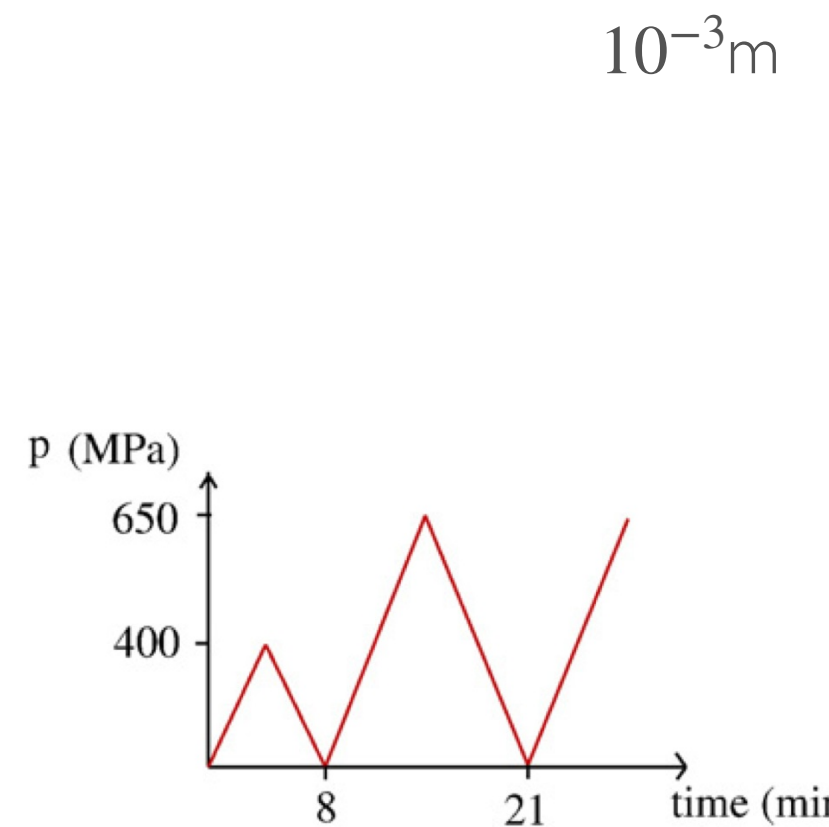
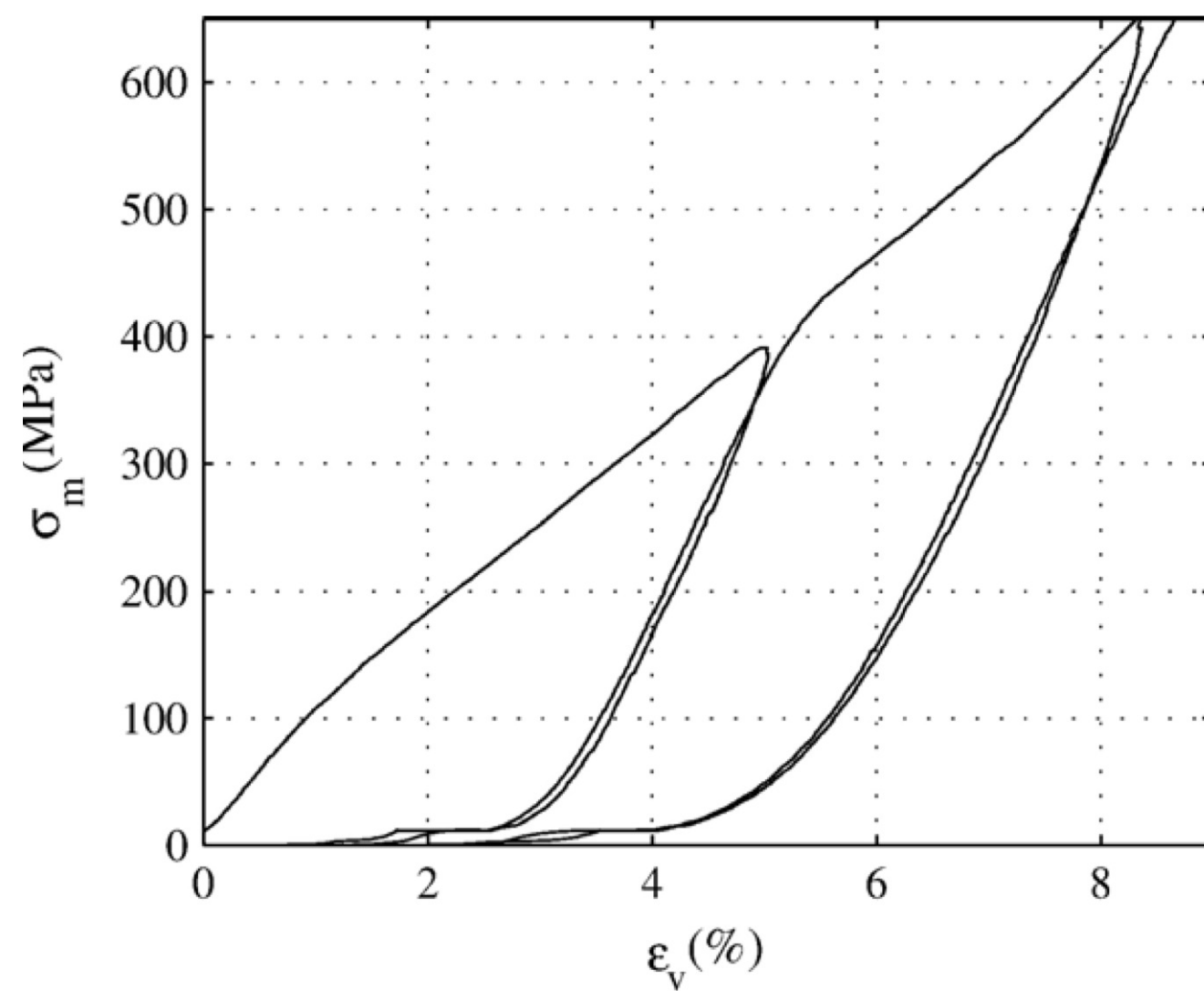


Constant strain amplitude tests for temper T4 (left) and temper T6 (right) at strain amplitude level 1.2%.

O. S. Hopperstad and M. Langseth, S. Remseth, Cyclic stress-strain behaviour of alloy AA6060, part I: Uniaxial experiments and modelling, International Journal of Plasticity, Vol. 11, pp. 725-739, 1995.

Cyclic loading test

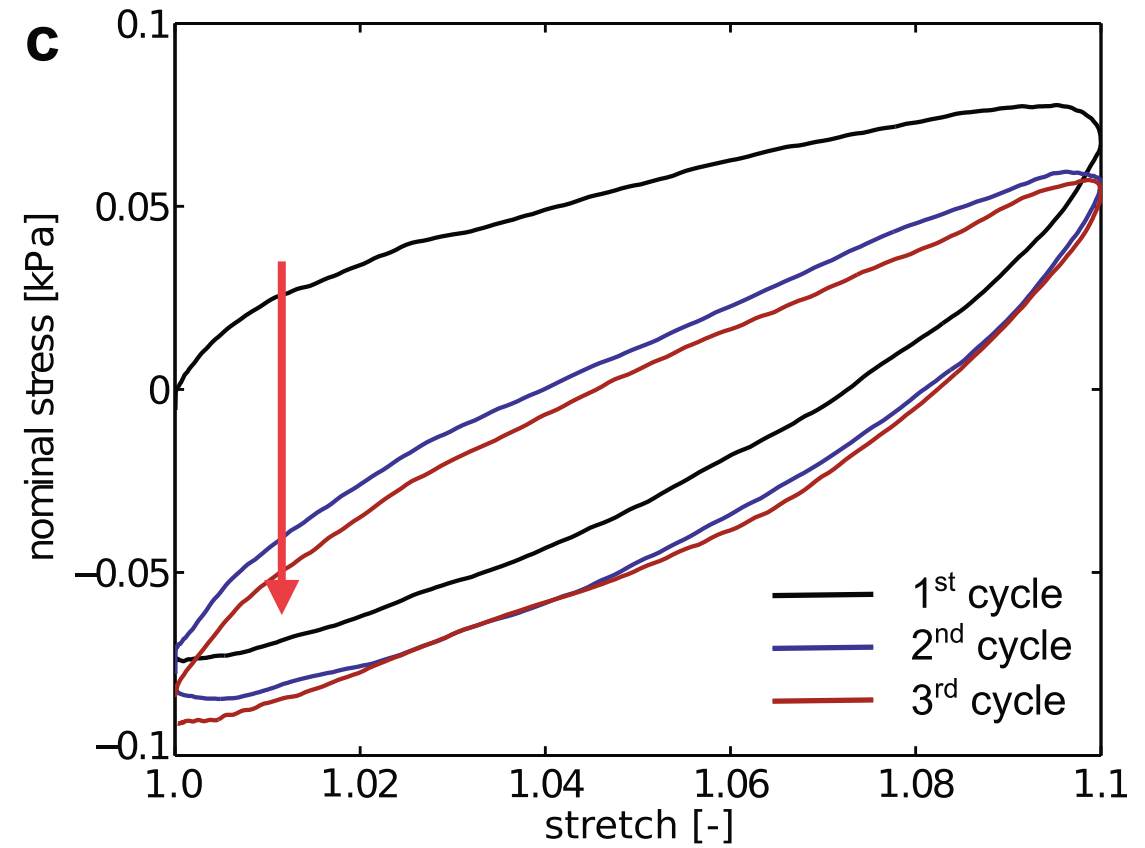
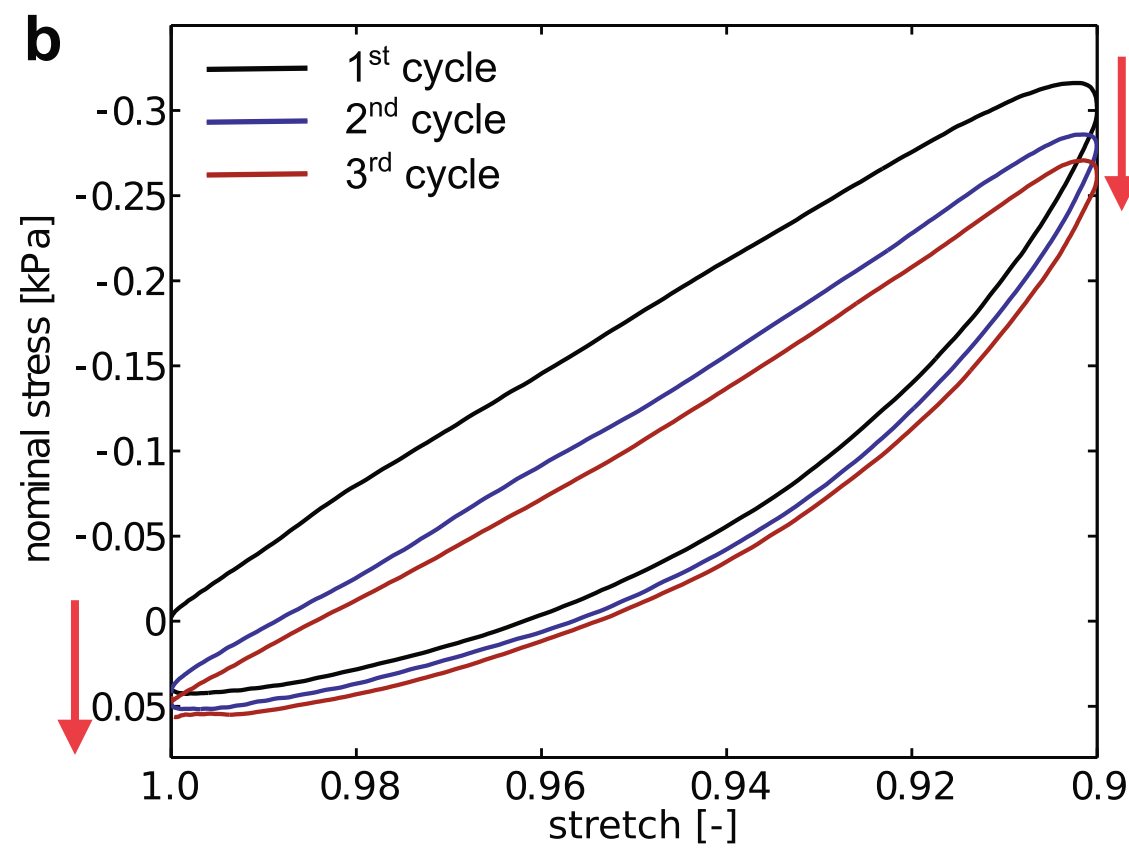
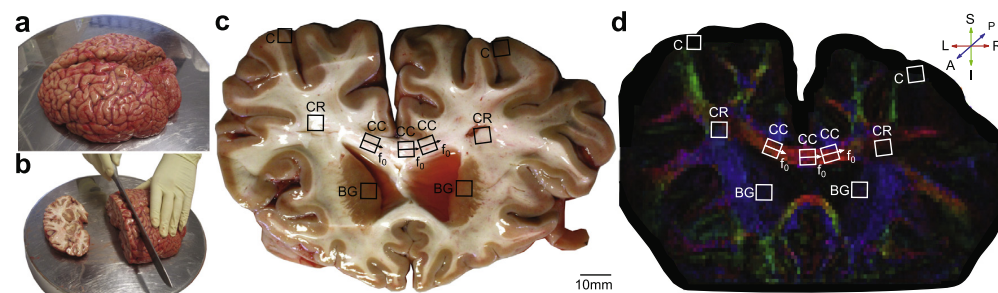
Concrete



T. Gabet, Y. Malécot, L. Daudeville, Triaxial behaviour of concrete under high stresses: Influence of the loading path on compaction and limit states, Cement and Concrete Research, Vol. 38, pp. 403-412, 2008.

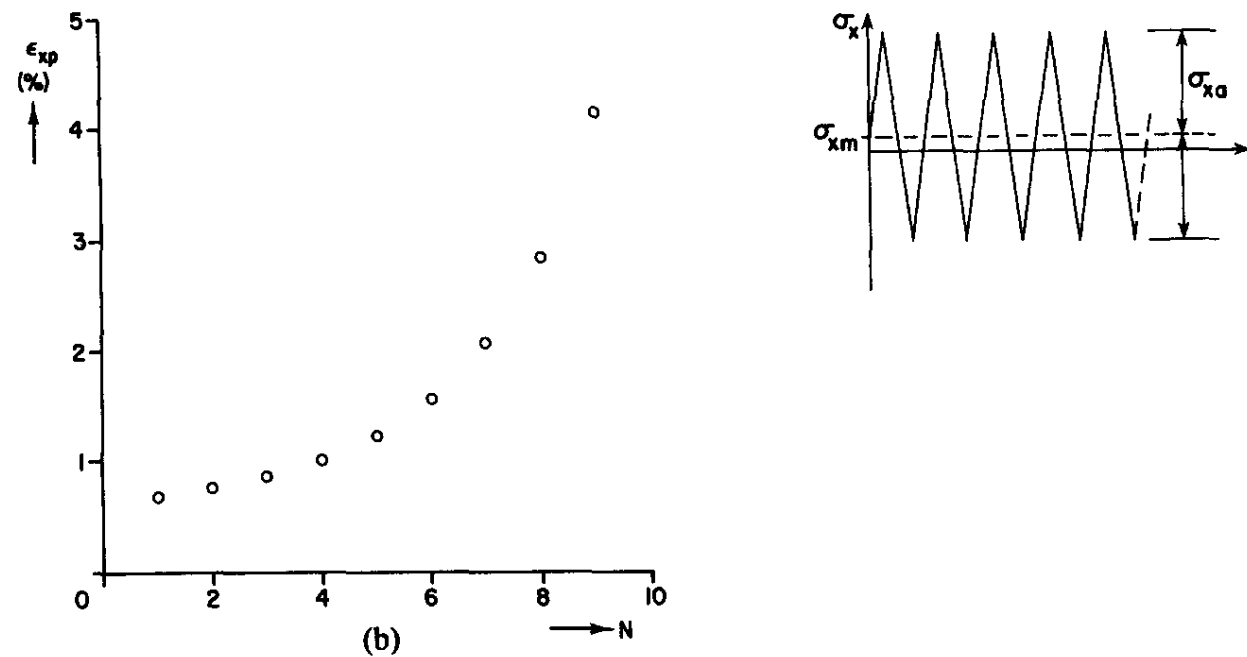
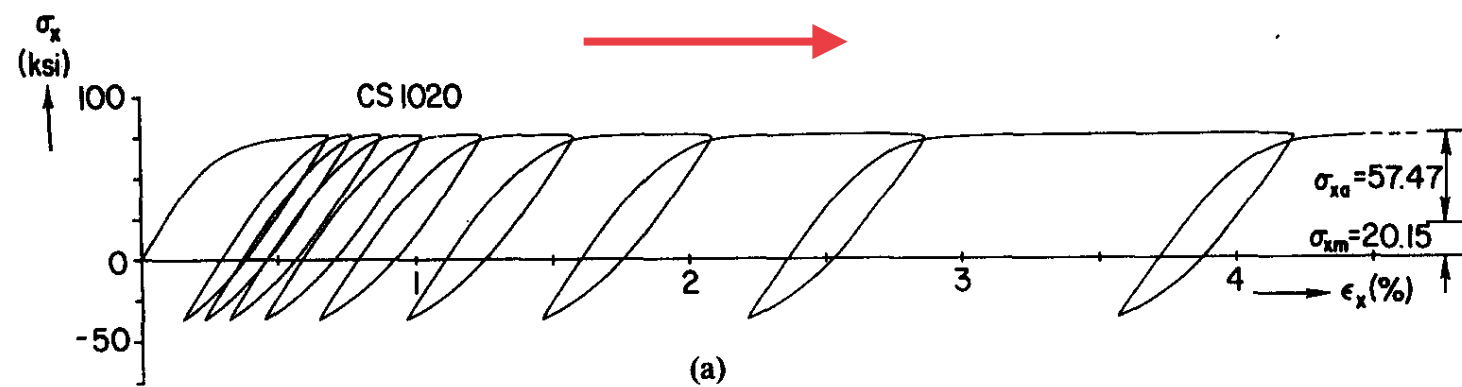
Cyclic loading test

Human brain tissue



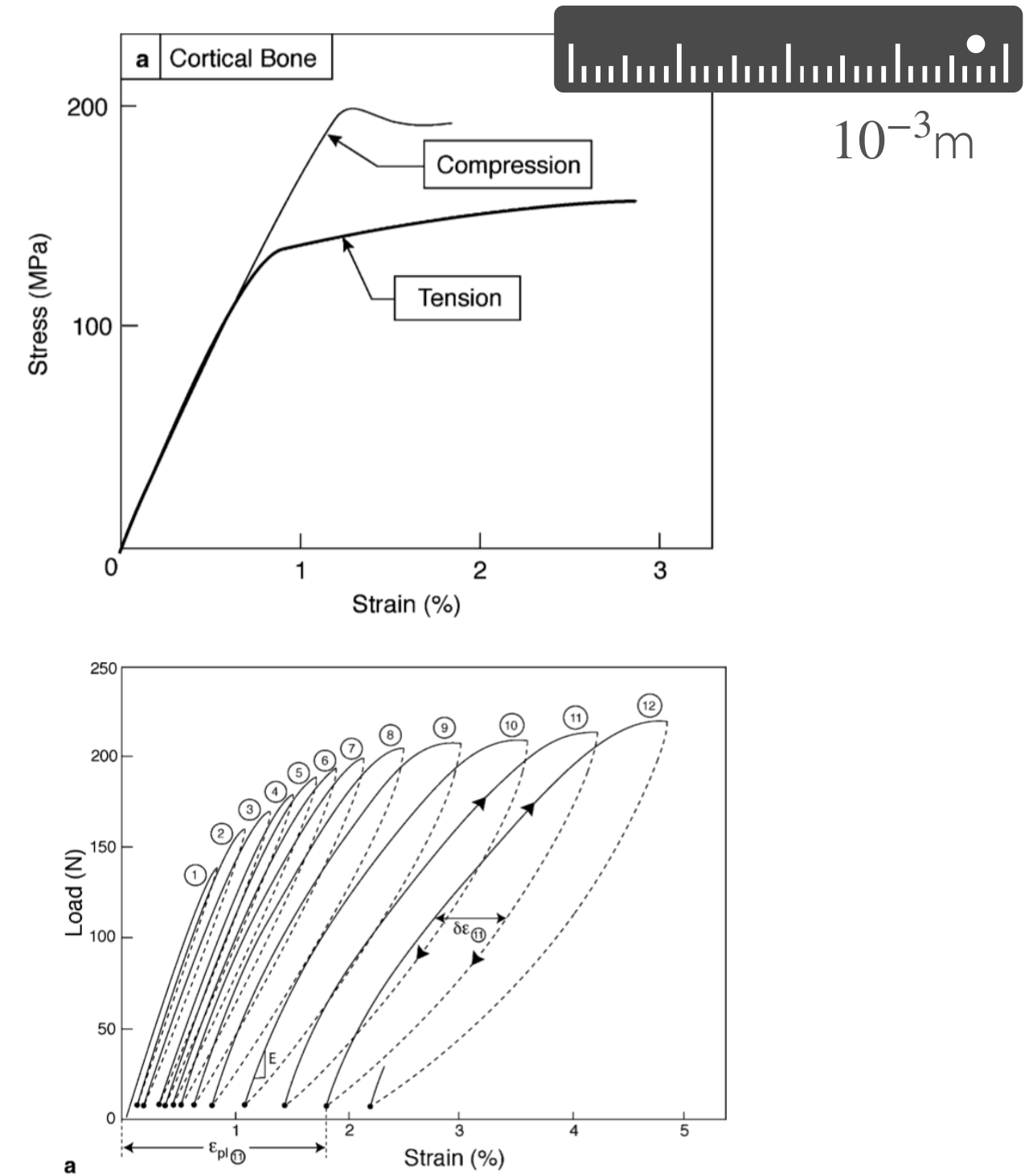
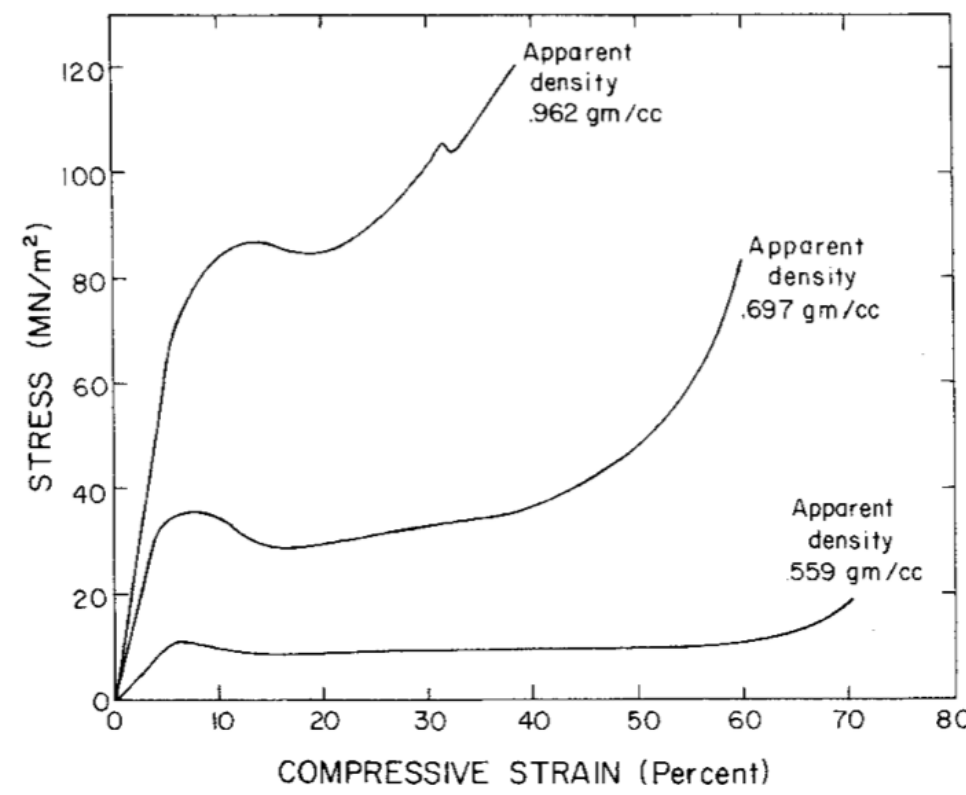
Cyclic loading test

Carbon steel CS1020



T. Hassan, S. Kyriakides, Ratcheting in cyclic Plasticity, Part I: uniaxial behavior, International Journal of Plasticity, Vol. 8, pp. 91-116, 1992.

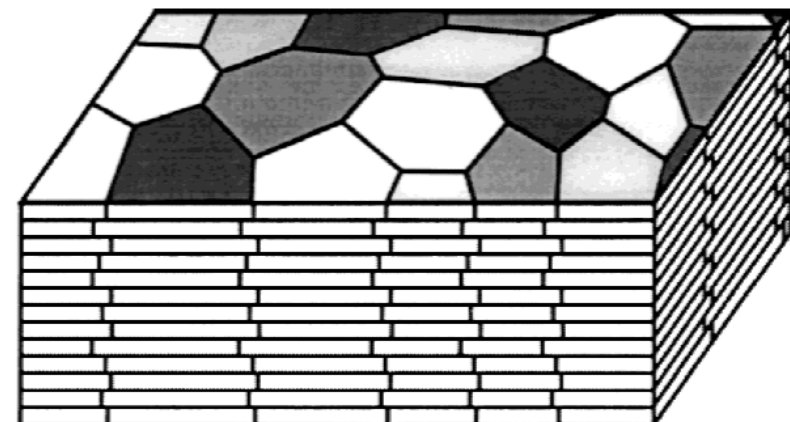
Post-yield behavior of bone



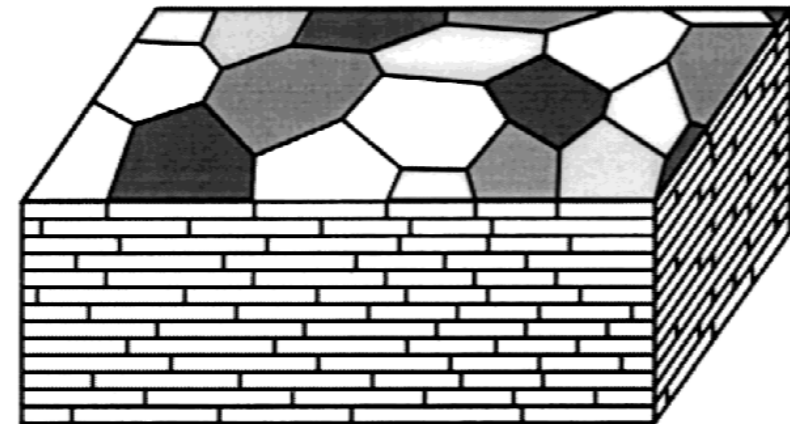
MERCER, C., et al. Mechanisms governing the inelastic deformation of cortical bone and application to trabecular bone. *Acta Biomaterialia*, 2006, 2.1: 59-68.

MERCER et al. BONE, Trabecular. Postyield Behavior of Subchondral.

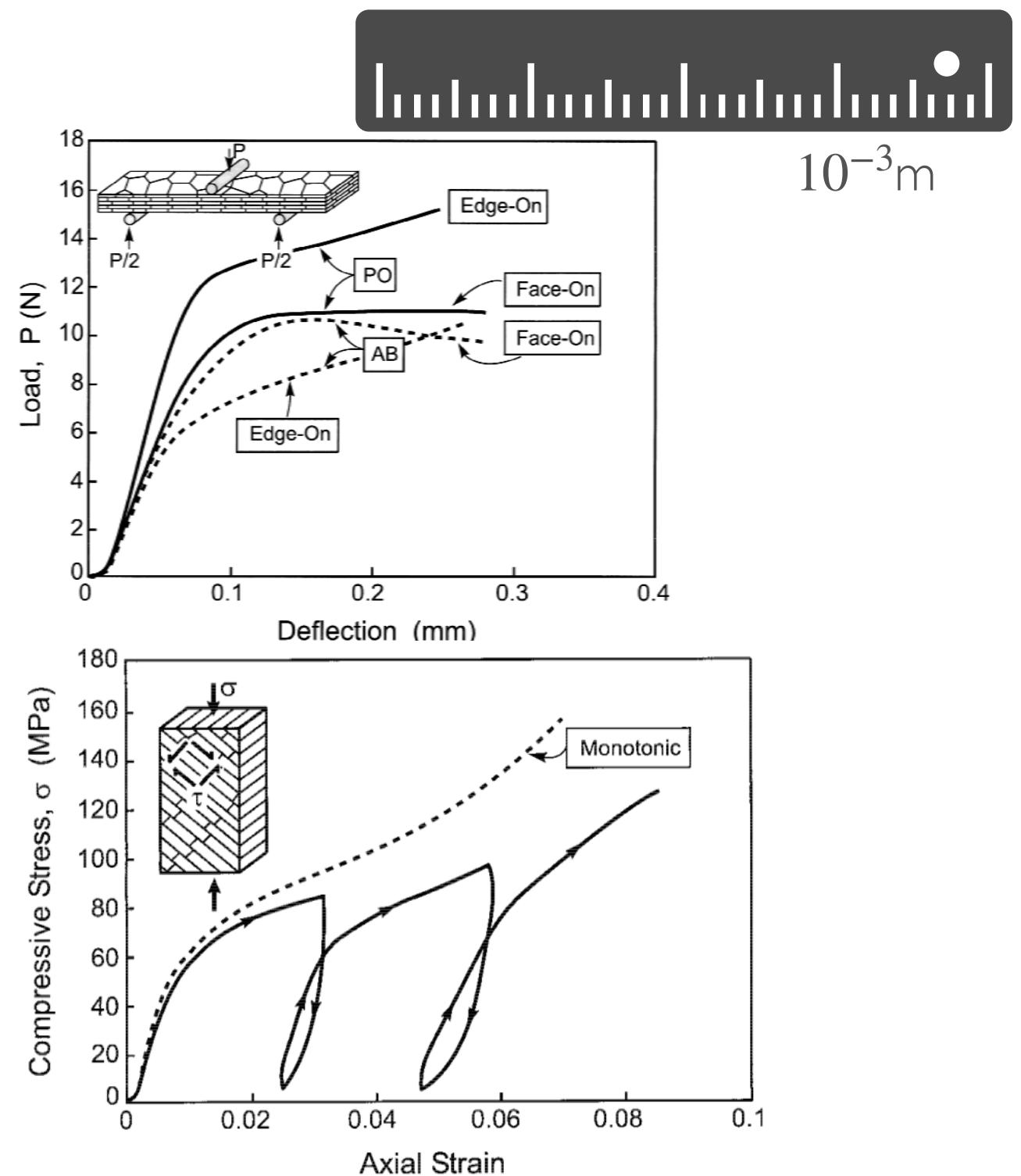
Post-yield behavior of bone



(a)

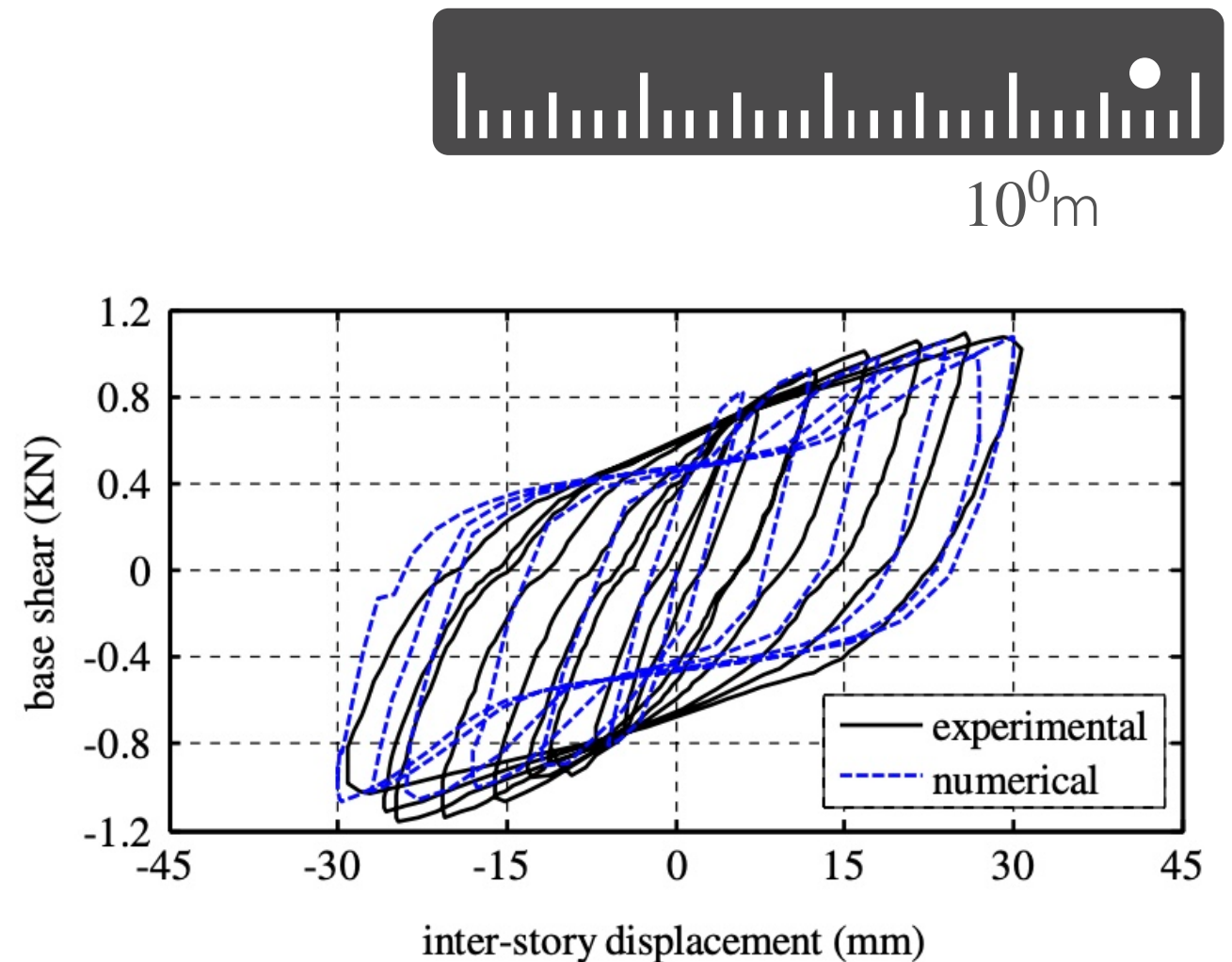
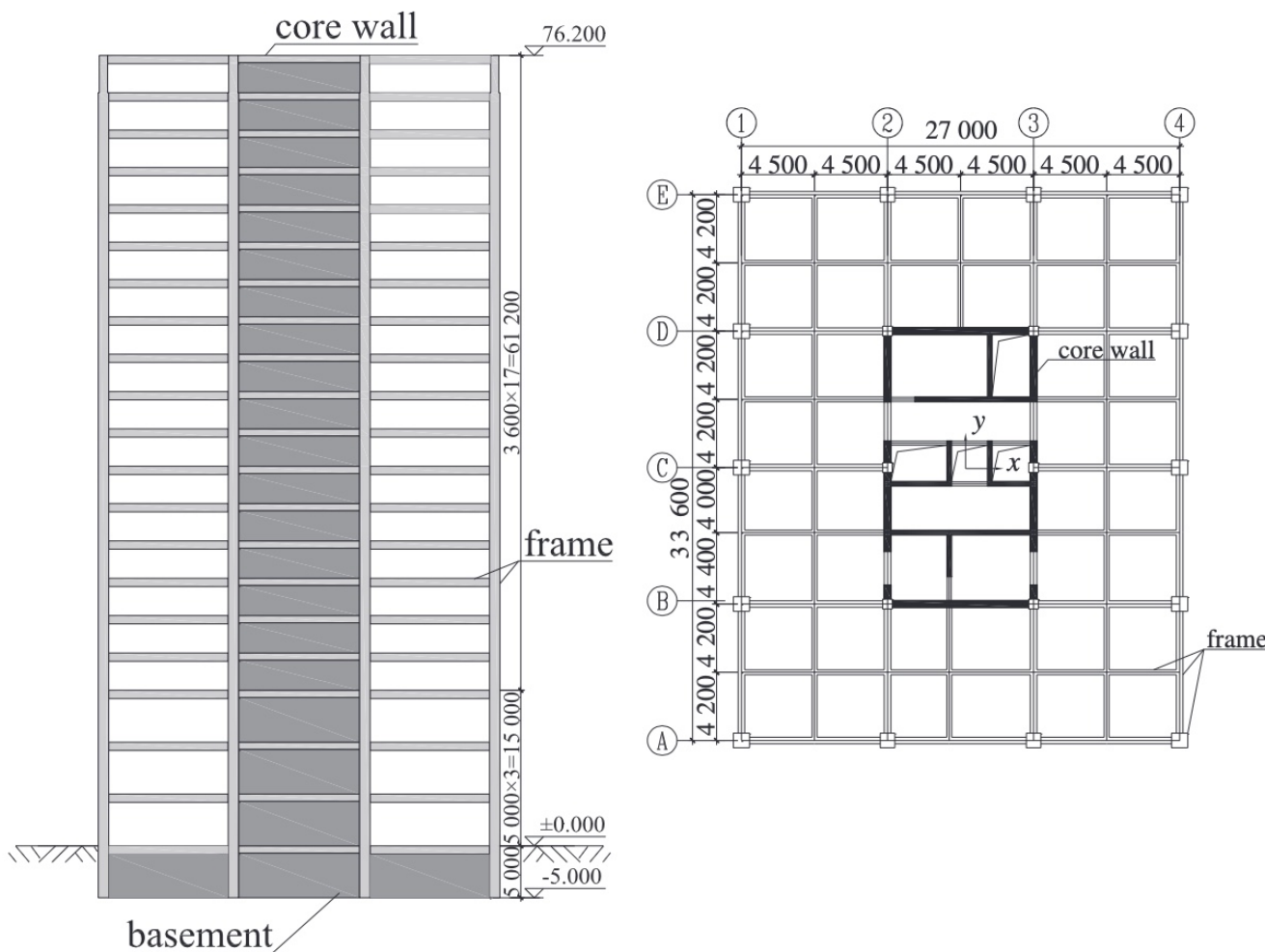


(b)



WANG, R. Z., et al. Deformation mechanisms in nacre. Journal of Materials Research, 2001, 16(9): 2485-2493.

Seismic behavior of tall buildings

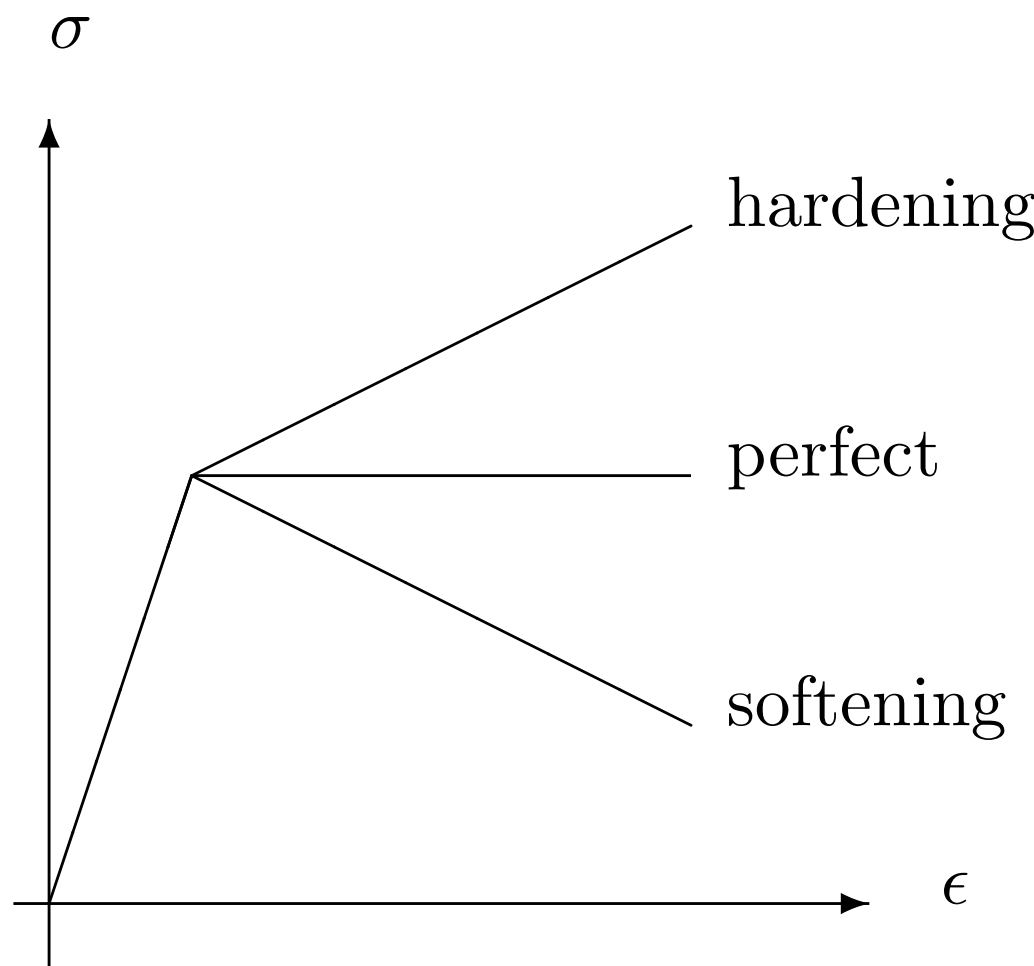


Ren X, Bai Q, Yang C, Li J. Seismic behavior of tall buildings using steel-concrete composite columns and shear walls. *Struct Design Tall Spec Build.* 2018; 27:e1441.

Evidence of plastic behavior in multi-scale mechanics

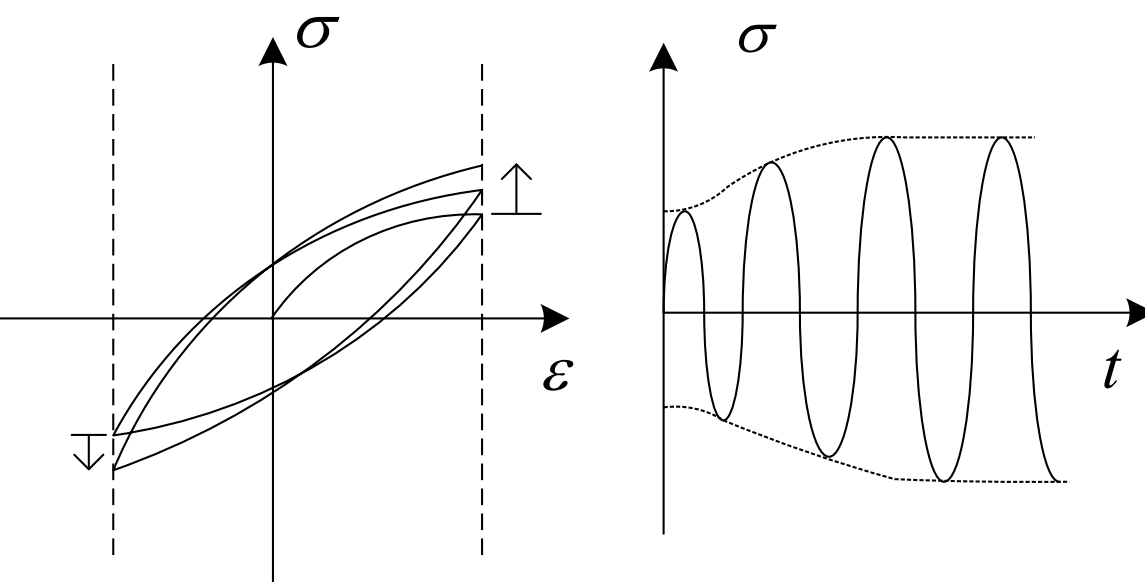
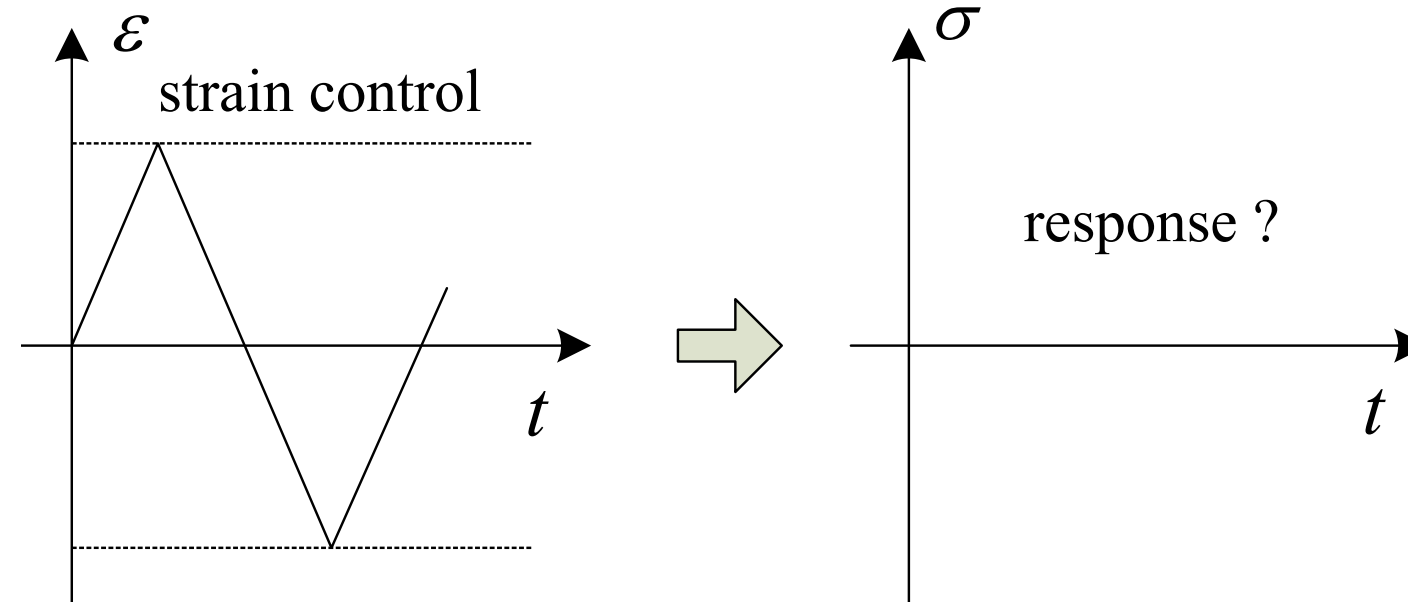
Plastic behavior—a 1D/classical viewpoint

Plastic plateau, hardening & softening

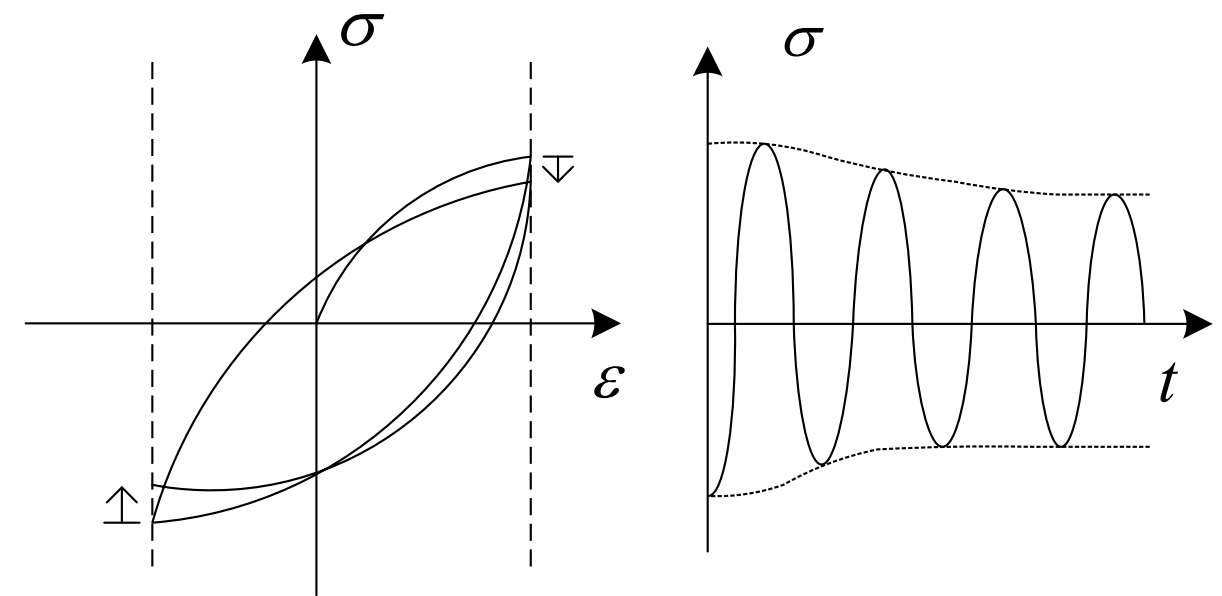


- Ludwick (1909): $\sigma = \sigma_0 + H\epsilon^n$
- $\epsilon = \frac{\sigma}{E} + H(\frac{\sigma}{E})^n$
- Prager (1941/1942): $\sigma = \sigma_0 \tanh(\frac{\epsilon}{\epsilon_0})$
- Holloman (1944): $\sigma = H\epsilon^n$
- Swift (1947): $\sigma = H(\epsilon_s + \epsilon)^n$
- Voce (1948): $\sigma = \sigma_0 + (\sigma_s - \sigma_0)[1 - e^{-n\epsilon}]$

Cyclic hardening & cyclic softening

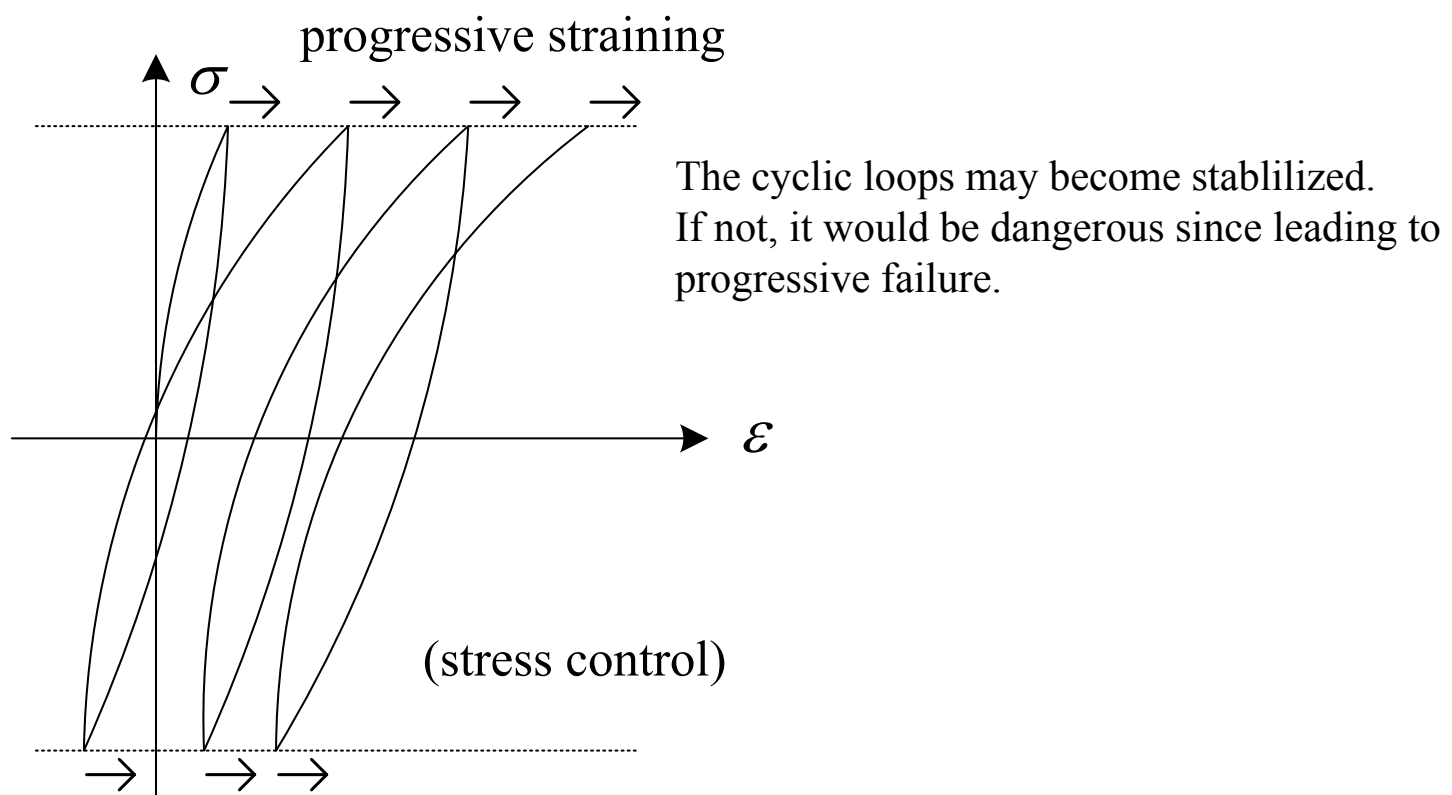
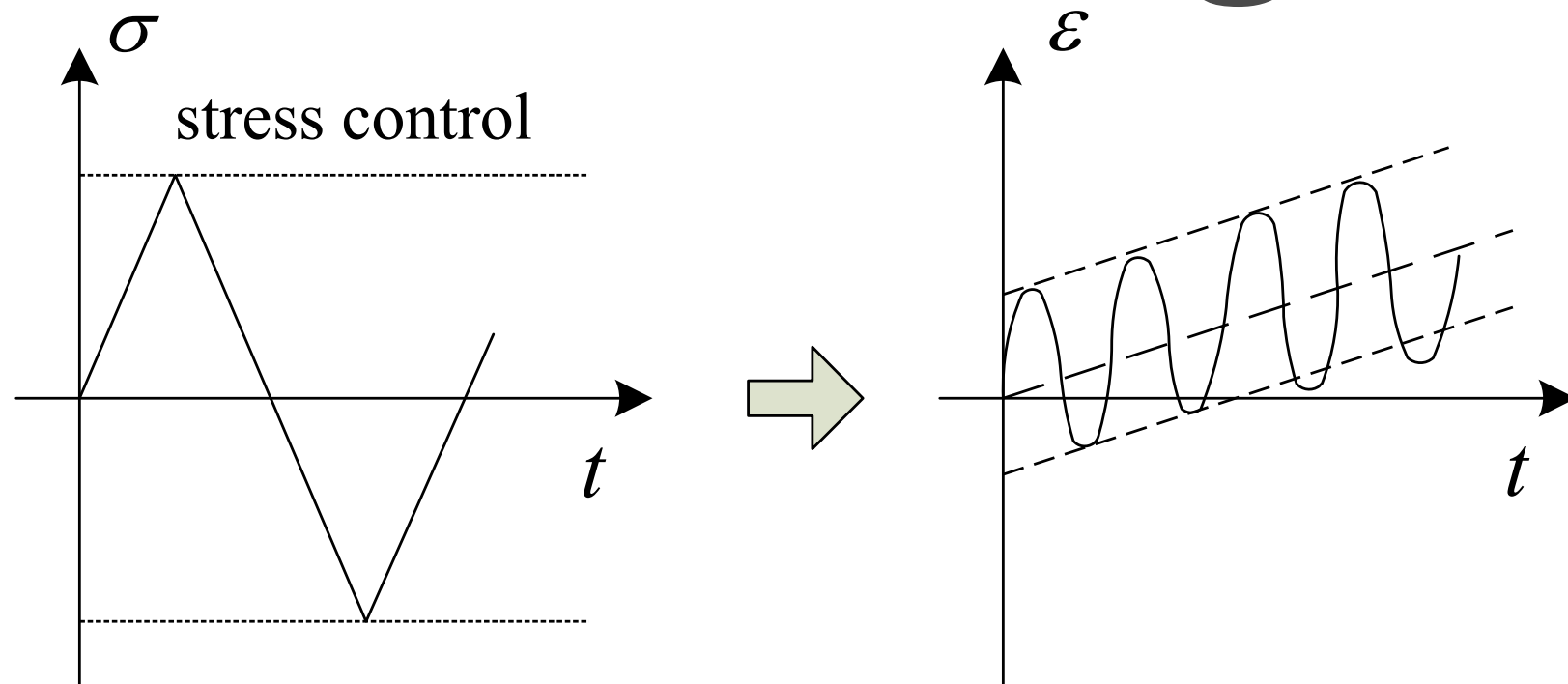


cyclic hardening

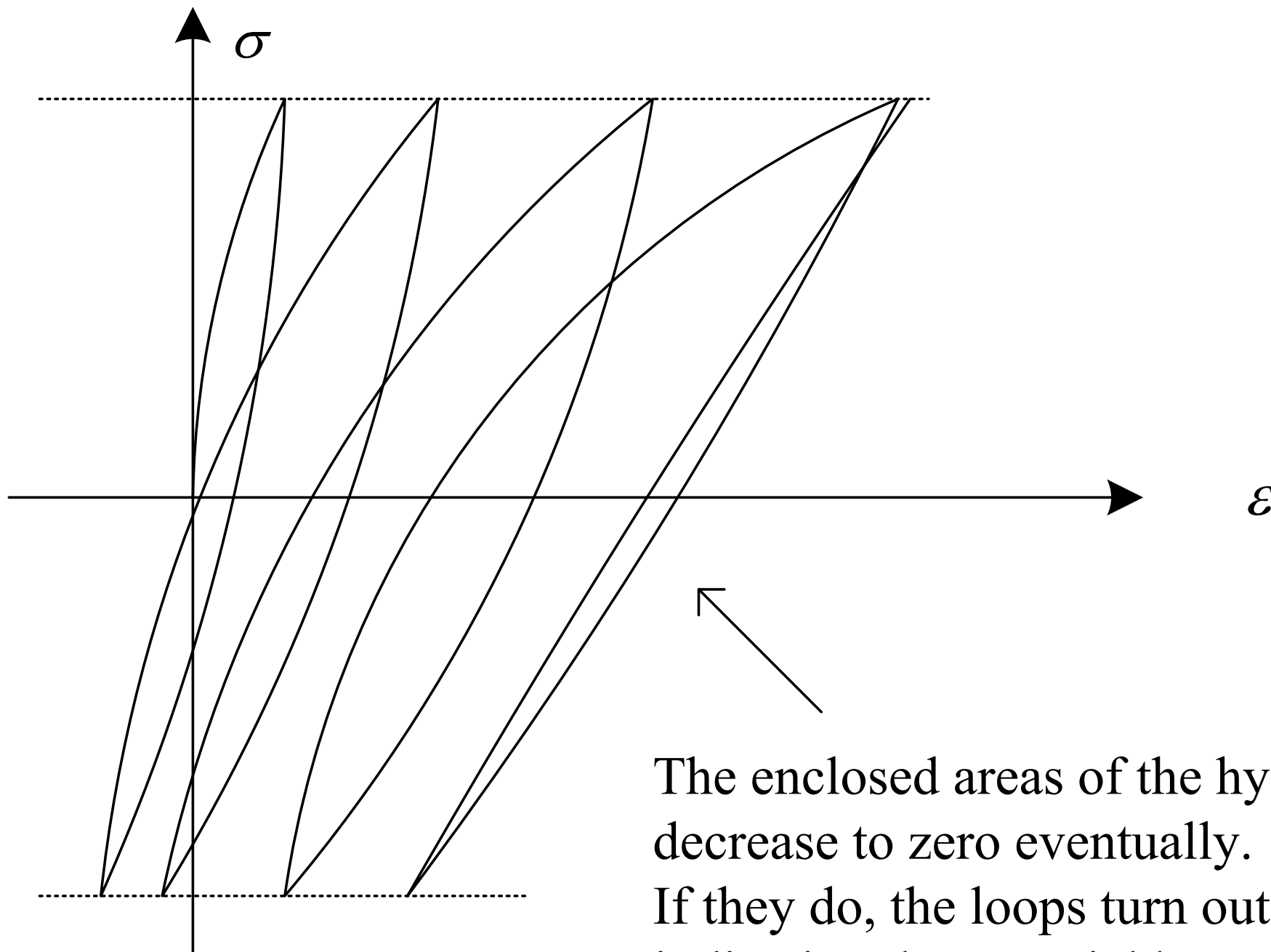


cyclic softening

Ratcheting



Shakedown

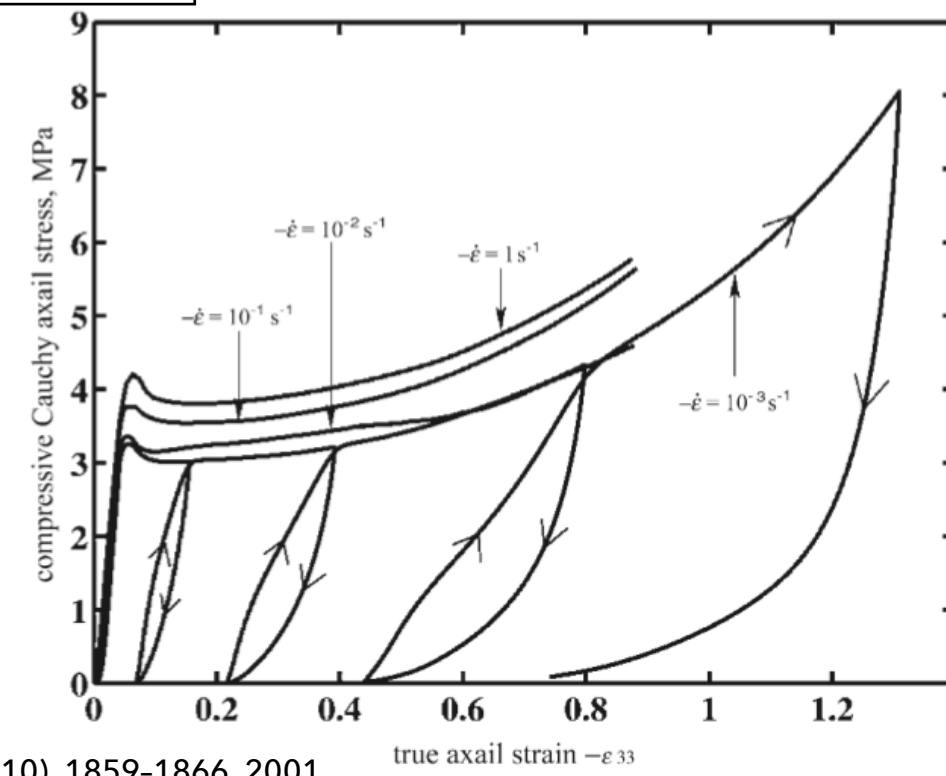
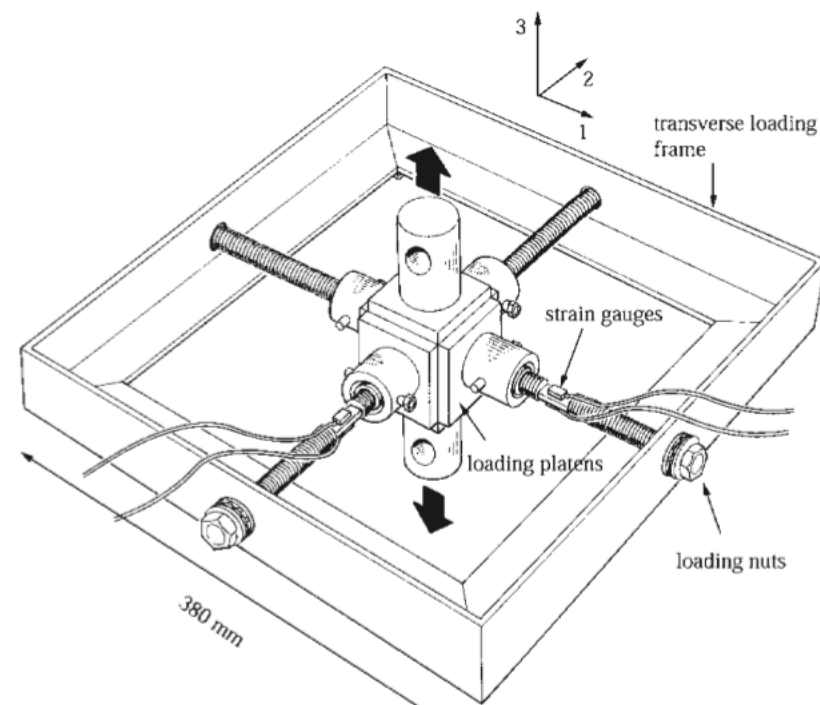
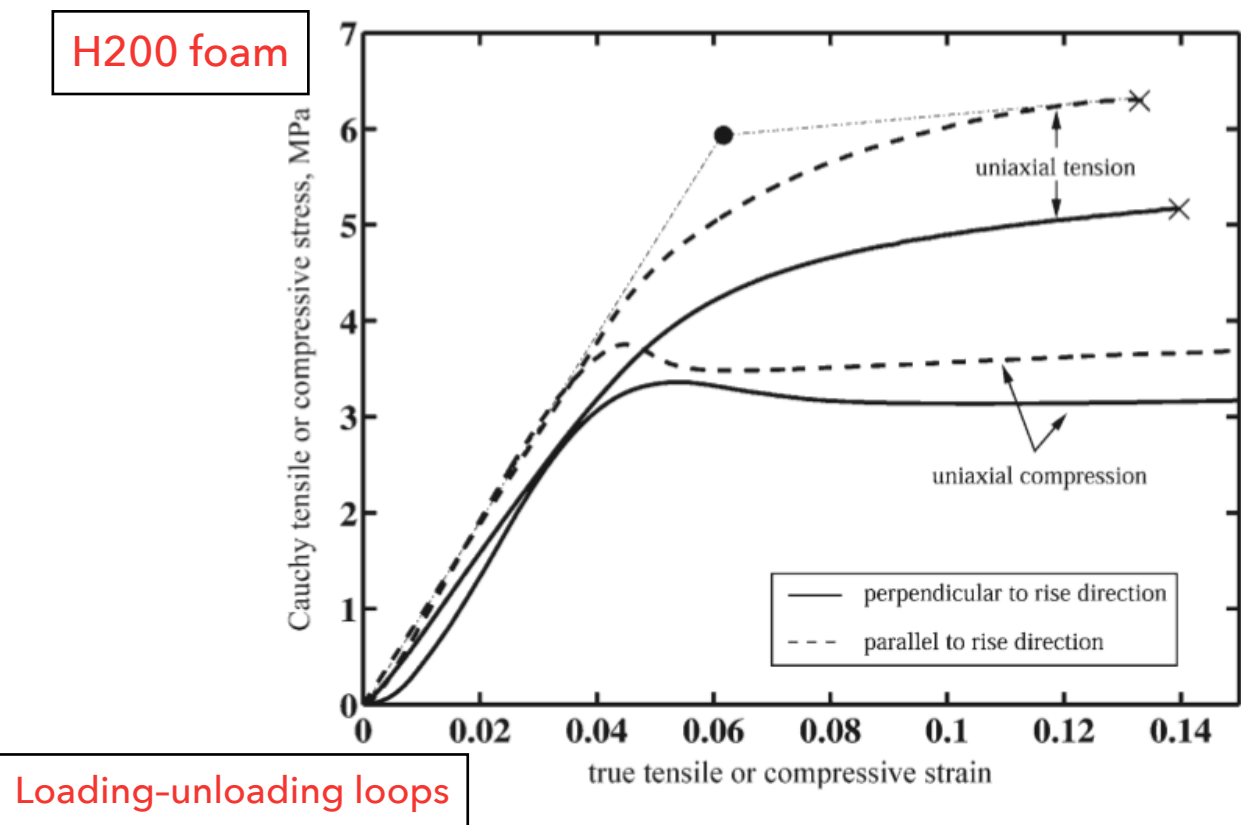
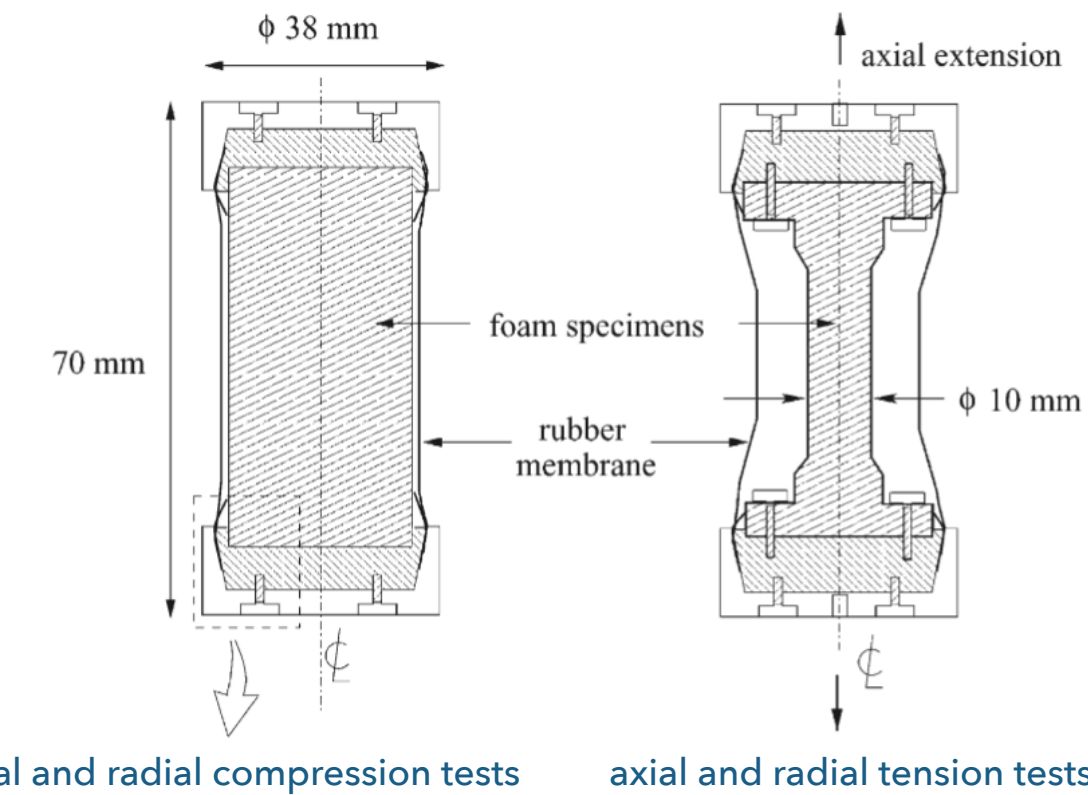


The enclosed areas of the hysteresis loops may decrease to zero eventually.
If they do, the loops turn out to be a linear line, indicating the material becomes elastic again.
That phenomenon is called shakedown.

Evidence of plastic behavior in multi-scale mechanics

Biaxial loading tests

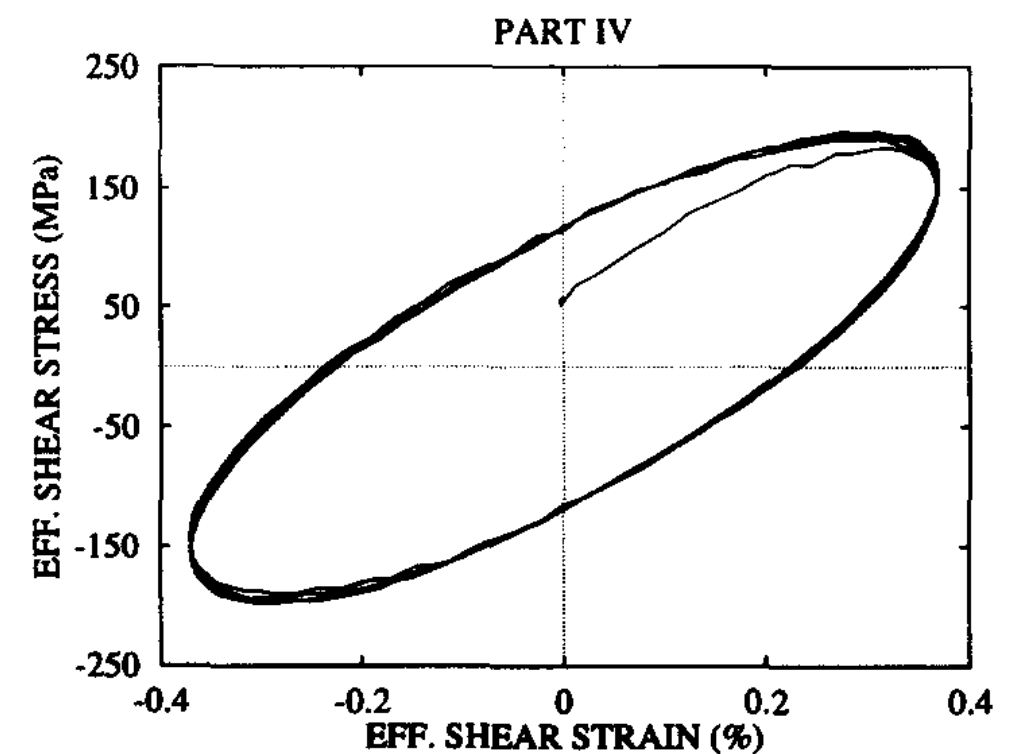
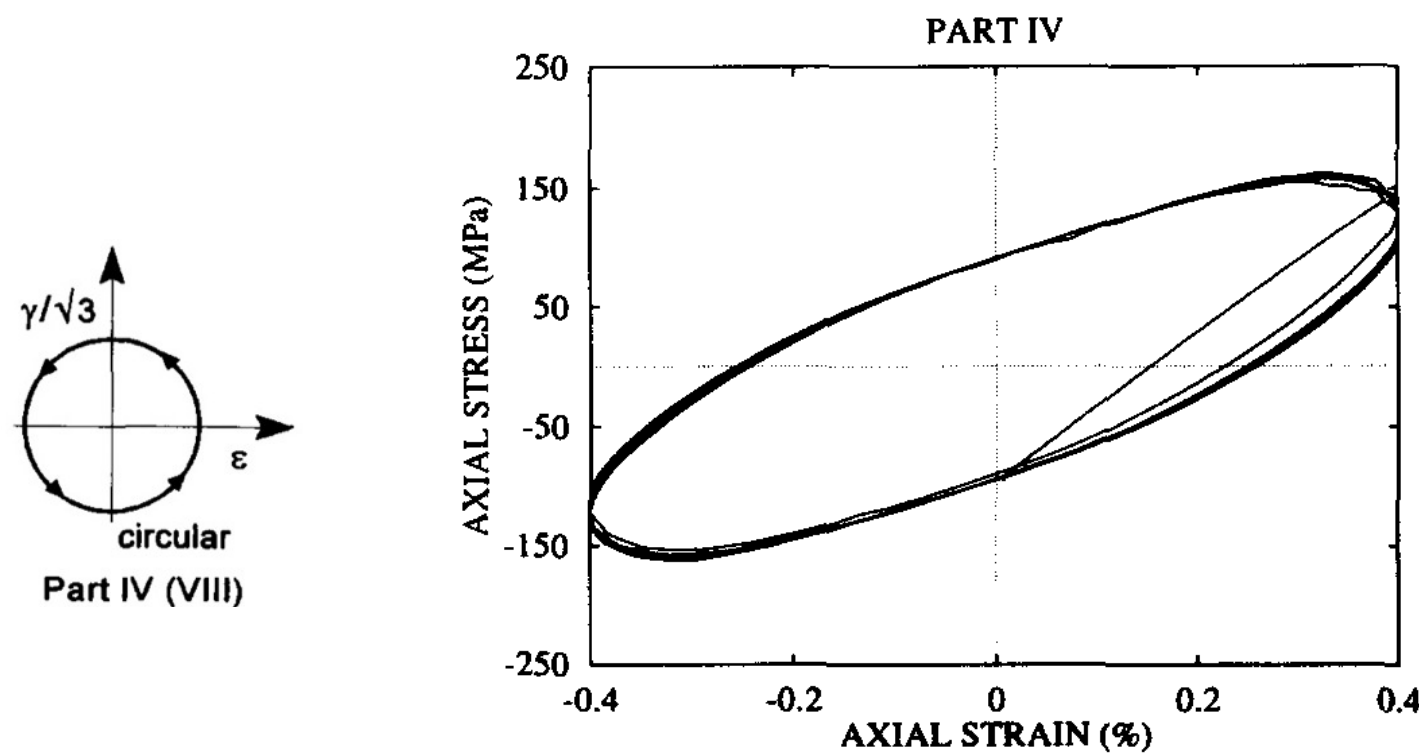
Yield behavior of polymer foams



Deshpande, V. S., Fleck, N. A., "Multi-axial yield behaviour of polymer foams," Acta Materialia, 49(10), 1859-1866, 2001.

Biaxial loading test

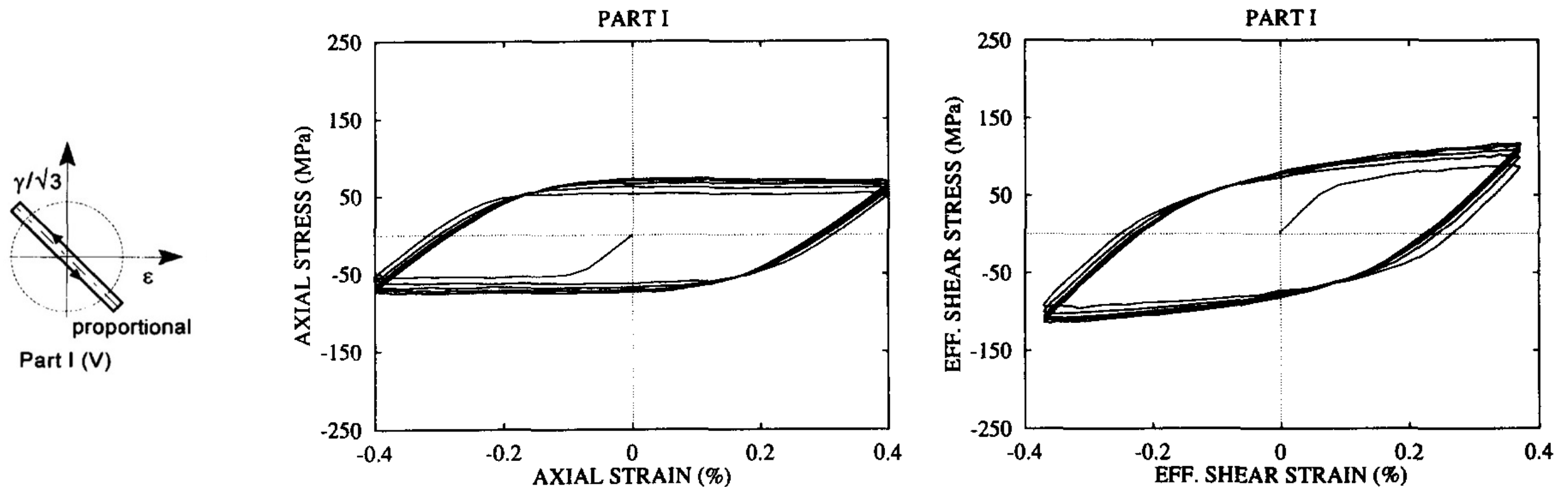
Aluminium alloy (Al6060)



O. S. Hopperstad and M. Langseth, S. Remseth, Cyclic stress-strain behaviour of alloy AA6060, part II: Biaxial experiments and modelling, International Journal of Plasticity, Vol. 11, pp. 741-762, 1995.

Biaxial loading test

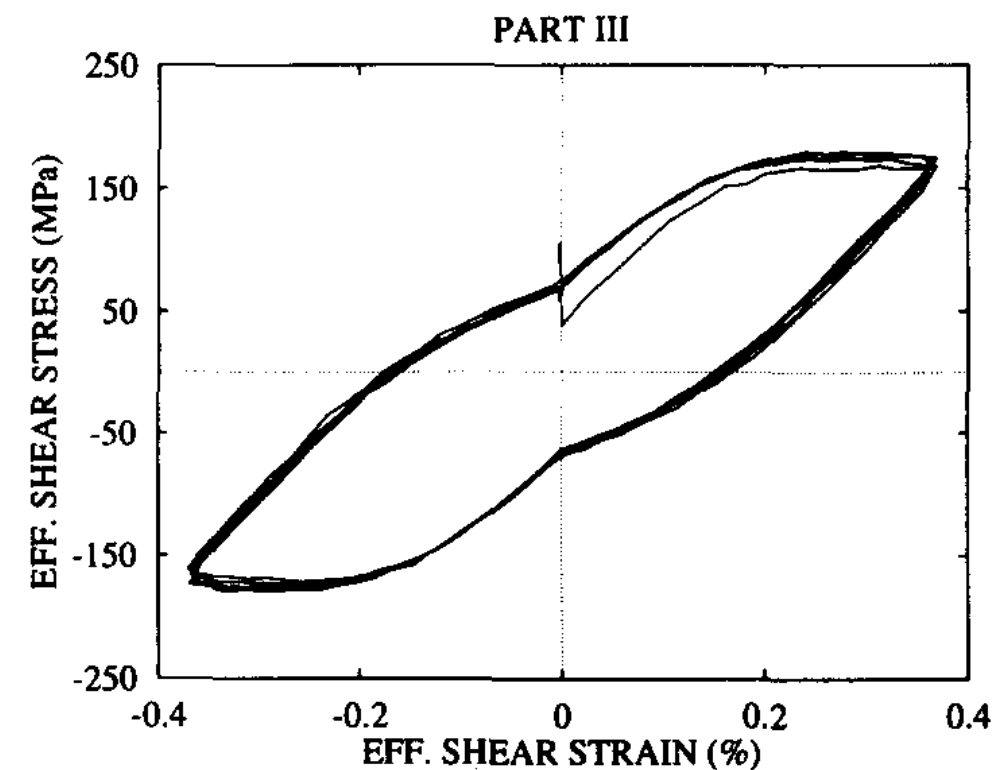
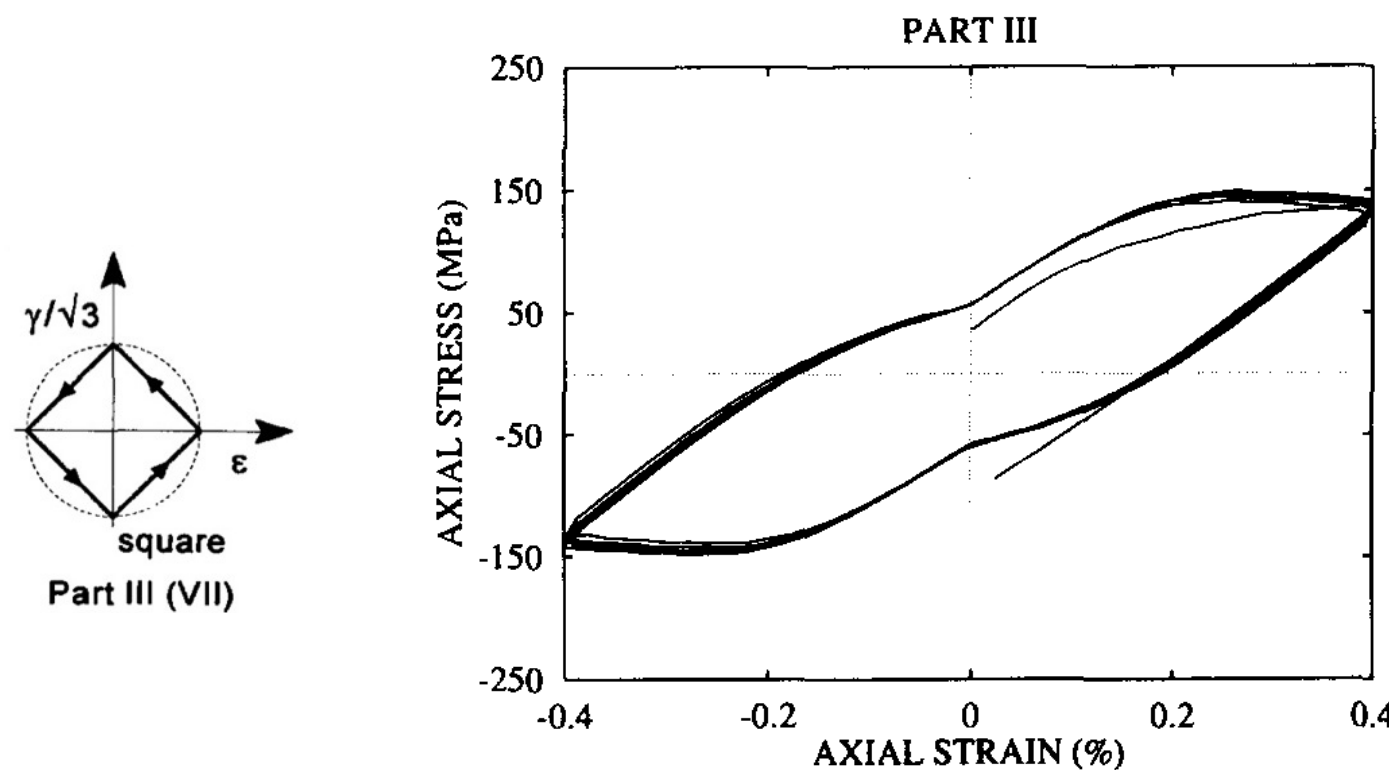
Aluminium alloy (Al6060)



O. S. Hopperstad and M. Langseth, S. Remseth, Cyclic stress-strain behaviour of alloy AA6060, part II: Biaxial experiments and modelling, International Journal of Plasticity, Vol. 11, pp. 741-762, 1995.

Biaxial loading test

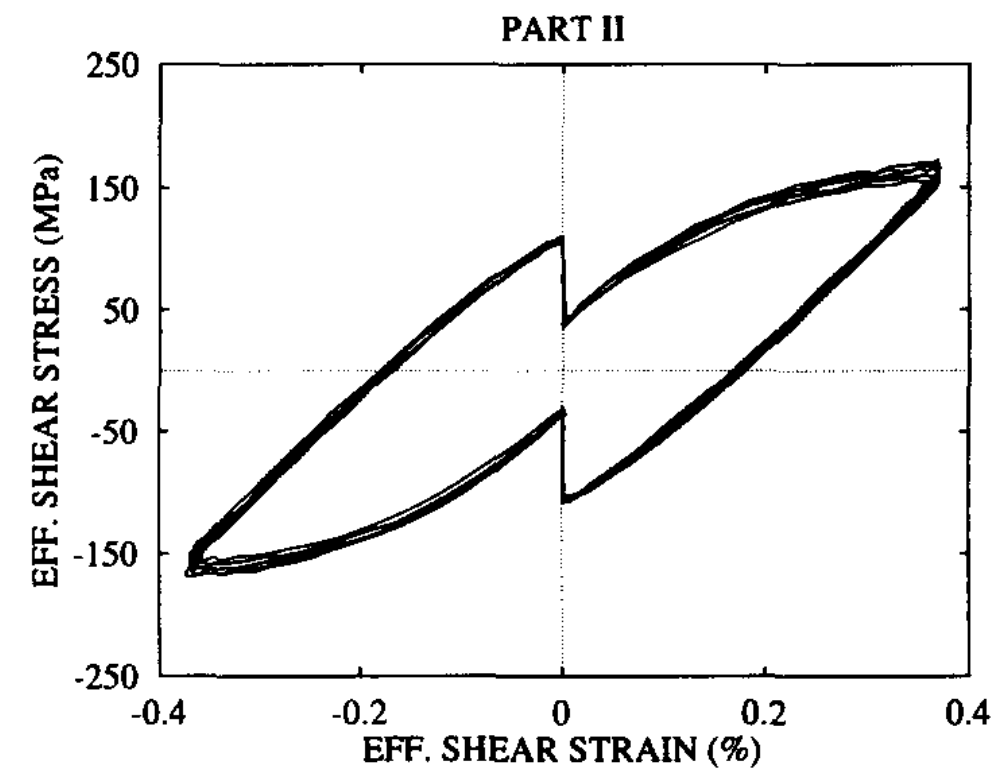
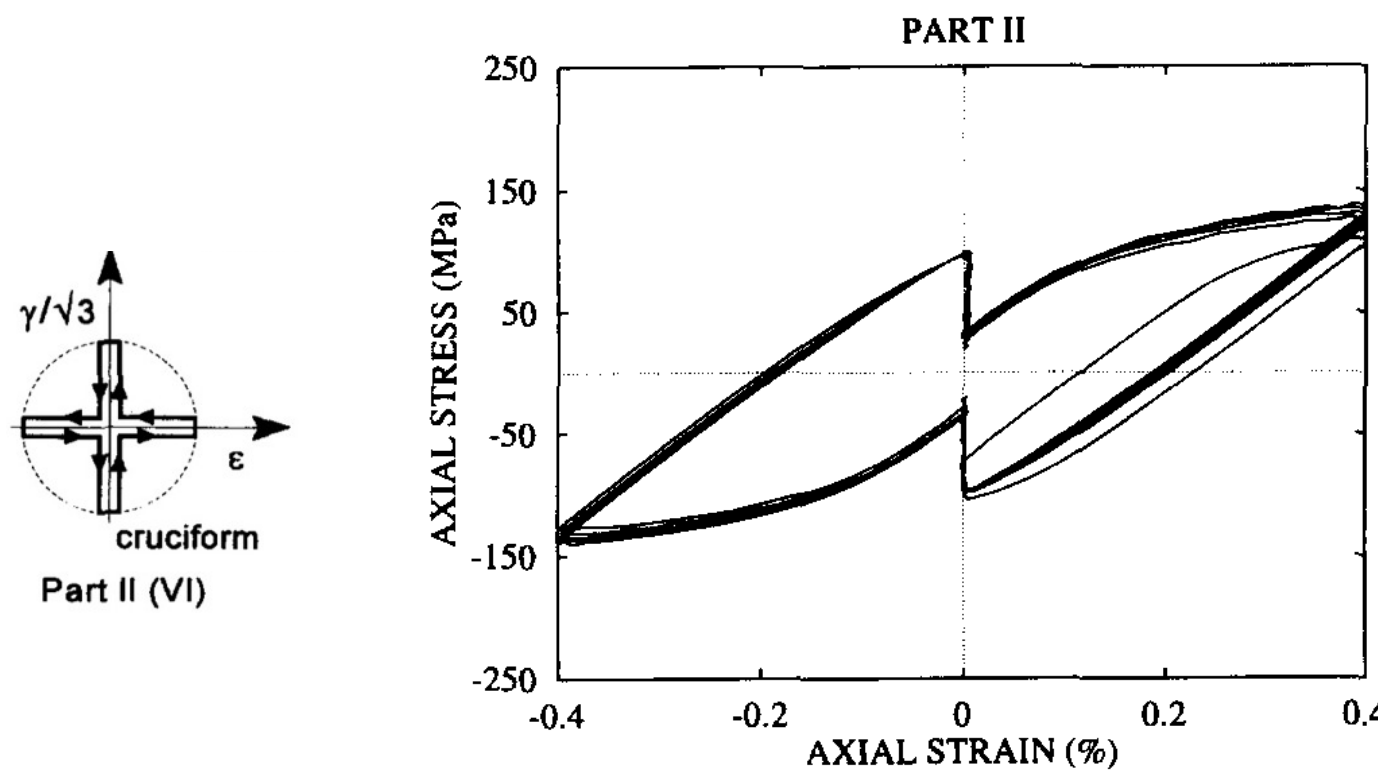
Aluminium alloy (Al6060)



O. S. Hopperstad and M. Langseth, S. Remseth, Cyclic stress-strain behaviour of alloy AA6060, part II: Biaxial experiments and modelling, International Journal of Plasticity, Vol. 11, pp. 741-762, 1995.

Biaxial loading test

Aluminium alloy (Al6060)



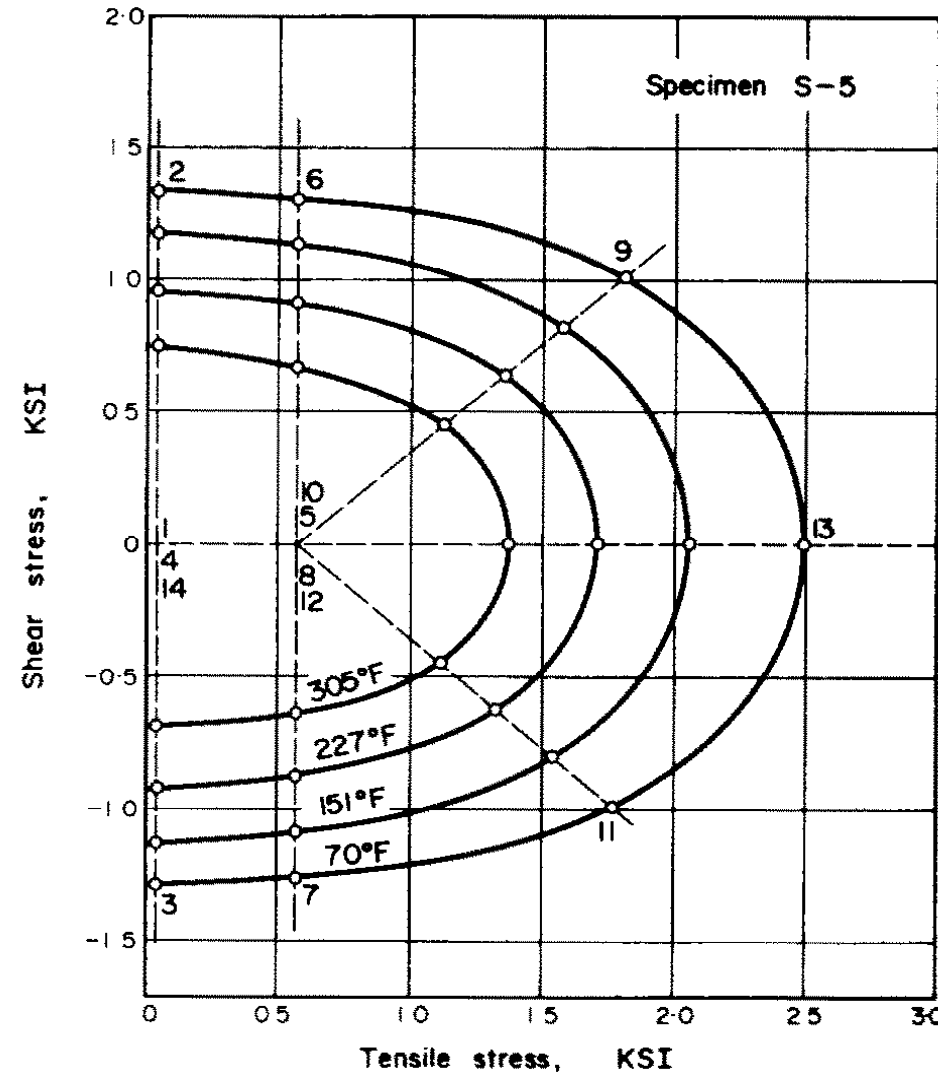
O. S. Hopperstad and M. Langseth, S. Remseth, Cyclic stress-strain behaviour of alloy AA6060, part II: Biaxial experiments and modelling, International Journal of Plasticity, Vol. 11, pp. 741-762, 1995.

Biaxial loading test

Aluminium alloy (Al1100)



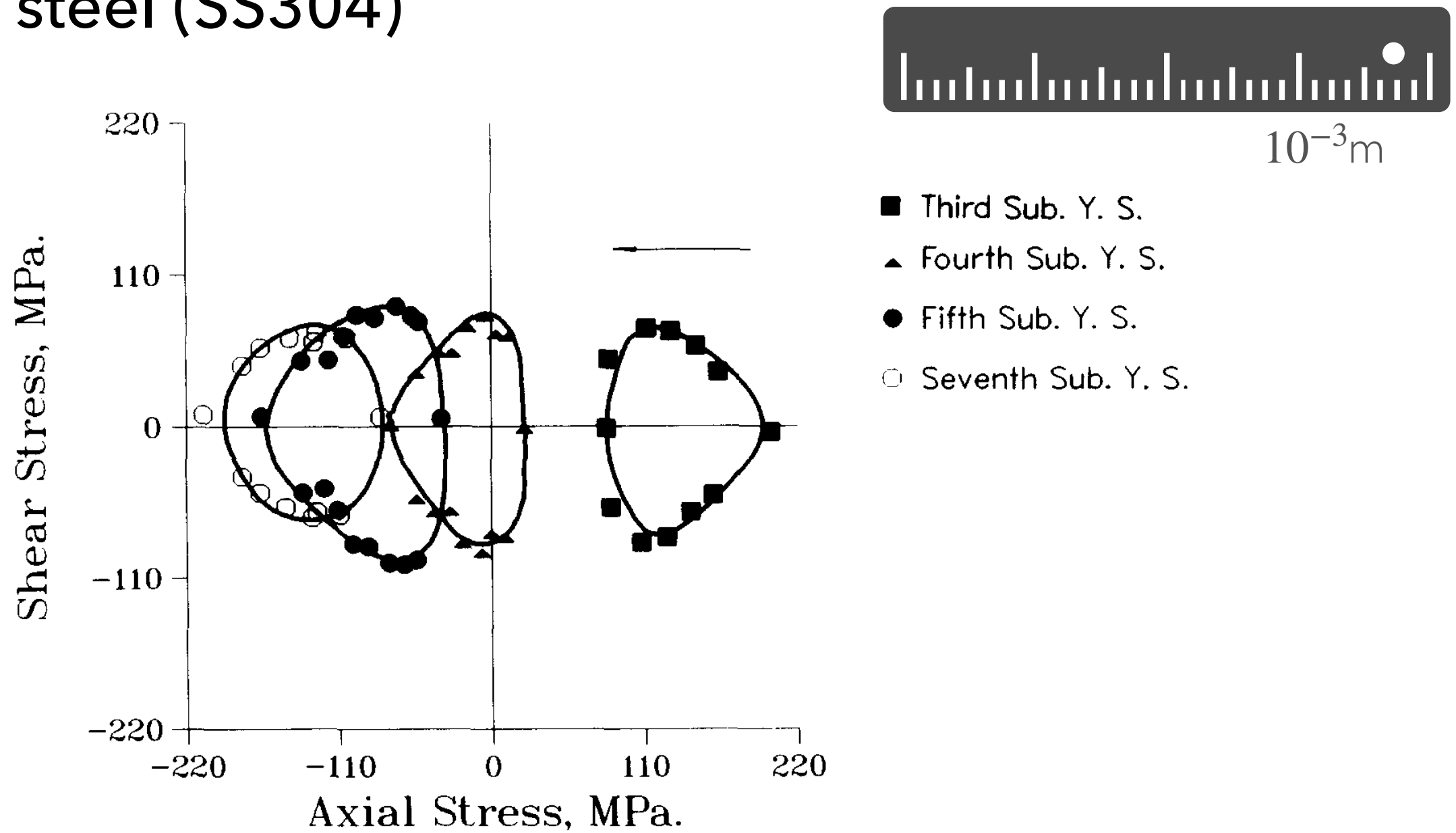
$10^{-3}m$



A. Phillips & P. K. Das, Yield surfaces and loading surfaces of aluminium and brass: An experimental investigation at room and elevated temperatures, International Journal of Plasticity, Vol. 1, pp. 89-109, 1985.

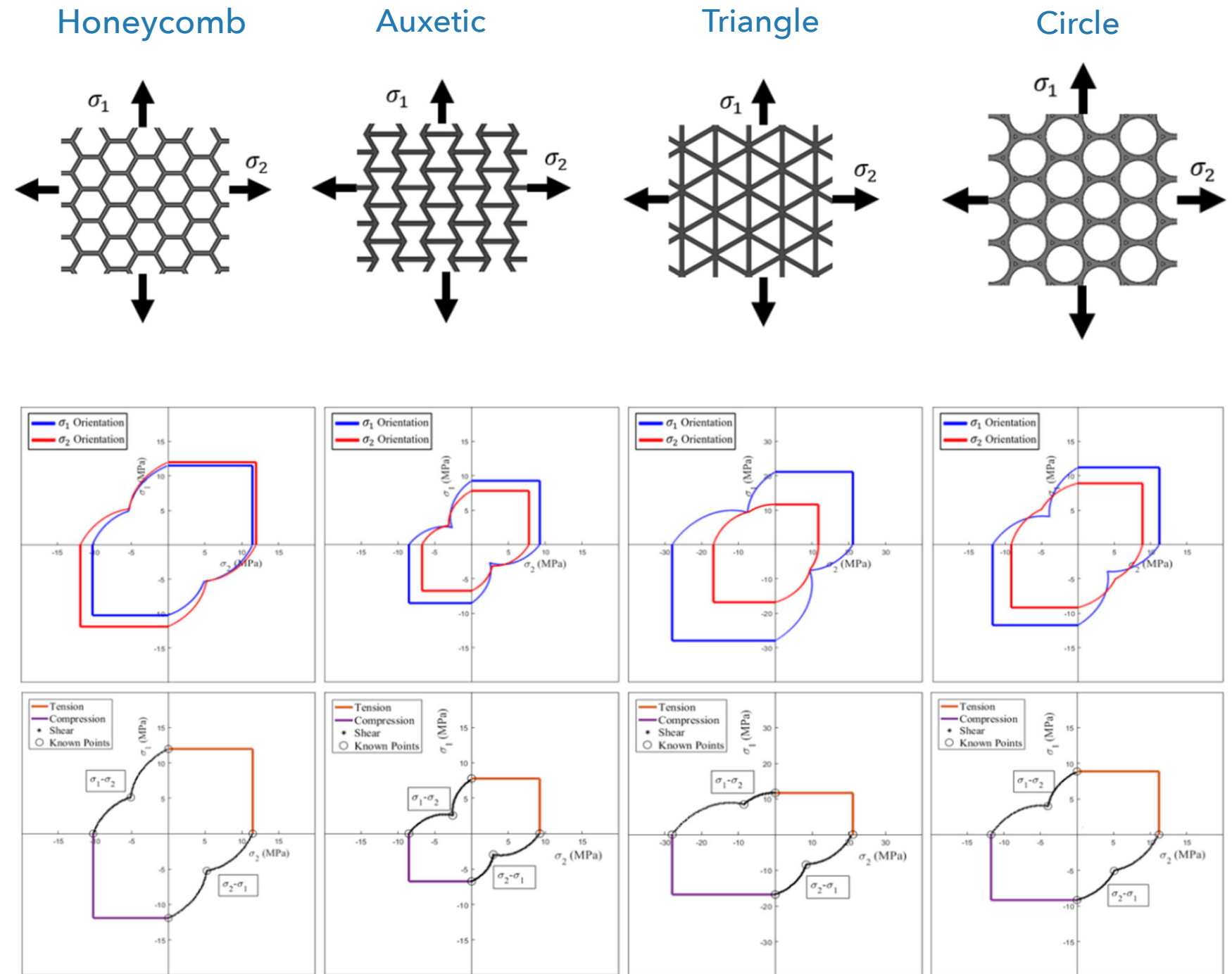
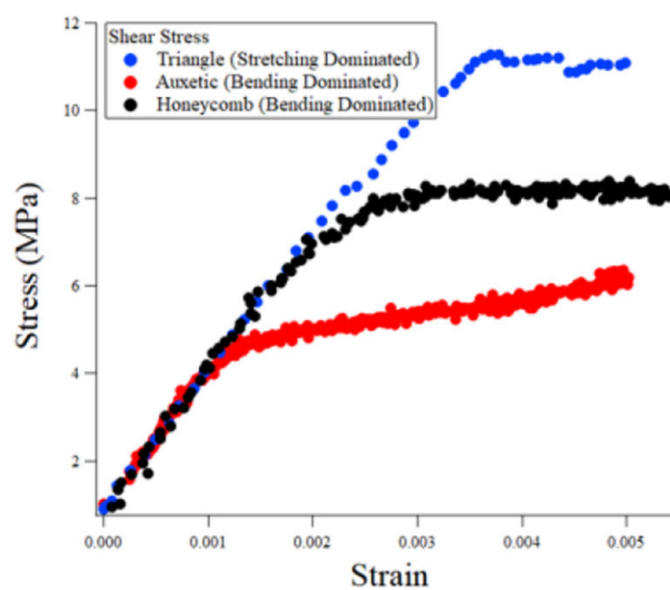
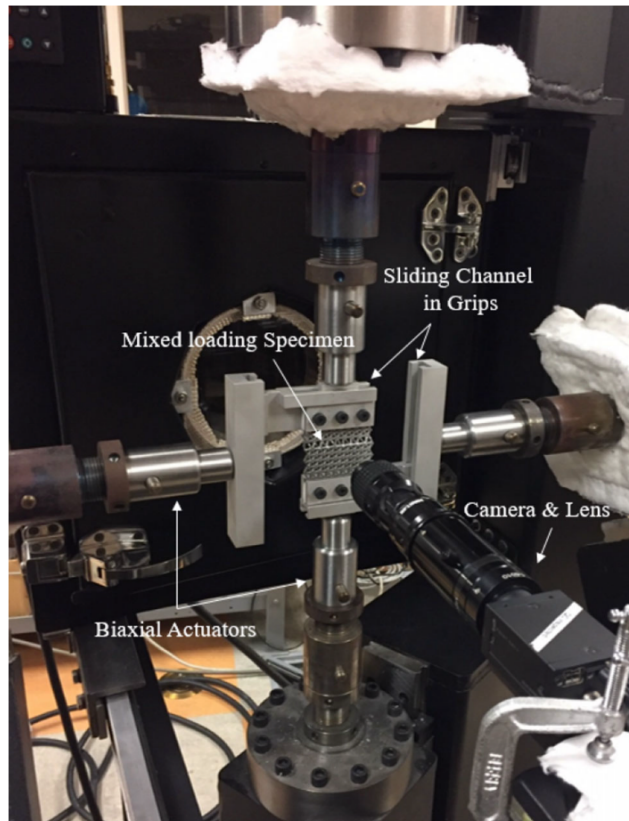
Biaxial loading test

Stainless steel (SS304)



H.-C. Wu & W. C. Yeh, On the experimental determination of yield surfaces and some results of annealed 304 stainless steel, International Journal of Plasticity, Vol. 7, pp. 803-826, 1991. (SS 304)

Yield surfaces of Anisotropic Cellular Materials

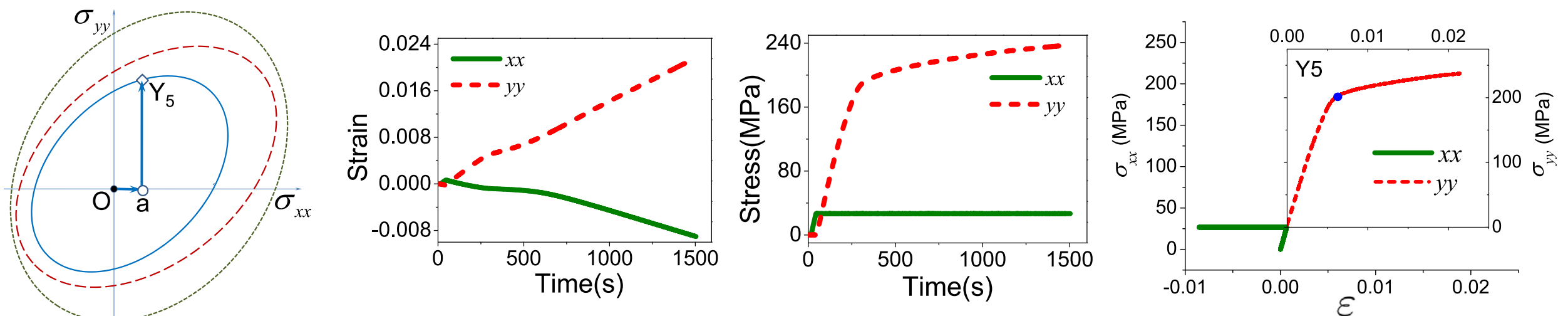
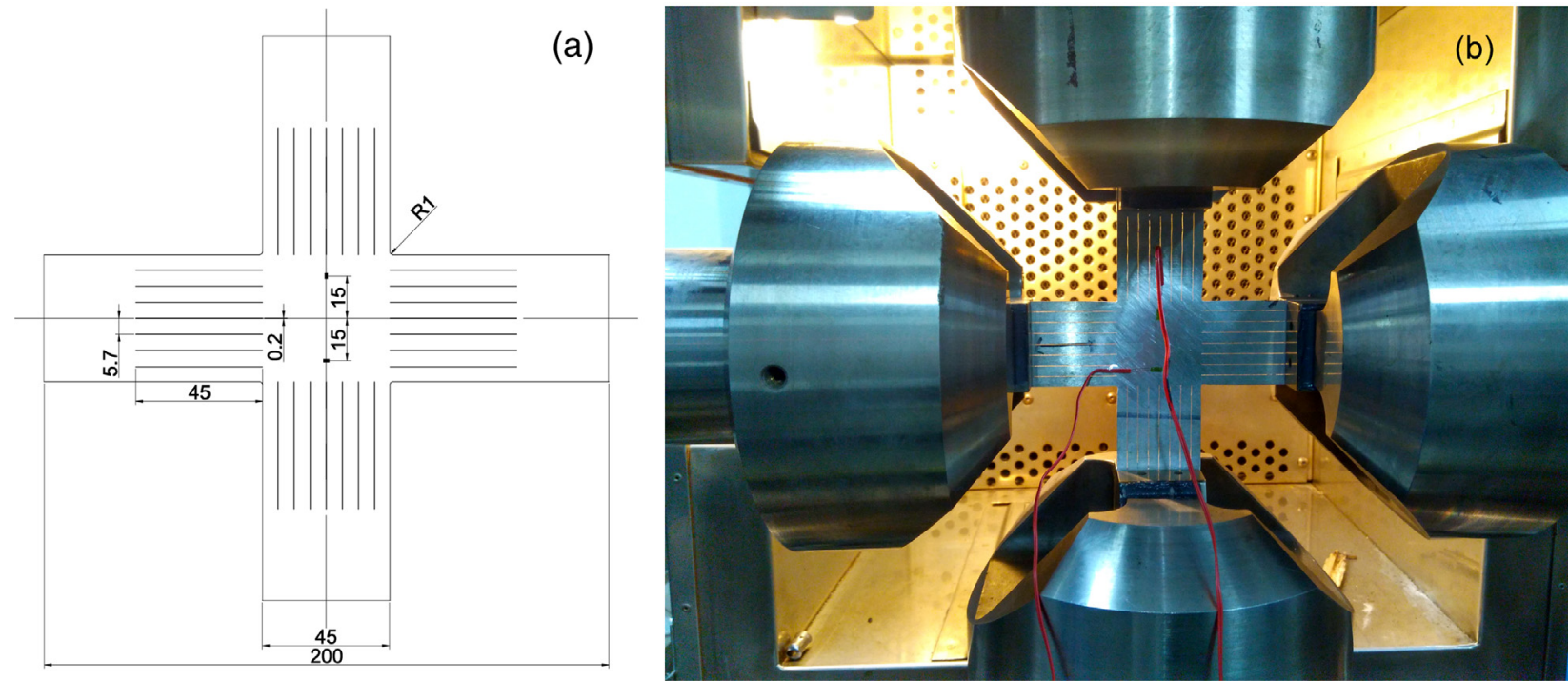


Conway, K. M., Romanick, Z., Cook, L. M., Morales, L. A., Despeaux, J. D., Ridlehuber, M. L., Fingar, C., Doctor, D., Nikhare, C. P., Pataky, G. J., "The anisotropic yield surface of cellular materials," JOM, pages 1-8, 2022.

Evidence of plastic behavior in multi-scale mechanics

Plastic behavior—a mD viewpoint

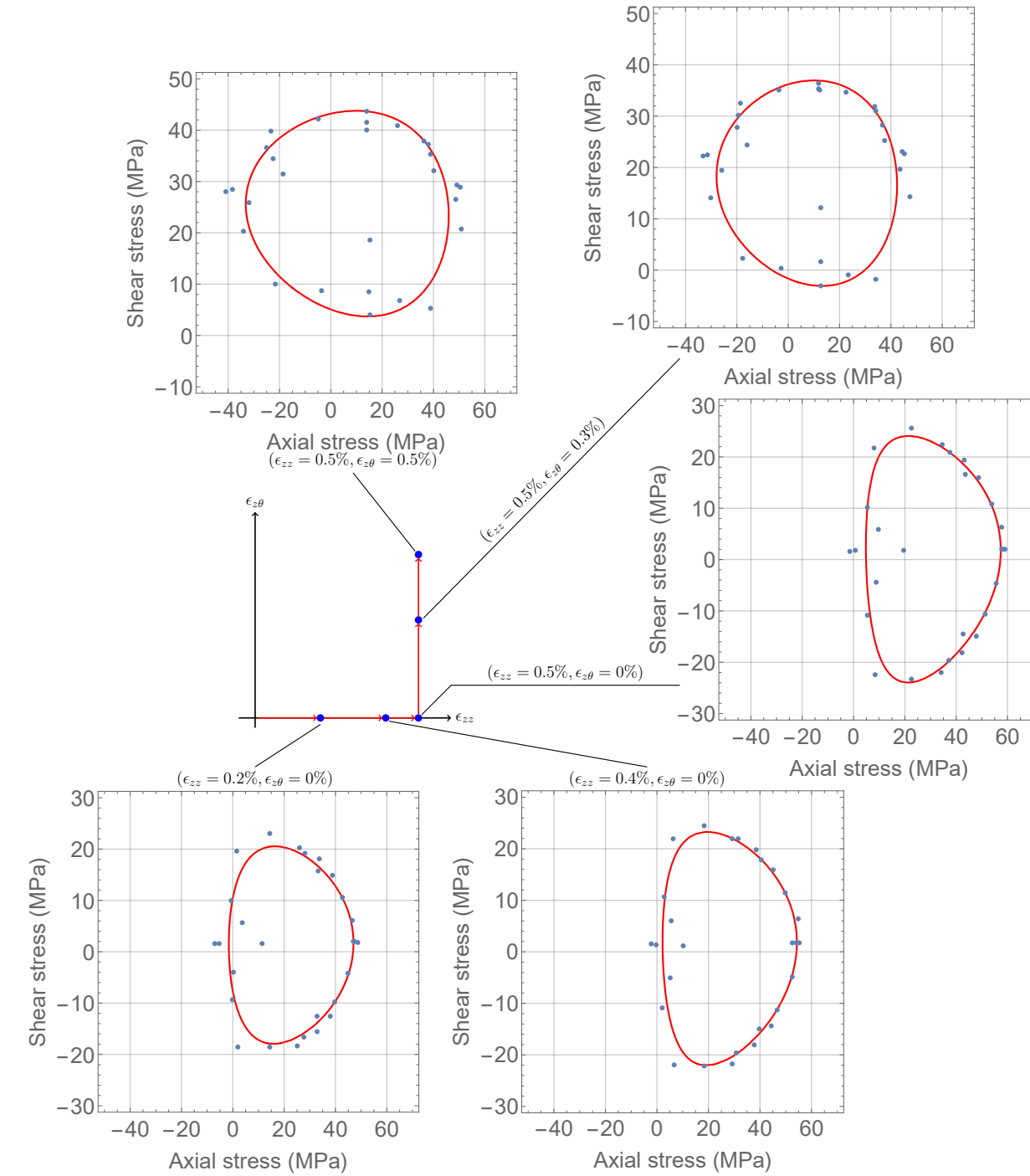
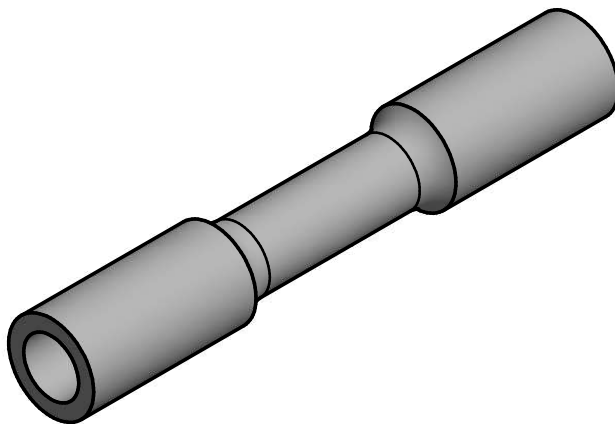
Yield surface evolution in 2D space



(b) Stress strain responses to probe Y_5 on initial yield surface

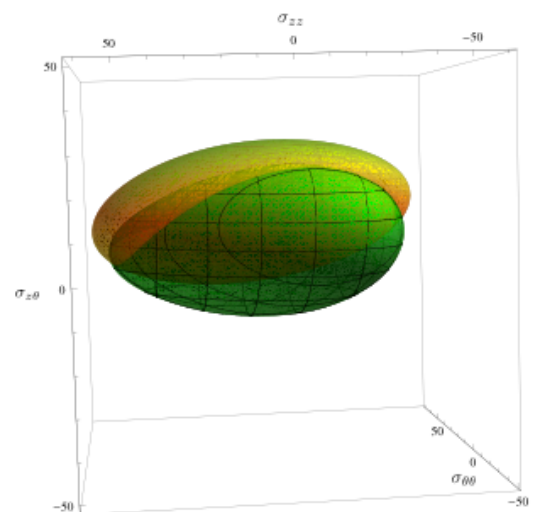
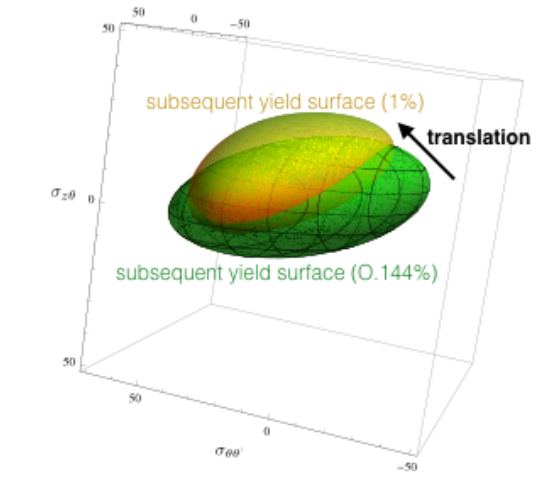
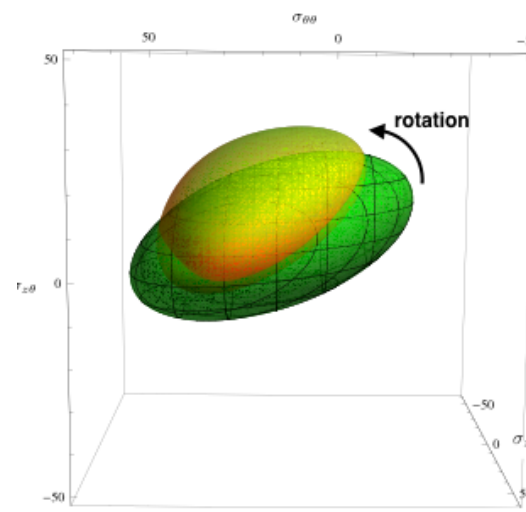
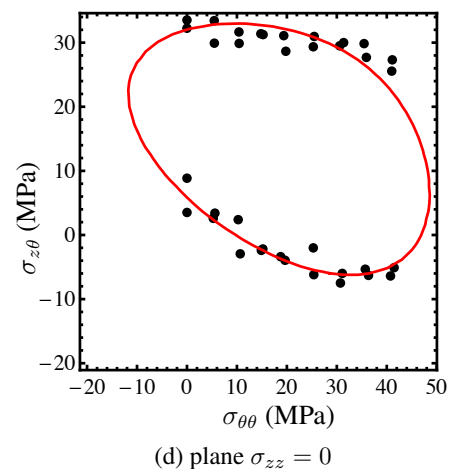
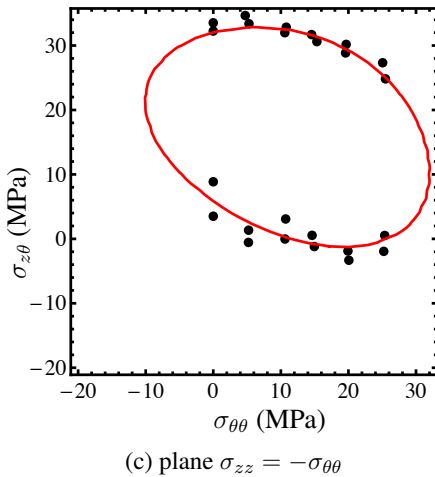
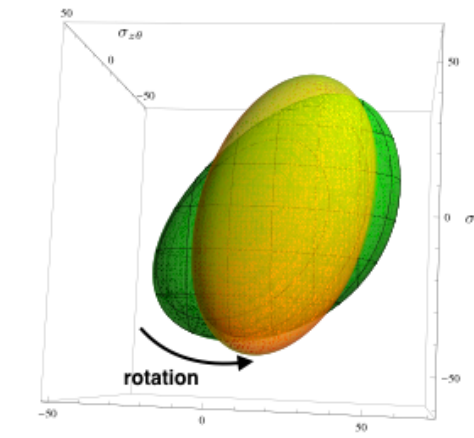
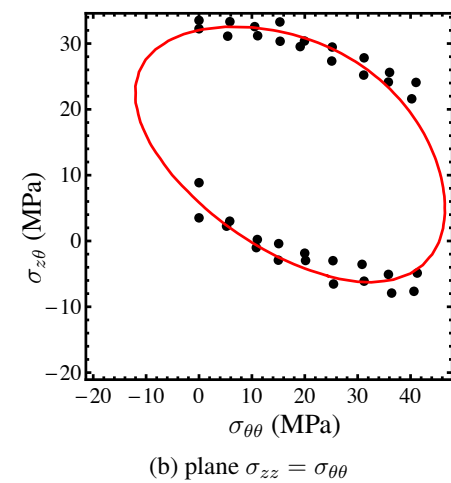
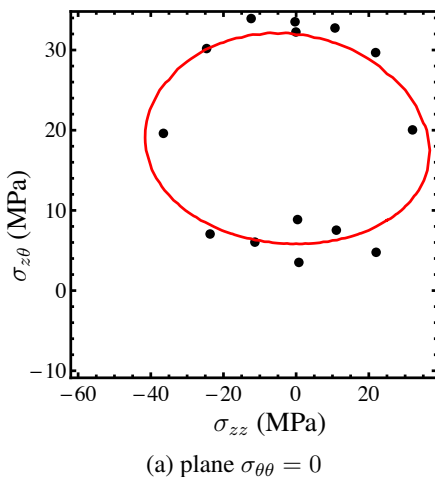
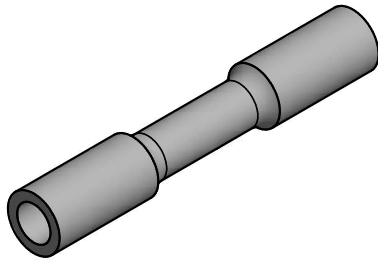
C. Yang, B. She, Y. Peng, & F. Pan, Loading path dependent distortional hardening of Mg alloys: Experimental investigation and constitutive modeling on cruciform specimens, International Journal of Mechanical Sciences, Vol. 160, pp. 282-297, 2019.

Yield surface evolution in 2D space



Hong-Ki Hong, Li-Wei Liu, Ya-Po Shiao, & Shao-Fu Yan, Yield surface evolution and an elastoplastic model with cubic distortional yield surface, Journal of Engineering Mechanics, , 148(6): 04022027, 2022.

Yield surface evolution in 3D space



Li-Wei Liu & Hong-Ki Hong, A description of three-dimensional yield surfaces by cubic polynomial, Journal of Engineering Mechanics, Vol. 143, No. 11, 04017129, 2017.

Features of elastoplastic behavior

Linearly elastic behavior

linear

constant moduli

reversible

conservative

single-valued

state vs. state

Elastoplastic behavior

linear or nonlinear

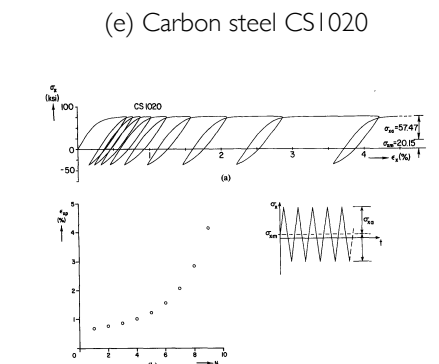
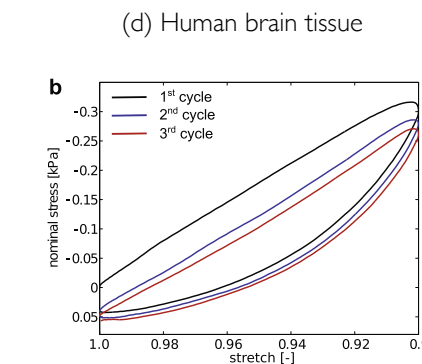
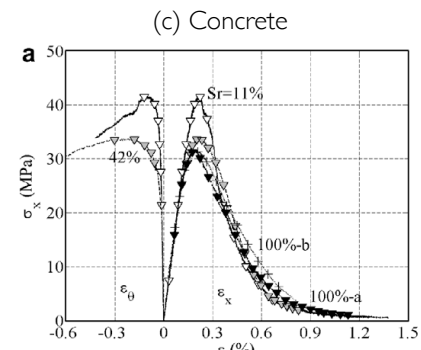
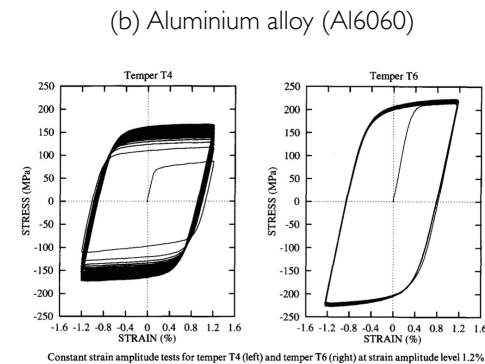
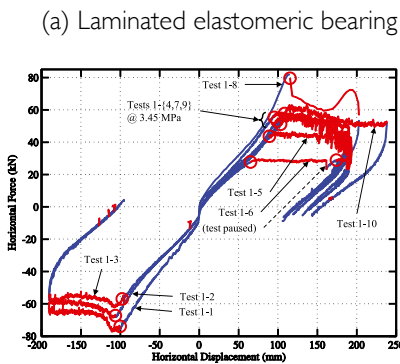
varying moduli

irreversible

conservative or dissipative

multi-valued

path vs. path



Mathematical frameworks of plastic models

Ingredient of elastoplastic models

1. Elastic-plastic decomposition

For infinitesimal deformation: $\varepsilon_{ij} = \varepsilon_{ij}^e + \varepsilon_{ij}^p$

2. Elastic constitutions

For large deformation: $F_{ij} = F_{ik}^e F_{kj}^p$ or $D_{ij} = D_{ij}^e + D_{ij}^p$

F_{ij} : deformation gradient, D_{ij} : Eulerian strain rate (stretching)

3. Plastic flow rules

4. Internal flow rules

(isotropic, kinematic, and distortion hardening/softening rules)

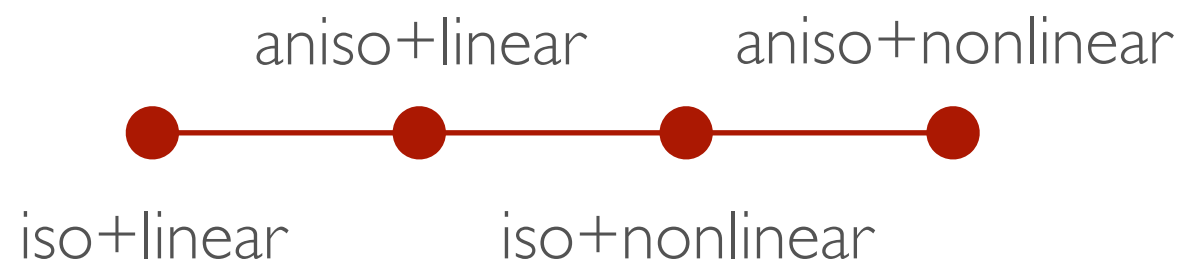
5. Admissible conditions

6. Non-negative conditions

7. Alternative conditions

Ingredients of elastoplastic models

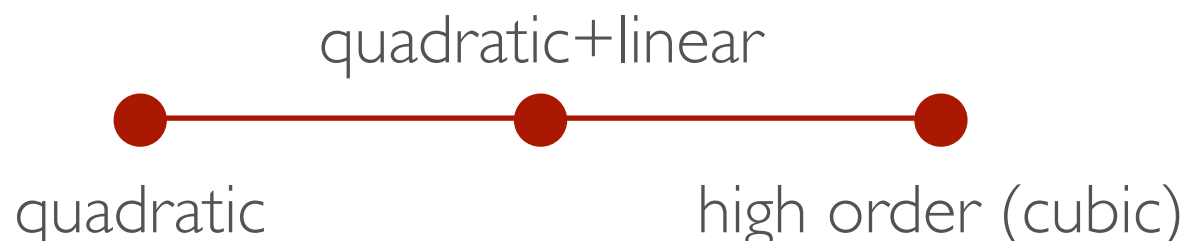
- elastic constitutions



- plastic flow rules

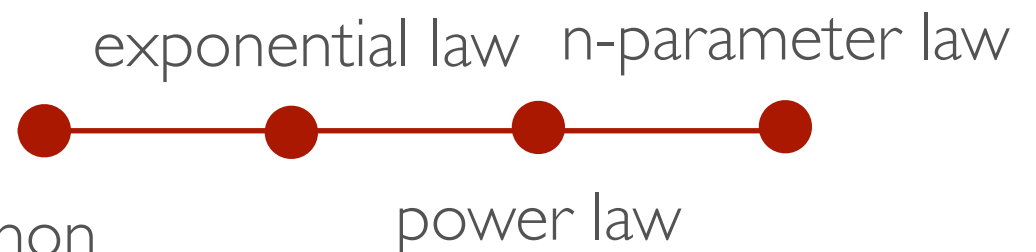


- stress admissible condition

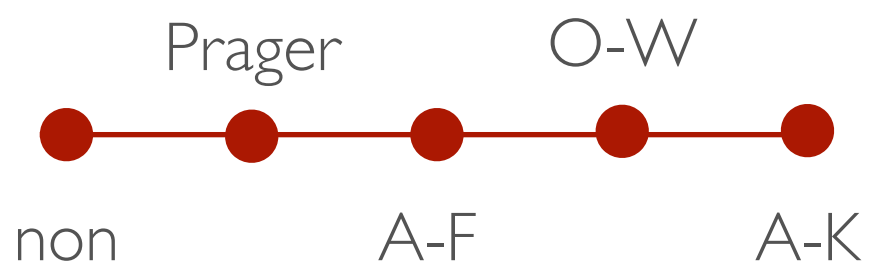


- hardening / softening rules

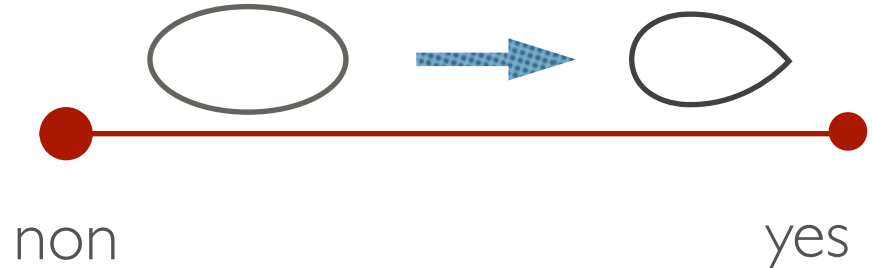
- isotropic hardening



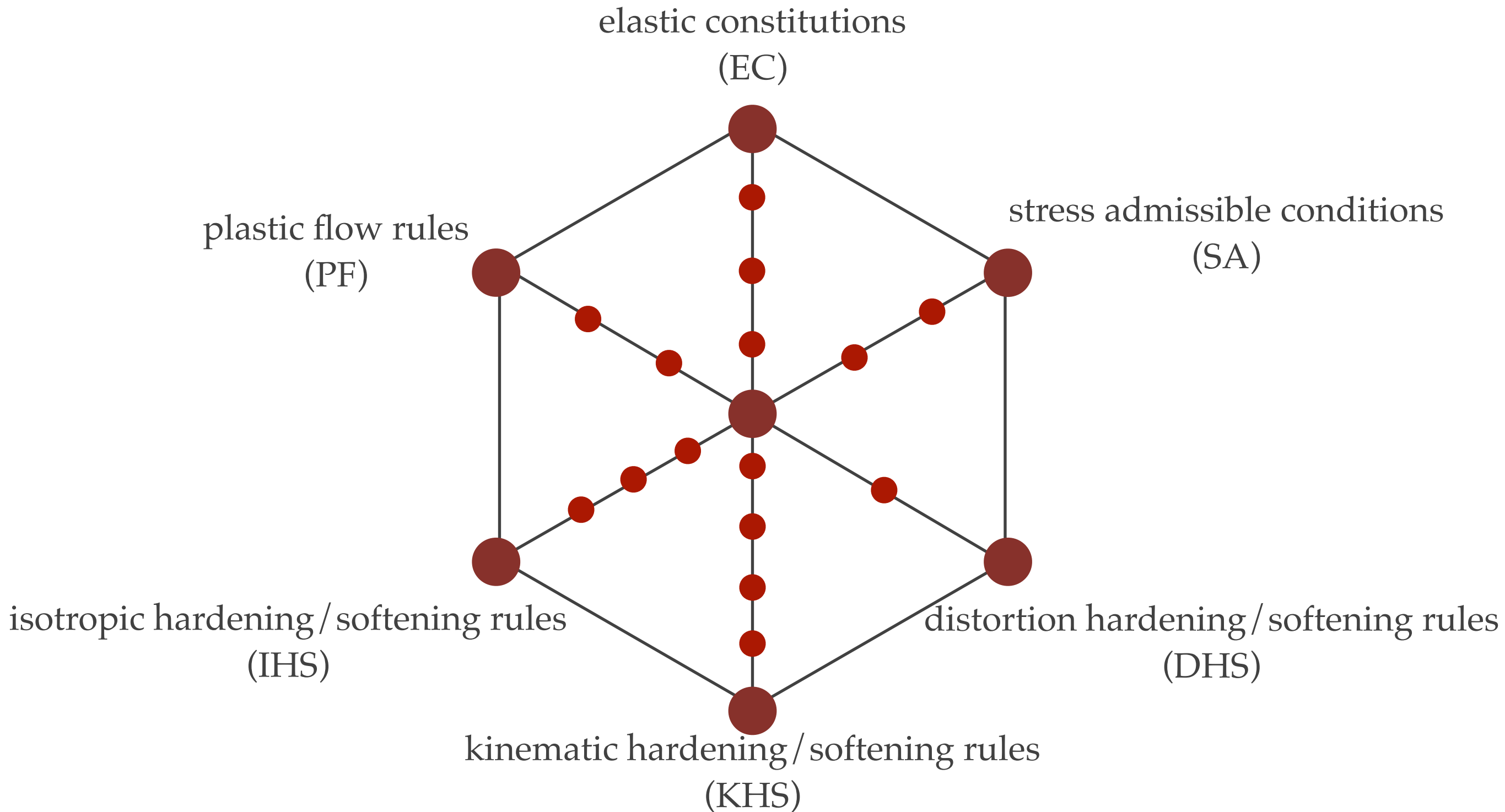
- kinematic hardening



- distortional hardening



Ingredients of elastoplastic models



Ingredients of elastoplastic models

Mechanical classification

- 1.elastic-plastic decomposition
- 2.elastic constitutions
- 3.plastic flow rules
- 4.hardening/softening rules
(isotropic, kinematic, and distortion)

- 5.stress admissible conditions
- 6.non-negative conditions
- 7.alternative conditions

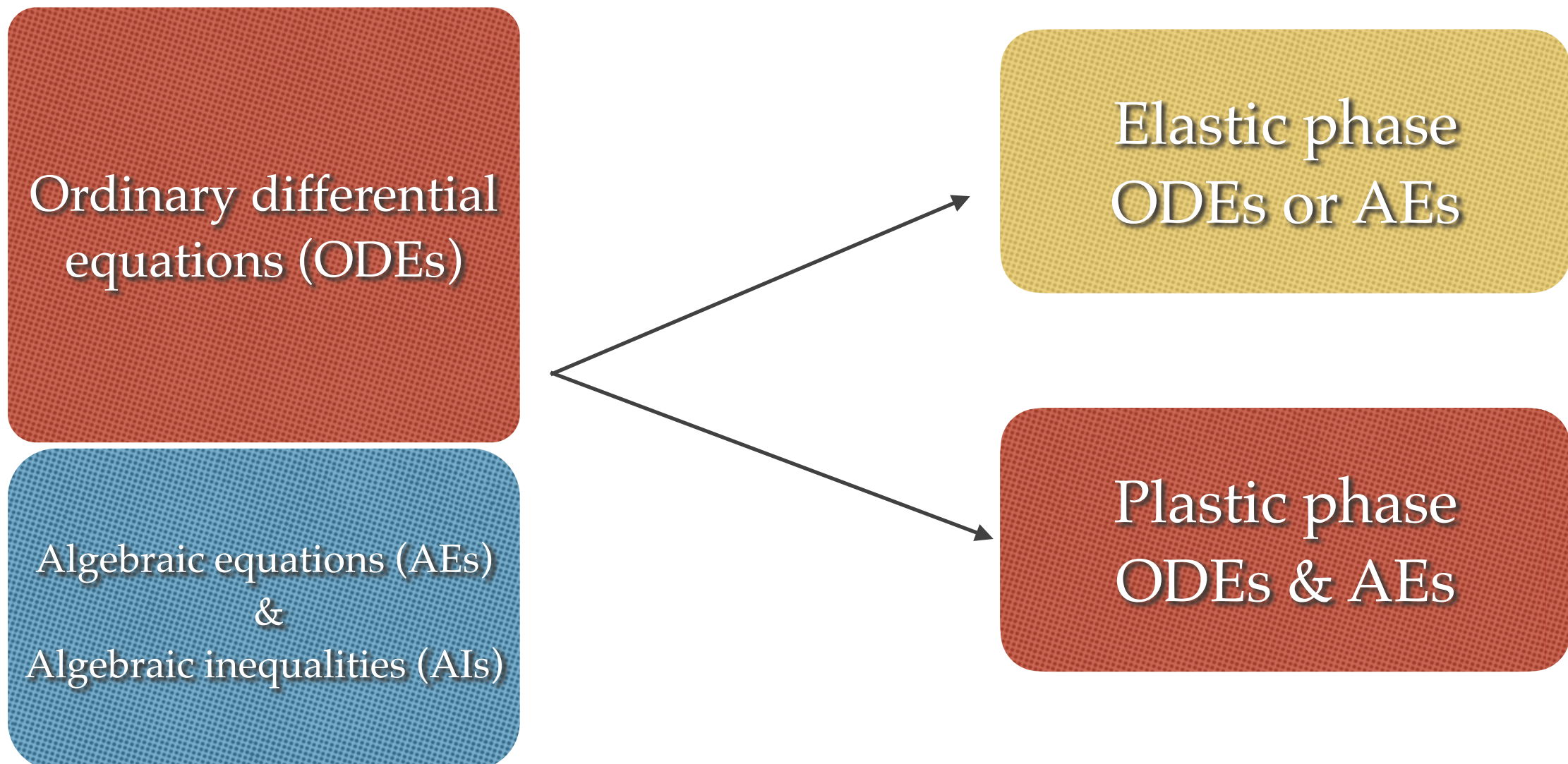
Mathematical classification

Ordinary differential
equations (ODEs)

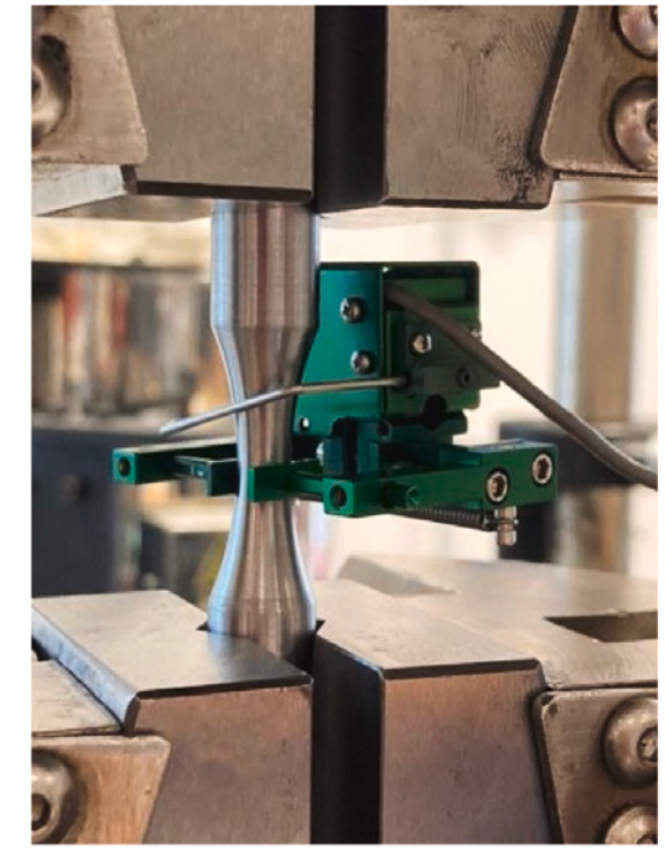
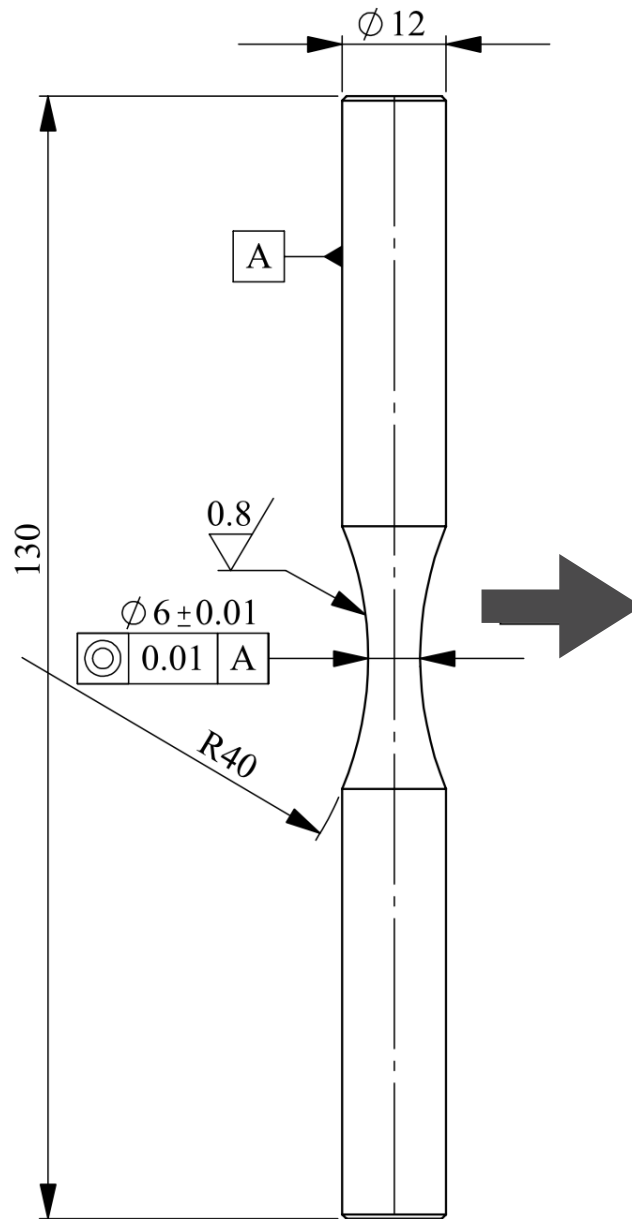
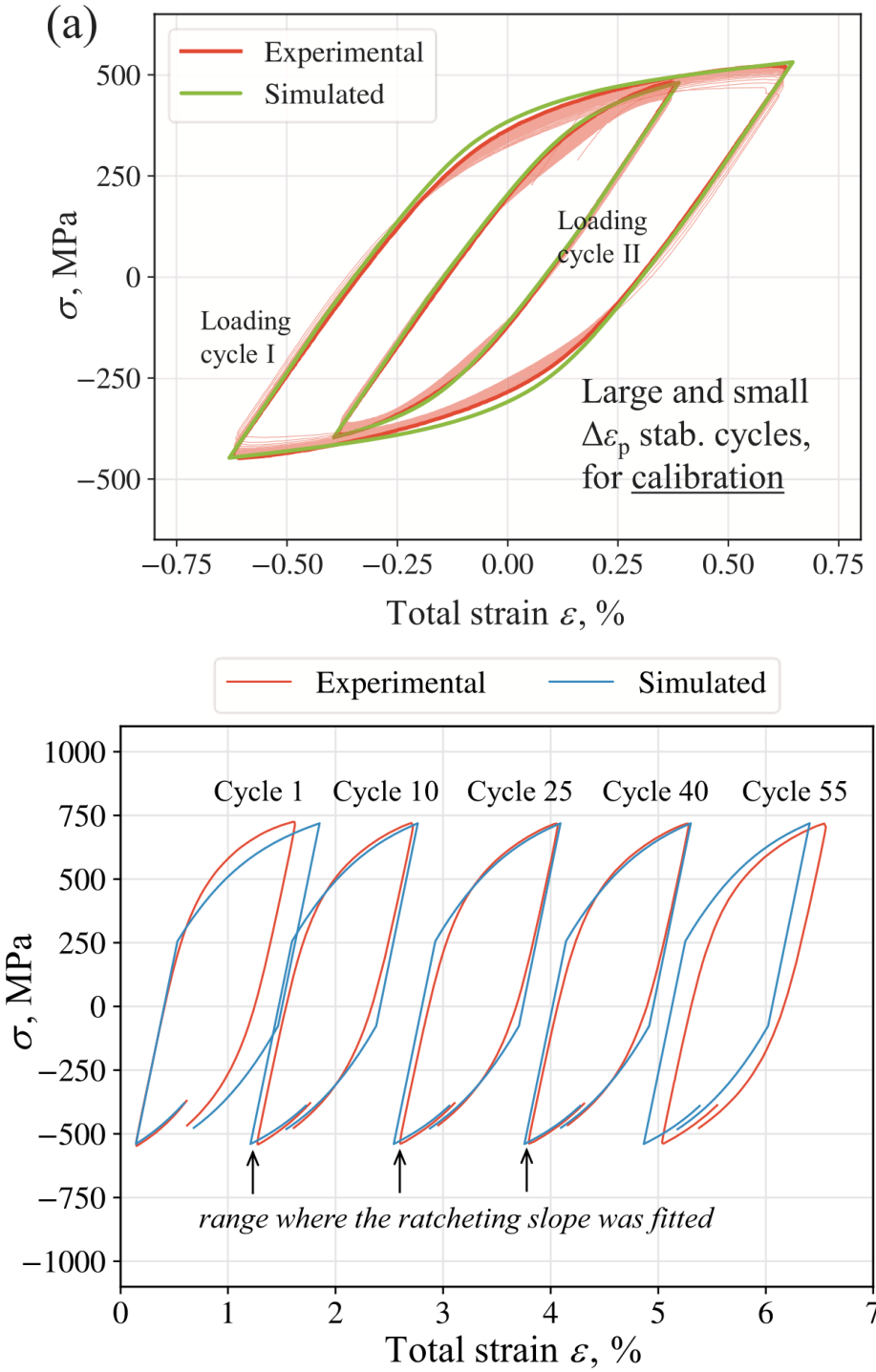
Algebraic equations (AEs)
&
Algebraic inequalities (AIs)

Ingredients of elastoplastic models

Mathematical classification



Chaboche isotropic-kinematic hardening model



C. Santus , T. Grossi , L. Romanelli , M. Pedranz , M. Benedetti, A computationally fast and accurate procedure for the identification of the Chaboche isotropic-kinematic hardening model parameters based on strain-controlled cycles and asymptotic ratcheting rate, International Journal of Plasticity, 160 (2023) 103503.

Enhanced homogeneous anisotropic hardening model

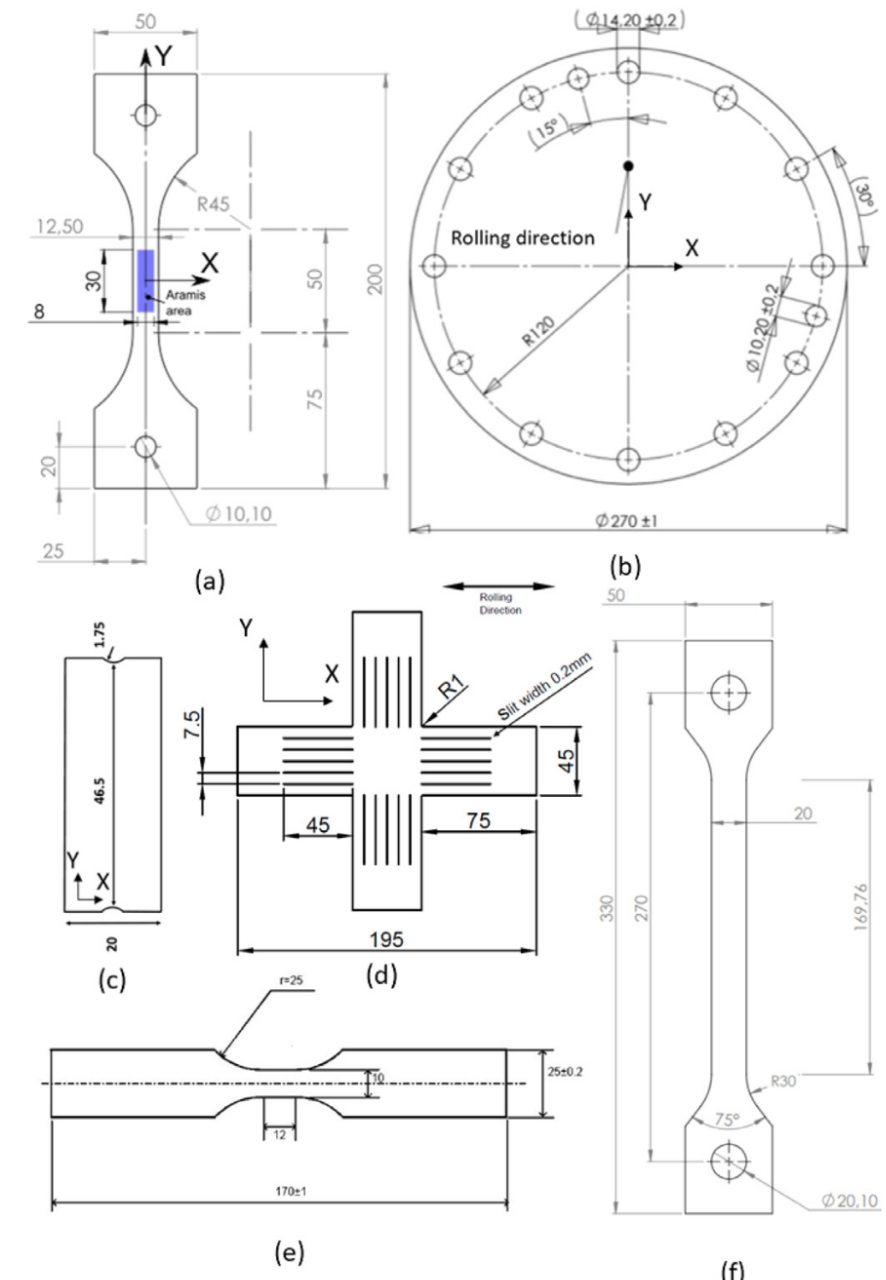
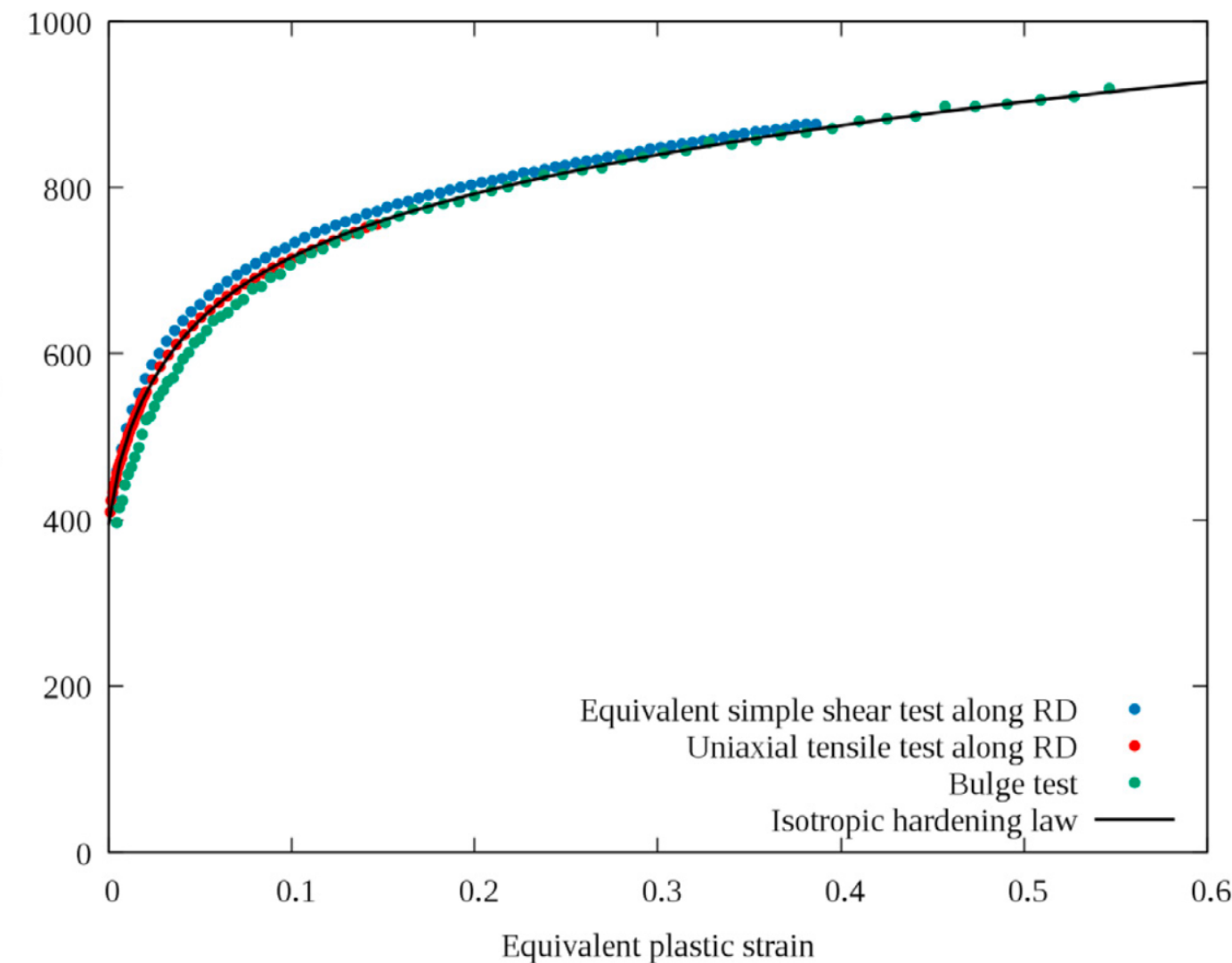
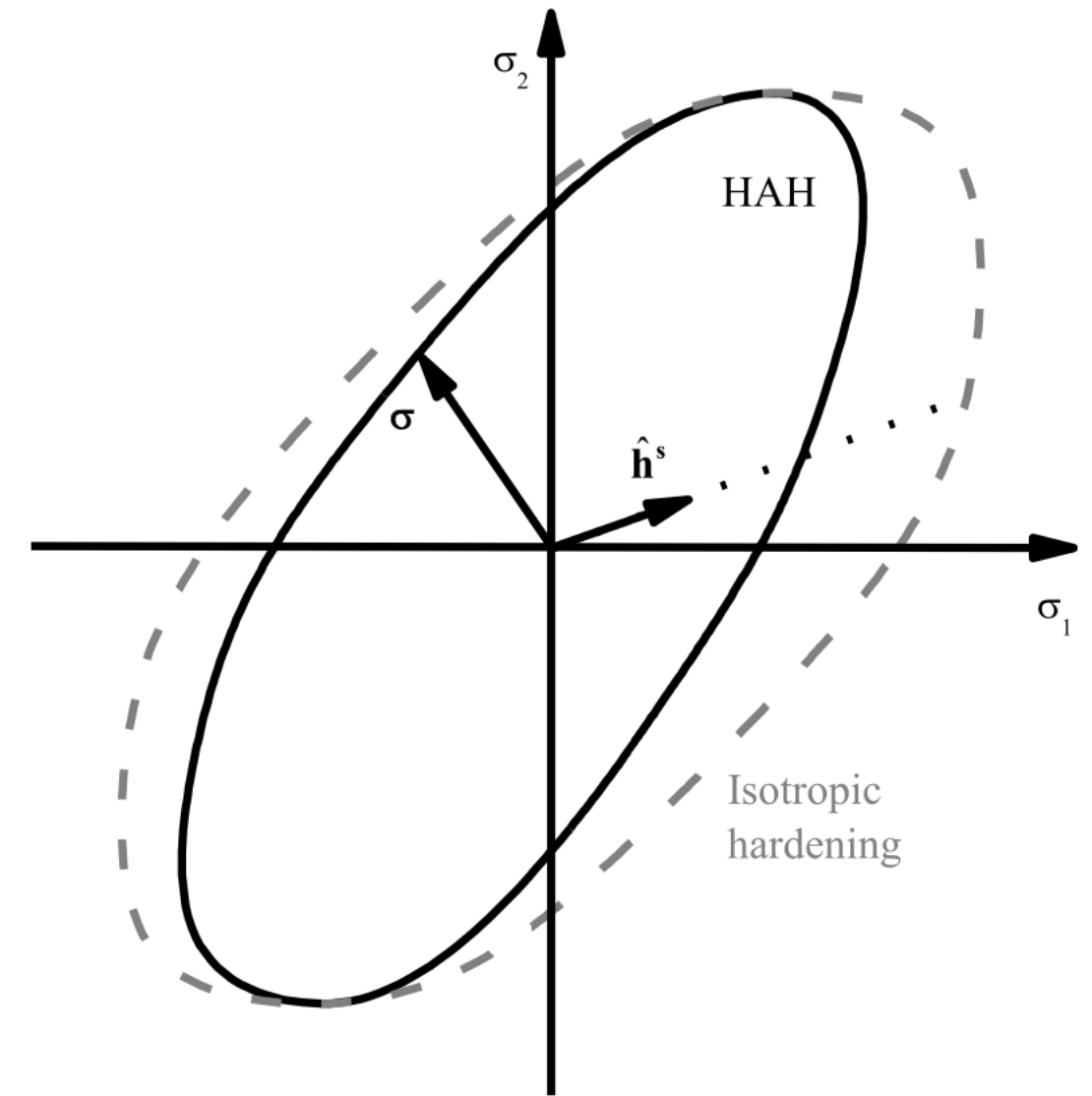
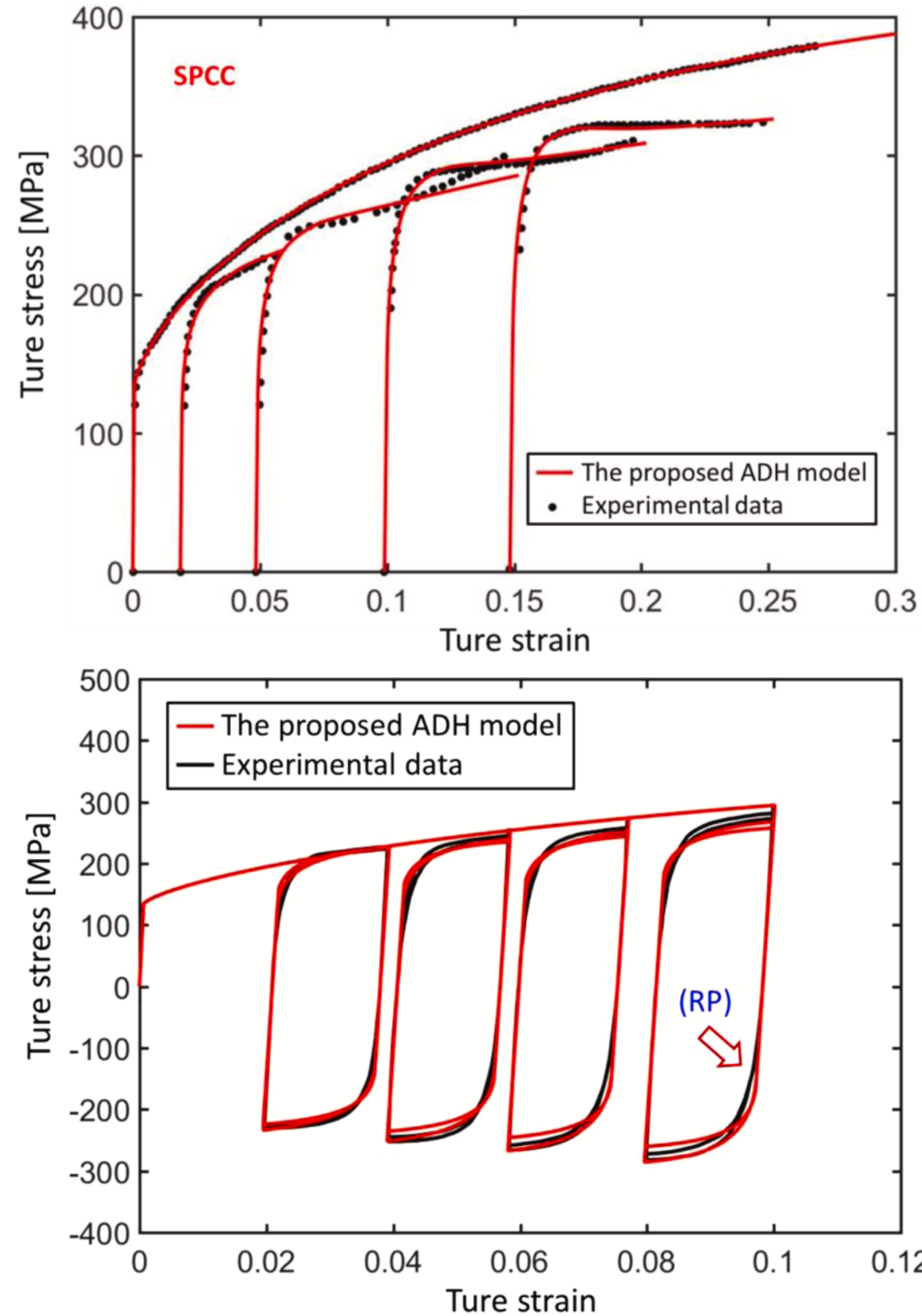


Fig. 1. Specimen geometries of the different tests (dimensions in mm, (a) Uniaxial tension, (b) Hydraulic bulge, (c) Simple shear, (d) Biaxial tension, (e) Tension-compression, (f) Pre-strain in tension).

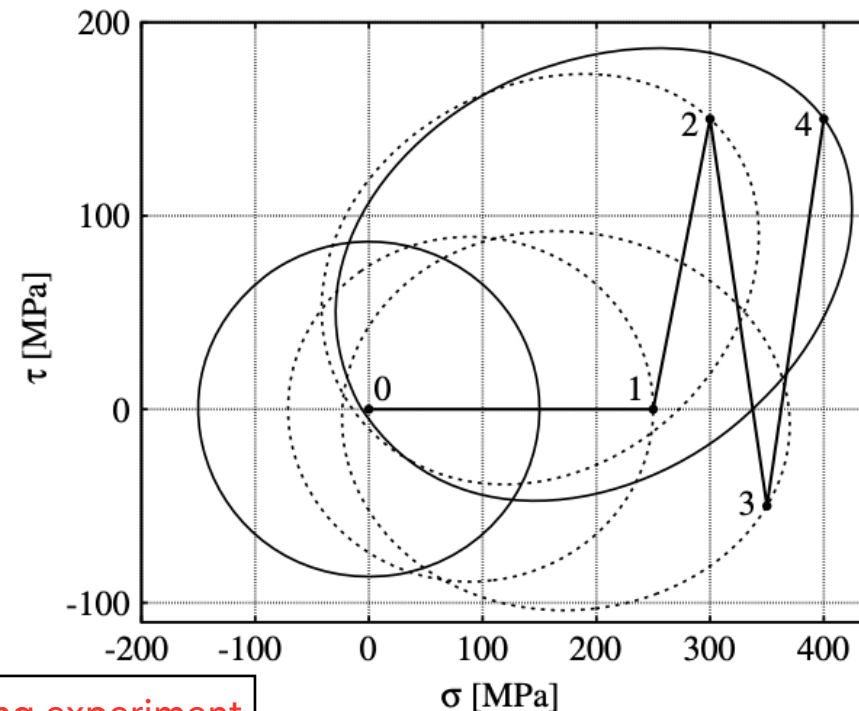
X. Diane Héault, Sandrine Thuillier, Shin-Yeong Lee, Pierre-Yves Manach, Frédéric Barlat, Calibration of a strain path change model for a dual phase steel, International Journal of Mechanical Sciences, 194 (2021) 106217

Anisotropic distortional hardening model

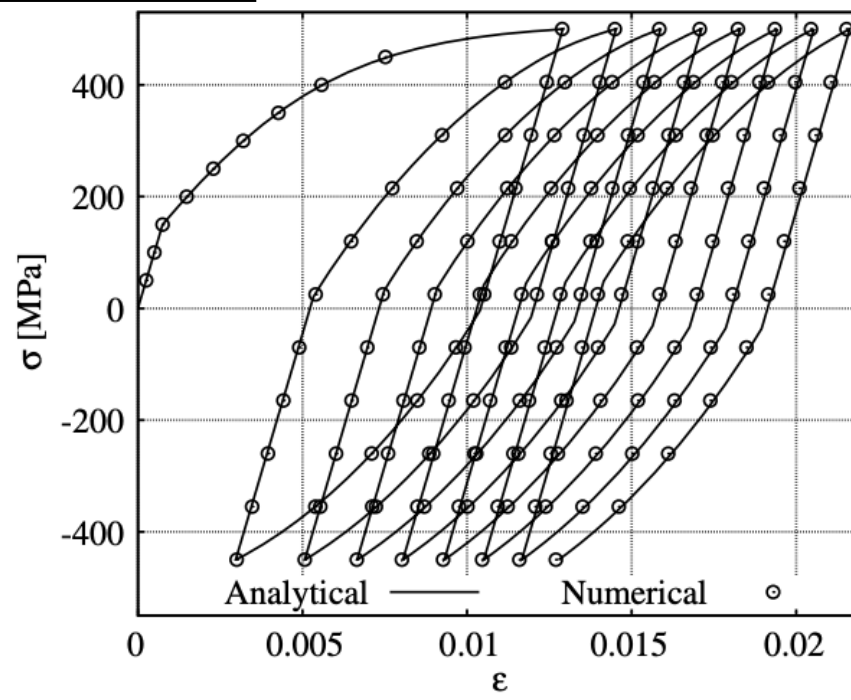


A model with directional distortional hardening

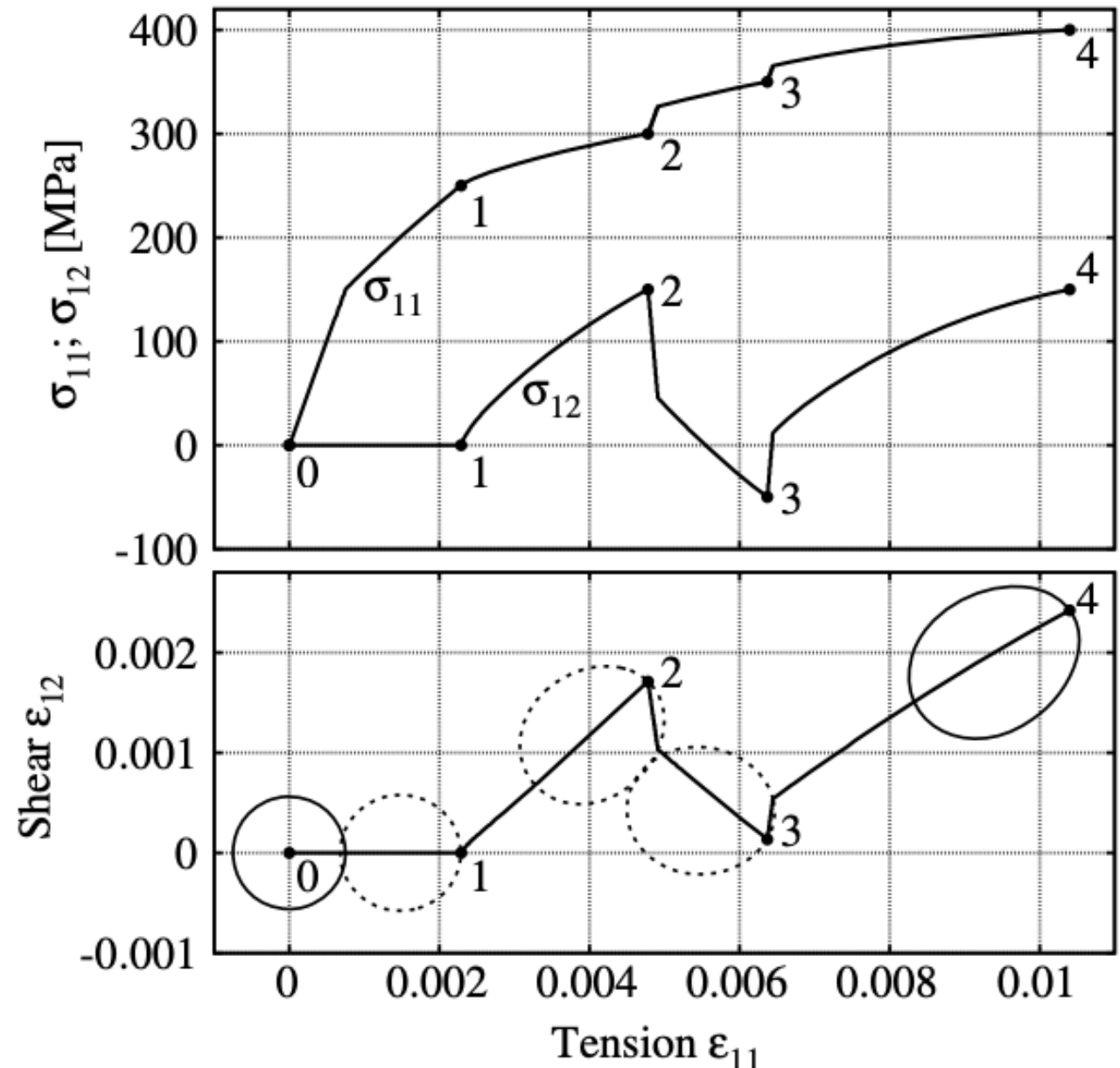
Subsequent yield surfaces in stress space



Ratcheting experiment



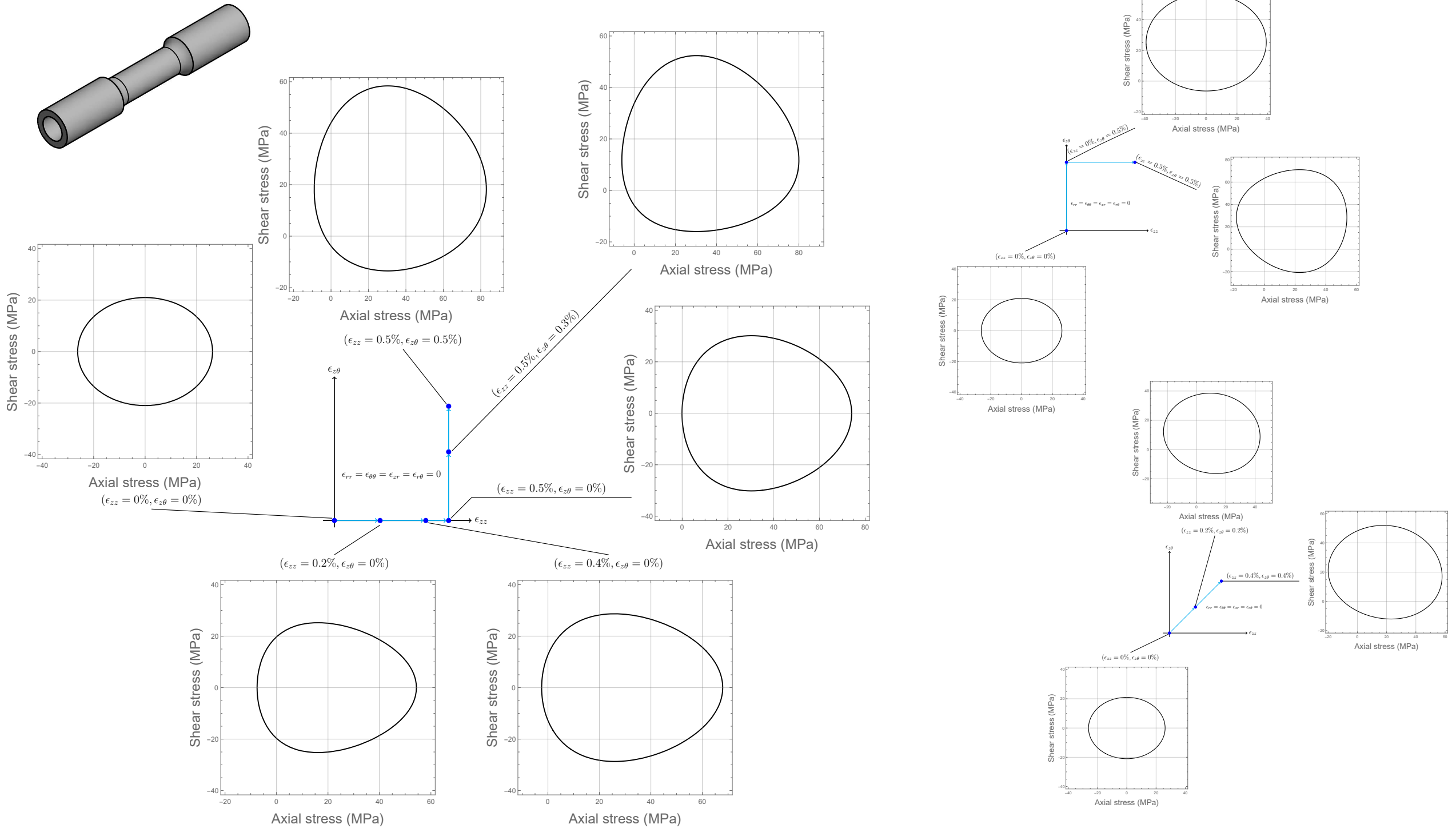
Loading path and subsequent elastic regions in strain space



René Marek ; Jiří Plešek; Zbyněk Hrubý ; Slavomír Parma; Heidi P. Feigenbaum; and Yannis F. Dafalias, M.ASCE Numerical Implementation of A Model With Directional Distortional Hardening, American Society of Civil Engineers, Volume 141, Issue 12, 2015

René Marek 2015

A model with cubic distortional yield surface

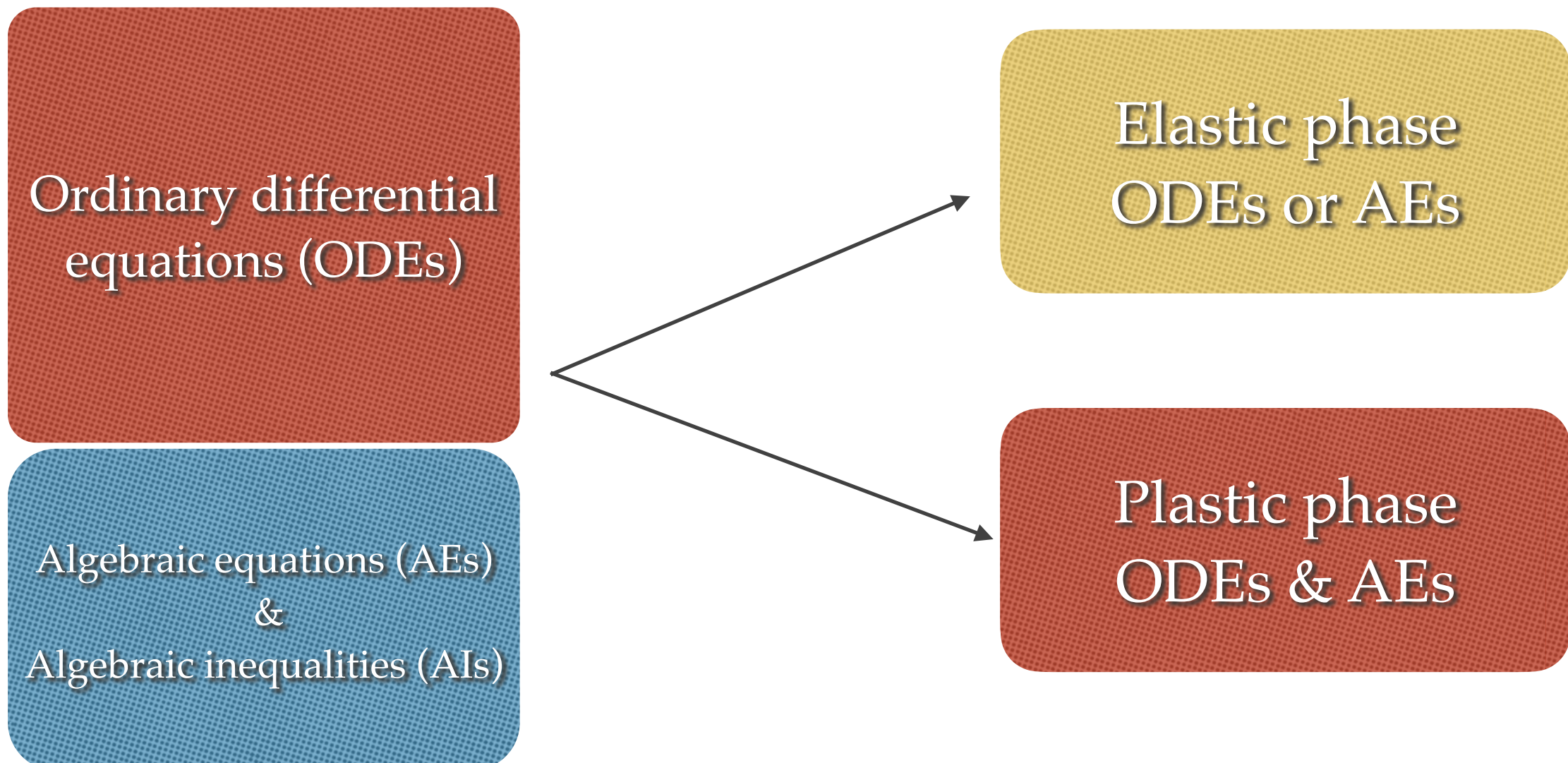


Hong-Ki Hong, Li-Wei Liu, Ya-Po Shiao, & Shao-Fu Yan, Yield surface evolution and an elastoplastic model with cubic distortional yield surface, Journal of Engineering Mechanics, , 148(6): 04022027, 2022.

Plastic integrations

Ingredients of elastoplastic models

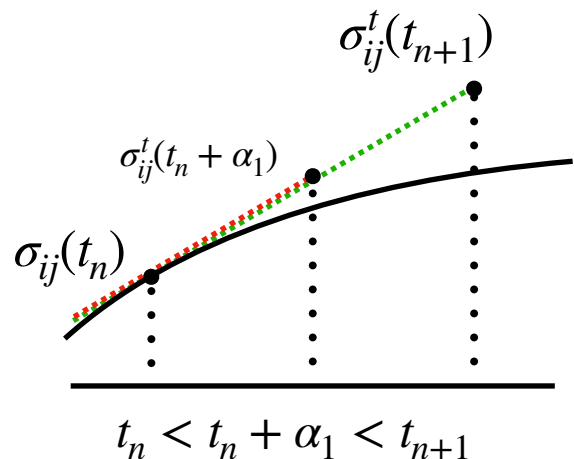
Mathematical classification



Plastic integrations

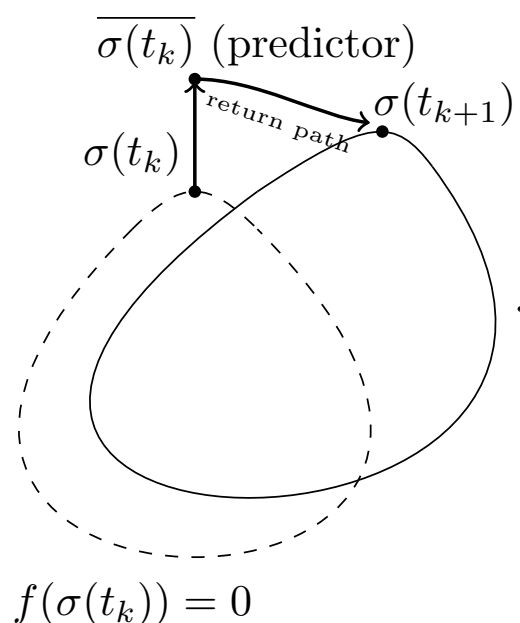
Plastic phase (ODEs & AEs)

Sub-stepping integrations



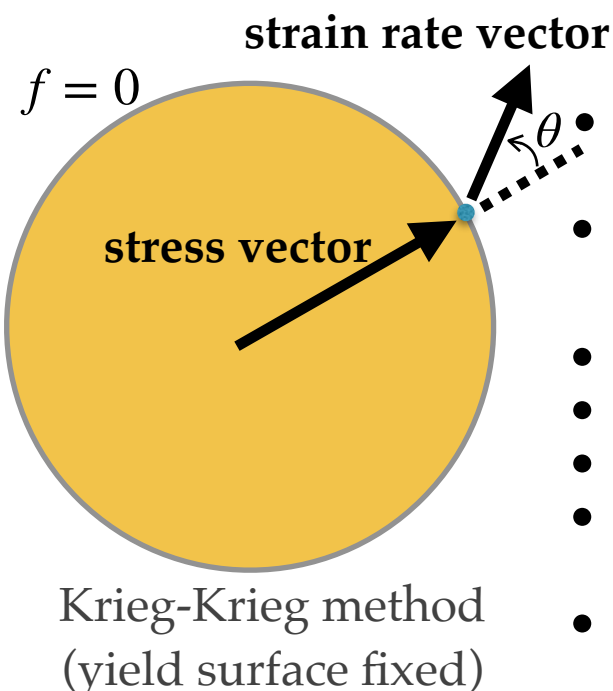
- Sloan (1987)
- Polat & Dokainish (1989)
- Potts & Ganendra (1994)
- Sloan et al. (2011)
- Ding et al. (2007)

Return-mapping integrations



- Wilkins (1964)
- Krieg & Krieg (1977)
- Scheryer et al. (1979)
- Ortiz et al. (1983)
- Ortiz & Popov (1985)
- Simo & Taylor (1985)
- Ortiz & Simo (1986)

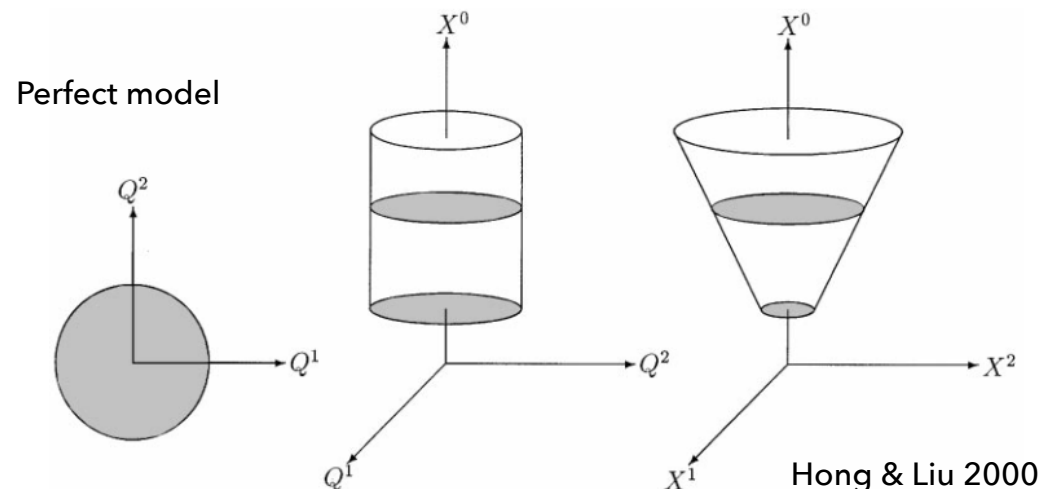
Angle-based integrations ("exact integrations")



- Initiated by Krieg & Krieg (1977) for von Mises yield surface
- $d\theta/dt=g(\theta)$, obtain exact solution of θ
- Szabo (2009)
- Kossa & Szabo (2009)
- Szabo & Kossa(2009)
- Rezaiee-Pajand & Sharifan (2012)
- Rezaiee-Pajand et al. (2014)

Plastic integrations based internal symmetry

Group preserving integrations



Generalized model

$$\mathbf{q} = \mathbf{q}^e + \mathbf{q}^p$$

$$\mathbf{Q} = k_e \mathbf{q}^e,$$

$$\dot{\mathbf{q}}^p = \lambda \frac{\mathbf{Q}}{Q_y},$$

$$\|\mathbf{Q}\| - Q_y \leq 0,$$

$$\lambda \geq 0,$$

$$\|\mathbf{Q}\| \lambda = Q_y \lambda.$$

Augmented stress space

$$\frac{d}{dt} \mathbf{X} = \mathbf{A} \mathbf{X}$$

$$\mathbf{A} = \frac{1}{q_y} \begin{bmatrix} \mathbf{0} & \dot{\mathbf{q}} \\ \dot{\mathbf{q}}^T & 0 \end{bmatrix}, \text{ if } \mathbf{X}^T \mathbf{g} \mathbf{X} = 0 \text{ and } \frac{d}{dt} [(\mathbf{X}^s)^T \mathbf{g}_{ss} \mathbf{X}^s] > 0.$$

$$\mathbf{A} = \frac{1}{q_y} \begin{bmatrix} \mathbf{0} & \dot{\mathbf{q}} \\ \mathbf{0} & 0 \end{bmatrix}, \text{ if } \mathbf{X}^T \mathbf{g} \mathbf{X} < 0 \text{ or } \frac{d}{dt} [(\mathbf{X}^s)^T \mathbf{g}_{ss} \mathbf{X}^s] \leq 0.$$

where $\mathbf{g} = \begin{bmatrix} \mathbf{g}_{ss} & \mathbf{g}_{s0} \\ \mathbf{g}_{0s} & g_{00} \end{bmatrix} = \begin{bmatrix} \mathbf{I} & \mathbf{0} \\ \mathbf{0} & -1 \end{bmatrix}$ is the Minkowski metric tensor.

The solution $\mathbf{X}(t) = [\mathbf{G}(t) \mathbf{G}^{-1}(t_1)] \mathbf{X}(t_1)$,

where $\mathbf{G} \in \text{SO}_o(n,1)$ since $\mathbf{A} \in \text{so}(n,1)$.

Hong & Liu 1999a; Hong & Liu 1999b; Hong & Liu 2000; Hong & Liu 2001;
Liu & Hong 2001; Liu 2003; Liu 2004a, b, c; Liu 2005; Liu & Li 2005; Artioli et al. 2005; Artioli et al. 2006; Artioli et al. 2007; Rezaiee-Pajand et al. 2010

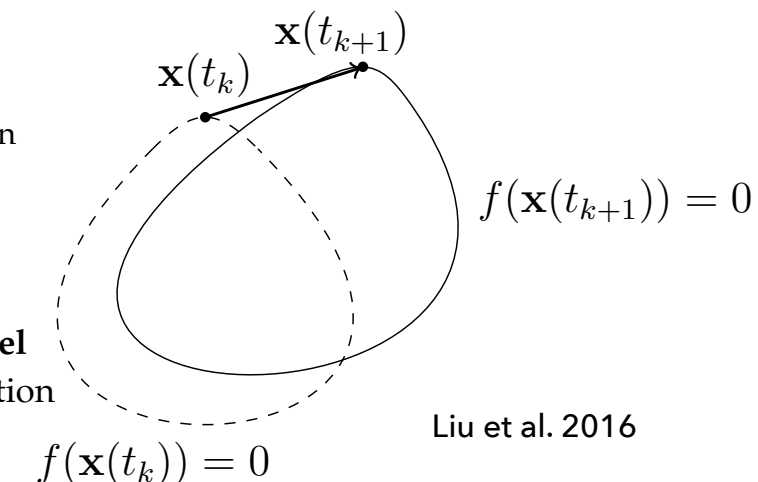
Return-free integrations

Perfect elastoplastic model

- Drucker-Prager yield condition
- cubic yield condition
- quartic yield condition

Kinematic and isotropic hardening elastoplastic model

- Drucker-Prager yield condition



Stress is updated on the yield surface automatically.

Model family

$$\varepsilon_{ij} = \varepsilon_{ij}^e + \varepsilon_{ij}^p$$

$$\varepsilon_{ij}^e = \mathcal{C}(\sigma_{kl}, \chi_\alpha)$$

$$\dot{\varepsilon}_{ij}^p = \dot{\lambda} g_{ij}(\sigma_{kl}, \chi_\alpha)$$

$$\dot{\chi}_\alpha = \dot{\lambda} h_\alpha(\sigma_{kl}, \chi_\beta)$$

$$f(\sigma_{kl}, \chi_\alpha) \leq 0$$

$$\dot{\lambda} \geq 0$$

$$f \dot{\lambda} = 0$$

Augmented stress space

$$\dot{\mathbf{x}} = -\dot{\lambda} \mathbf{S}(\mathbf{x}) \nabla_{\mathbf{x}} f + \mathbf{D}(\mathbf{x}) \mathbf{u}$$

$$f(\mathbf{x}) \leq 0$$

$$\dot{\lambda} \geq 0$$

$$f \dot{\lambda} = 0$$

plastic phase

Space with internal symmetry

$$\dot{\mathbf{y}} = \mathbf{A} \mathbf{y}, \mathbf{A} \in \text{so}(p, g) \text{ (Lie algebra)}$$

$$f = \mathbf{y}^T \mathbf{g} \mathbf{y} = 0,$$

$$\mathbf{A}^T \mathbf{g} + \mathbf{g} \mathbf{A} = 0,$$

$$\mathbf{g} = \begin{bmatrix} \mathbf{I}_p & \mathbf{0}_{p \times q} \\ \mathbf{0}_{q \times p} & -\mathbf{I}_q \end{bmatrix}$$

$$\mathbf{y}(t) = [\mathbf{G}(t) \mathbf{G}^{-1}(t_i)] \mathbf{y}(t_i), \quad \mathbf{G}(t) \in \text{SO}(p, g) \text{ (Lie group)} \\ \mathbf{G}(0) = \mathbf{I}_{p+q},$$

Angle-based integrations

- Perfectly elastoplastic model with spherical yield surface

$$\mathbf{q} = \mathbf{q}^e + \mathbf{q}^p$$

$$\mathbf{Q} = k_e \mathbf{q}^e$$

$$\dot{\mathbf{q}}^p = \frac{\partial f}{\partial \mathbf{Q}} \dot{\lambda}$$

$$f = \|\mathbf{Q}\| - Q_y \leq 0$$

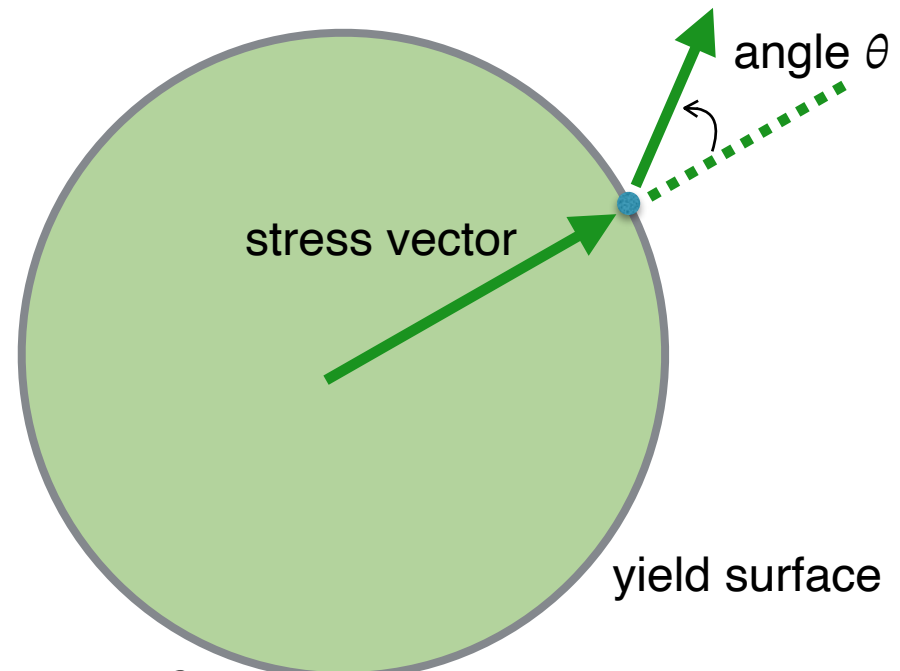
$$\dot{\lambda} \geq 0$$

$$f\dot{\lambda} = 0$$

$$\begin{aligned} \dot{\mathbf{Q}} &= k_e \dot{\mathbf{q}} && \text{if } \|\mathbf{Q}\| - Q_y < 0 \\ \dot{\mathbf{Q}} &= -k_e \frac{\mathbf{Q}^T \dot{\mathbf{q}}}{Q_y^2} \mathbf{Q} + k_e \dot{\mathbf{q}} && \text{if } \|\mathbf{Q}\| - Q_y = 0 \end{aligned}$$

or $\mathbf{Q}^T \dot{\mathbf{q}} \leq 0$
 and $\mathbf{Q}^T \dot{\mathbf{q}} > 0$

strain rate vector



- Krieg-Krieg method ($\dot{\mathbf{q}}(\tau)$ is constant $\forall \tau \in [t_0, t]$)

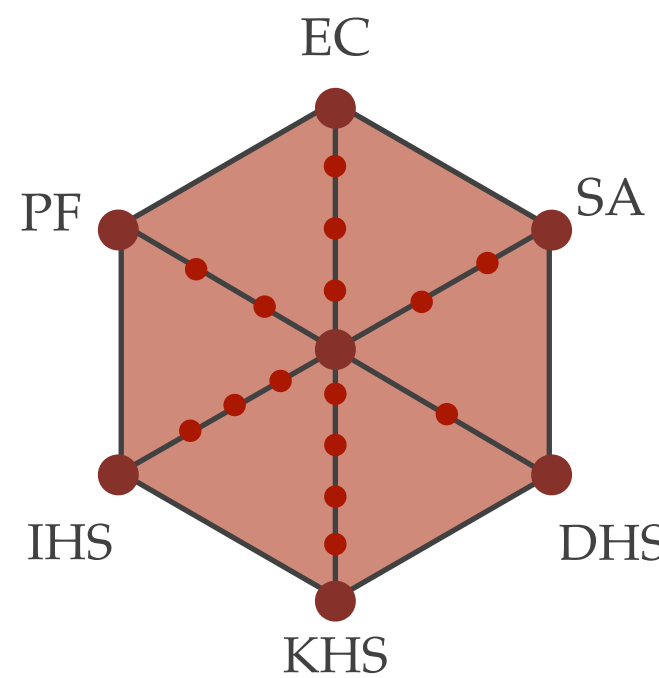
$$\text{plastic phase} \left\{ \begin{array}{l} \dot{\mathbf{Q}} = -k_e \frac{\mathbf{Q}^T \dot{\mathbf{q}}}{Q_y^2} \mathbf{Q} + k_e \dot{\mathbf{q}} \\ \|\mathbf{Q}\| - Q_y = 0 \end{array} \right. \leftrightarrow \text{ODE of angle} \quad \dot{\theta} = -\frac{k_e}{Q_y} \|\dot{\mathbf{q}}\| \sin \theta$$

$$\leftrightarrow \tan \frac{\theta}{2} = \exp\left(-\frac{k_e \|\dot{\mathbf{q}}\|(t - t_0)}{Q_y}\right) \tan \frac{\theta_0}{2}$$

R. D. Krieg and D. B. Krieg. Accuracies of numerical solution methods for the elastic- perfectly plastic model. *Journal of Pressure Vessel Technology*, 99, 510–515, 1977.

Limitation of plastic integrations

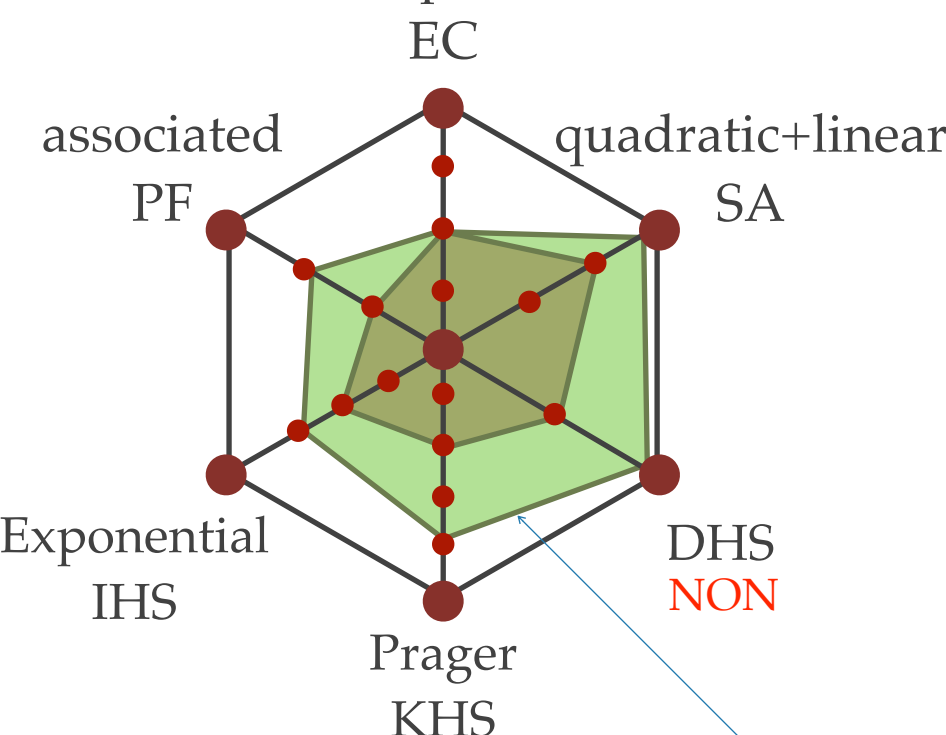
Substepping / return-mapping integrations



- Time-consuming
- Predict-correct need to design in each model

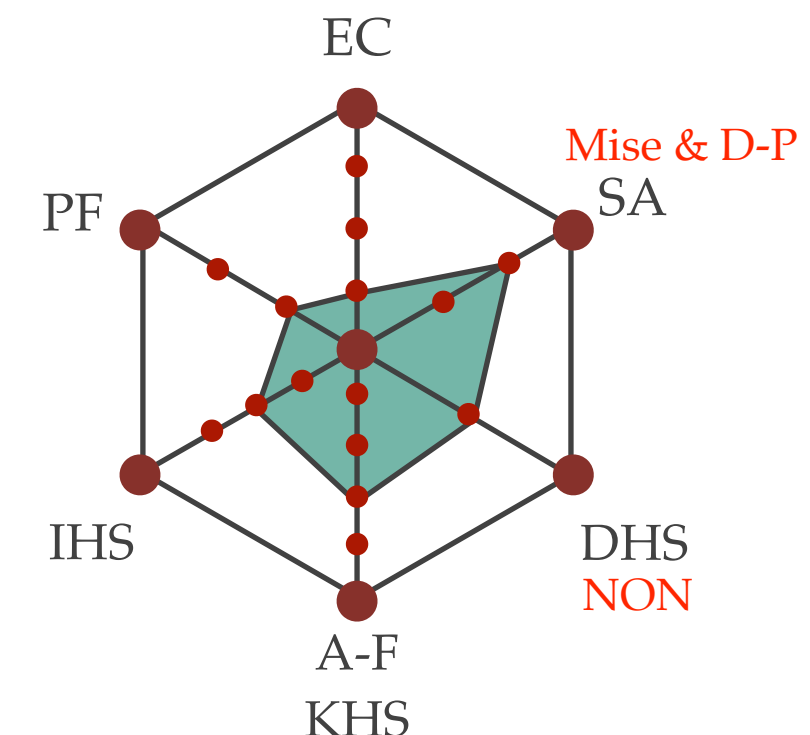
Group-preserving integrations

anisotropic+linear



Internal symmetry must be explored & obtained in each model.

Angle-based integrations



The exact solution only for elastoplastic models with von Mise or D-P yield surface.

Thanks for your attention